VOL. 6 NO. 5 NOVEMBER 1963

Journal of

ELECTROANALYTICAL CHEMISTRY

International Journal Dealing with all Aspects of Electroanalytical Chemistry, Including Fundamental Electrochemistry

E·L S E V I E R

GENERAL INFORMATION

See also Suggestions and Instructions to Authors which will be sent free, on request to the Publishers.

Types of contributions

(a) Original research work not previously published in other periodicals.
(b) Reviews on recent developments in various fields.
(c) Short communications.
(d) Bibliographical notes and book reviews.

Languages

Papers will be published in English, French or German.

Submission of papers

Papers should be sent to one of the following Editors:

Professor J. O'M. BOCKRIS, John Harrison Laboratory of Chemistry, University of Pennsylvania, Philadelphia 4, Pa., U.S.A.
Dr. R. PARSONS, Department of Chemistry, The University, Bristol 8, England.
Professor C. N. REILLEY, Department of Chemistry, University of North Carolina, Chapel Hill, N.C., U.S.A.

Authors should preferably submit two copies in double-spaced typing on pages of uniform size. Legends for figures should be typed on a separate page. The figures should be in a form suitable for reproduction, drawn in Indian ink on drawing paper or tracing paper, with lettering etc. in thin pencil. The sheets of drawing or tracing paper should preferably be of the same dimensions as those on which the article is typed. Photographs should be submitted as clear black and white prints on glossy paper.
All references should be given at the end of the paper. They should be numbered and the numbers should appear in the text at the appropriate places.
A summary of 50 to 200 words should be included.

Reprints

Twenty-five reprints will be supplied free of charge. Additional reprints can be ordered at quoted prices. They must be ordered on order forms which are sent together with the proofs.

Publication

The *Journal of Electroanalytical Chemistry* appears monthly and has six issues per volume and two volumes per year, each of approx. 500 pages.

Subscription price (post free): £ 10.15.0 or $ 30.00 or Dfl. 108.00 per year; £ 5.7.6 or $ 15.00 or Dfl. 54.00 per volume.
Additional cost for copies by air mail available on request.
For advertising rates apply to the publishers.

Subscriptions

Subscriptions should be sent to:

ELSEVIER PUBLISHING COMPANY, P.O. Box 211, Spuistraat 110-112, Amsterdam-C., The Netherlands.

SUMMARIES OF PAPERS PUBLISHED IN JOURNAL OF ELECTROANALYTICAL CHEMISTRY

Vol. 6, No. 5, November 1963

CHRONOPOTENTIOMETRIC DEPOSITION AND STRIPPING OF SILVER, LEAD AND COPPER AT PLATINUM ELECTRODES

The effect of pre-treatment (pre-oxidation, pre-plating, or platinization) of a platinum electrode on the chronopotentiometric deposition and stripping of silver, lead and copper in various media is considered. Depositions were found to occur less reversibly at a pre-oxidized electrode. Evidence for retention of some deposited metal, even at potentials considerably more positive than the reversible stripping potential is presented and possible mechanisms for this retention are suggested.

A. R. NISBET AND A. J. BARD,

J. Electroanal. Chem., 6 (1963) 332–343.

THE REDUCTION MECHANISM OF PERMANGANIC ION IN MINERAL ACID MEDIA

The reduction of MnO_4^- in nitric, perchloric and sulphuric acids on a bubbling platinum electrode and the influence of the acid anion on the behaviour of the permanganic ion in the presence of Mn(II) were studied. The rôle of Mn(II) and Mn(III) in the permanganate reduction process was fully investigated. Evidence is given for the formation of an Mn(III)–acid complex in sulphuric and perchloric acids. The presence of a surface film of $MnMnO_3$ on the platinum electrode and its reduction were observed and studied.

P. G. DESIDERI,

J. Electroanal. Chem., 6 (1963) 344–356.

POLAROGRAPHIC BEHAVIOUR OF HALIDE IONS

I. CHLORIDE

The wave obtained in the a.c. polarography of chloride is attributed mainly to the adsorption of chloride ion which results in a high differential capacity of the electrical double-layer. The alternating current at potentials more negative than the summit of this a.c. wave is non-faradaic in character since no faradaic direct current can be detected in this potential region. D.c. polarographic current–time curves indicate that discharge of chloride ion begins almost discontinuously at a potential corresponding to the summit of the a.c. wave.

T. BIEGLER,

J. Electroanal. Chem., 6 (1963) 357–364.

POLAROGRAPHIC BEHAVIOUR OF HALIDE IONS

II. BROMIDE

The a.c. wave of bromide consists of two distinct portions, one, at more negative potentials, arising from the adsorption of bromide ion and the other resulting from the electron transfer process involved in the formation of mercurous bromide. Diffusion-control of adsorption of bromide ion can be detected at low concentrations. Evidence obtained from the shape of the a.c. wave and from current–time curves, both a.c. and d.c., for individual drops suggests that the faradaic process is reversible only over a narrow potential range corresponding to the formation of a mono-layer of mercurous bromide. Bromide ion gives a d.c. pre-step of origin similar to that of chloride.

T. BIEGLER,

J. Electroanal. Chem., 6 (1963) 365–372.

POLAROGRAPHIC BEHAVIOUR OF HALIDE IONS

III. IODIDE

A.c. polarograms of iodide ion at concentrations less than $4 \cdot 10^{-4}$ *M* shows two separate waves, one of which occurs near the potential region of the anodic d.c. step and is probably due to adsorption of iodide ion and the other at a considerably more positive potential, resulting from desorption of mercurous iodide from the electrode sur face. At higher iodide concentrations a third a.c. wave is evident and is connected with the occurrence of convection phenomena at the electrode surface.

T. BIEGLER,

J. Electroanal. Chem., 6 (1963) 373–380.

APPLICATION OF OSCILLOGRAPHIC POLAROGRAPHY IN QUANTITATIVE CHEMICAL ANALYSIS

XX. THE OSCILLOGRAPHIC DETERMINATION OF TRACE AMOUNTS OF HEAVY METALS IN HYDROCHLORIC ACID, PURE ALUMINIUM AND ZIRCONIUM

A method has been developed for the oscillopolarographic determination of trace amounts of copper, lead, cadmium and zinc in hydrochloric acid. This method has also been applied to the simultaneous determination of these metals at concentrations of 10^{-4}–10^{-5}% in pure aluminium and zirconium. A new method for the quantitative evaluation of the results has been proposed.

P. BERAN, J. DOLEŽAL AND D. MRÁZEK,

J. Electroanal. Chem., 6 (1963) 381–396.

AN IMPROVED TECHNIQUE IN IMPEDANCE TITRATION

The precision of the end-point of the impedance titration can be improved by compensating the alternating voltage of the titration cell with that from an external alternating voltage with the help of a difference amplifier. The output signal of the difference amplifier is A-B if the input signals are A and B. There will be a sharp jump in the output of the difference amplifier at the end-point of the titration.

U. H. NARAYANAN AND K. SUNDARARAJAN,

J. Electroanal. Chem., 6 (1963) 397–400.

STUDIES OF THE MECHANISM OF THE ANODIC OXIDATION OF ETHYLENE IN ACID AND ALKALINE MEDIA

The ethylene oxidation reaction on smooth and platinized platinum has been studied at 80°C in solutions of $H_2SO_4 + K_2SO_4$ and $NaOH + K_2SO_4$ of constant ionic strength = 1.5. Reaction rates were measured as a function of potential, pH and partial pressure of ethylene. Coulombic efficiency of the reaction was determined by measurements of CO_2 production in acidic solutions, and of C_2H_4 consumption in alkaline solutions. The following parameters have been found:

$$\left(\frac{dV}{d\log i}\right)_p = \frac{2.3 \cdot 2RT}{F}; \left(\frac{d\log i}{d\,pH}\right)_V \simeq 0.45; \left(\frac{d\eta}{d\,pH}\right)_i \simeq 0;$$

$$\left(\frac{d\log i_0}{d\,pH}\right) \approx 0; \left(\frac{di}{dp}\right)_V < 0;$$

Coulombic efficiency is 100 ± 1% in acidic and 90 ± 5% in alkaline solutions. $i_0 = 10^{-8}$ A cm^{-2} on platinized and 10^{-10} A cm^{-2} on smooth Pt respectively. Activation energy A = 17 ± 2 kcals. At higher overpotentials diffusion limiting current was obtained. At V = 0.9 (R.H.E.), the current drops to negligible values due to the oxide formation. Coverage of the electrode with the ethylenic radical at 1 atm has been evaluated by two independent methods as $\theta_E = 0.55 \pm 0.2$.

The reaction mechanism in the Tafel potential range was interpreted in terms of water discharge as the rate-determining step over the complete pH range investigated. In the potential range higher than that of the Tafel region the rate control is shifted to mass transport of ethylene. At P_E = 1 atm, the Tafel potential range is limited by oxide formation before diffusion control sets in. A possible explanation of the anomalous pH effect in reactions concerning water discharge has been given.

H. WROBLOWA, B. J. PIERSMA AND J. O'M. BOCKRIS,
J. Electroanal. Chem., 6 (1963) 401–416.

POLAROGRAPHY OF CYCLIC HYDRAZIDES

(Short Communication)

E. T. SEO AND T. KUWANA,
J. Electroanal. Chem., 6 (1963) 417–418.

Announcement

Authors and readers of the Journal will have noticed that we have now succeeded in reducing the publication time of papers to 10–12 weeks after submission. We should like to maintain this situation which, we believe, provides the best service to the Sciences of Electrochemistry and Electroanalytical Chemistry.

This short publication time, however, means that each stage of the process of preparing the Journal must be completed smoothly and in as short a time as possible. We, therefore, appeal to Authors to return the proofs of their papers to the publishers as quickly as possible. Late return may delay the appearance of the issue or cause the paper to be transferred to a later issue.

The Editors

CHRONOPOTENTIOMETRIC DEPOSITION AND STRIPPING OF SILVER, LEAD AND COPPER AT PLATINUM ELECTRODES

ALEX R. NISBET* AND ALLEN J. BARD

Department of Chemistry, University of Texas, Austin 12, Texas (U.S.A.)

(Received June 26th, 1963)

INTRODUCTION

Recent studies have been concerned with the effect of surface oxidation and platinization on the behavior of a platinum electrode. This study is concerned with the effect of electrode pre-treatment on the deposition and stripping of metals at a platinum electrode. When a platinum electrode is oxidized, either anodically or chemically, the surface becomes covered with a film of adsorbed oxygen or platinum oxide (called for convenience throughout this paper, PtO). If this oxidized electrode is used for the chronopotentiometric reduction of a metal ion, the PtO may be completely reduced,

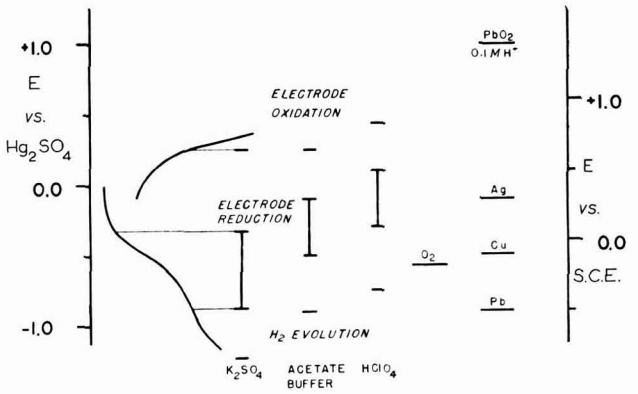

Fig. 1. Potentials for processes discussed. The left-hand scale indicates potentials *vs.* S.M.S.E., and the right-hand scale shows the same potentials *vs.* S.C.E.
Deposition of metals. These potentials may vary (in this work) up to 0.1 V, depending on the metal-ion concentration and on the electrode pre-treatment.
Reduction of oxidized platinum surface. These values were obtained from chronopotentiograms taken at about 80 $\mu A/cm^2$, one of which is shown. At higher current densities the values will be more negative.
Oxidation of platinum surface. As can be seen from the anode potential–time curve shown, the point at which the oxidation process can be said to begin is not well-defined.
Reduction of oxygen on a platinum electrode which has not recently been oxidized. This potential is independent of the pH of the solution over the pH range studied.

* Present address: Department of Chemistry, Ouachita Baptist College, Arkadelphia, Arkansas, U.S.A.

partially reduced, or unreduced before deposition of the metal occurs. Since the potential for the reduction of PtO is pH-dependent, the case which describes the deposition of a particular metal depends upon the pH of the solution. The approximate potentials for the formation and reduction of PtO and for the deposition of the metals studied are shown in Fig. 1. The anodic stripping of deposited metals also depends upon the state of the platinum electrode surface. If the last few mono-layers of metal are anodically stripped at sufficiently positive potentials, oxidation of the platinum electrode may be encountered before all of the metal is removed. Furthermore, this study indicates that metal deposited on top of PtO, or at different sites on the electrode surface, may be removed only at potentials much more positive than those characteristic of the oxidation of the bulk metal.

EXPERIMENTAL

Chronopotentiograms were recorded with a Varian G-10 recorder with 50-mV span and one-sec full-scale balancing time; the input was taken from a voltage divider which placed about 0.9 MΩ between the working and reference electrodes. The current source consisted of either three or four 90-V B batteries in series with appropriate resistances. Precise current measurements were made by measuring the voltage across a General Radio GR-500 precision resistor in the electrolysis circuit with a Leeds and Northrup Model 7651 potentiometer.

The working electrodes in most experiments were platinum discs in glass shields oriented downward[1]. The reference electrodes were equipped with salt bridges with constricted tips pointing upwards; the end of the reference-electrode tip was placed inside the working-electrode shield so as to minimize the contribution of iR drop to the measured potentials. Mercury–mercurous sulfate reference electrodes with either saturated K_2SO_4 or 0.5 F H_2SO_4 as electrolyte (S.M.S.E.) were used, except that a saturated-calomel electrode (S.C.E.) was used for most work with lead. The difference in the potentials of the Hg_2SO_4 electrodes is negligible in this work. The auxiliary electrode was a one-inch square of platinum foil. The electrolytic cell had two compartments connected by a fritted-glass disc; thus the auxiliary electrode was isolated so that its products did not contaminate the solution at the working electrode. The working-electrode compartment had a volume of about 200 ml; the decrease in concentration due to the taking of one chronopotentiogram was from 1–10 parts/10,000. The cell compartments were closed with rubber stoppers, and the stopper in the working-electrode compartment was coated with paraffin.

Unless otherwise stated, all solutions were de-aerated for at least 15–20 min by bubbling with nitrogen and stirring, and during the work nitrogen was passed over the surface of the solution. All work was done at 25.0°. The stirring of the thermostatic bath was stopped at least one minute before the taking of a chronopotentiogram, and before each one was recorded the solution was stirred and allowed to become quiet for one minute. Stock solutions 0.050 M in metal ion were prepared by direct weighing of reagent-grade salts.

SILVER

Deposition

The cathodic chronopotentiograms for the deposition of silver at pre-oxidized and pre-plated electrodes are shown in Fig. 2. In a neutral solution (Curve 1), deposition

of silver begins before reduction of PtO; the transition is not sharp, because PtO reduction immediately follows silver-ion reduction. The additional wave noted at both pre-oxidized and pre-plated electrodes is probably due to residual oxygen in the solution. In a solution buffered at about pH 4.8 with acetic acid and potassium acetate, reduction of PtO and silver ion occur at about the same potential, and a single long wave is obtained for both processes (Curve 2). Reduction of PtO occurs before deposi-

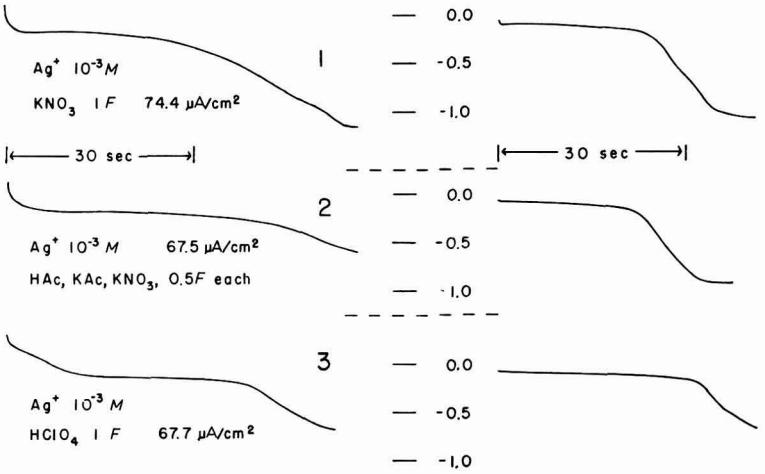

Fig. 2. Chronopotentiometric reduction waves of silver taken with pre-oxidized electrodes and pre-plated electrodes.

tion of silver from 1 F $HClO_4$ (Curve 3), and a wave corresponding to the reduction of about one-half of the PtO precedes the silver-deposition wave. The remaining oxidized platinum is reduced during the transition, thus causing the potential break to be less sharp than it is on a pre-reduced electrode. In all cases the potential break is sharper at a pre-plated electrode. Sharper breaks are also found with an electrode which is reduced by shorting it to a mercurous-sulfate electrode. This procedure reduces a large part of the PtO as shown by the absence of the PtO-reduction wave for such an electrode when it is cathodized in a silver-free solution.

Anodic dissolution

When the product of the electrode reaction is insoluble and is deposited on the electrode, reversal of the current at any time up to the transition time should lead to a reverse transition time equal to the first deposition time. When the deposition reaction is continued past the transition, the current efficiency for metal plating falls below 100%, and the stripping transition time τ_s is shorter than the deposition time and can be calculated from the following equation:

$$\tau_s = \frac{t}{2} + \frac{2}{\pi}(\tau t')^{1/2} + \frac{t}{\pi}\arcsin\frac{\tau - t'}{t} \qquad (1)$$

where t is the time from the start of the electrolysis, τ is the cathodic transition time,

and $t' = t - \tau$. This equation is equivalent to one obtained by REINMUTH[2] and can be shown to be equivalent to the expression of ANSON AND LINGANE[3].

However, the anodic transition time was found to depend upon the pre-treatment of the electrode. In the case of silver in 1 F $HClO_4$, precise agreement of the plating time and the stripping time (as measured to the first potential rise) was obtained for several minutes after the electrode was subjected to the following treatment. The electrode was placed in a cell containing 1 F $HClO_4$ and fitted with auxiliary and reference electrodes. A biased a.c. voltage was applied such that the peaks of the potential, as observed with an oscilloscope, were at +0.4 and −0.6 V *vs.* S.M.S.E. This condition was maintained for one minute, and then the electrode was reduced almost to the point of hydrogen evolution. The peak potentials were chosen to be in the vicinity of those for oxidation of platinum and evolution of hydrogen, respectively. The beneficial effect is lost within an hour and is destroyed by oxidation of the electrode. According to ANSON AND KING[4] this treatment lightly platinizes the electrode.

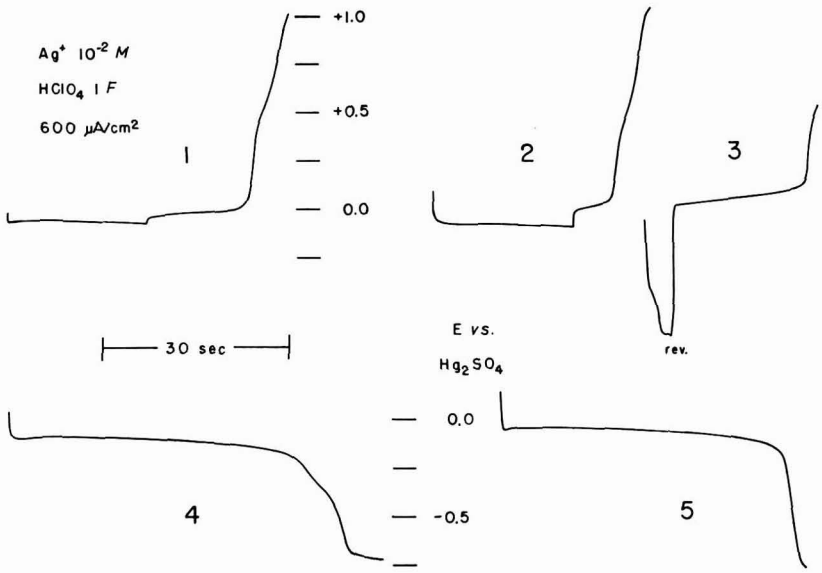

Fig. 3. Retention of silver: (1), cathodization followed by reversal, not preceded by strong oxidation (electrode was previously anodized to about +0.4 V); (2), plating/stripping cycle repeated for the fifth time; (3), in silver-free solution of 1 F $HClO_4$; (4), chronopotentiogram recorded with electrode which had been subjected to four plating/stripping cycles, as above; (5), normal chronopotentiogram.

When silver was deposited on an oxidized electrode, stripping times shorter than the deposition times were observed. For example, when silver was deposited from 1 F $HClO_4$ on to an electrode which had been anodically pre-oxidized, part of the cathodic process was due to reduction of PtO, and the stripping time was less than the plating time (Curve 1, Fig. 3). After the first oxidation to +1.0 V *vs.* S.M.S.E., the electrode was again plated (for less than the transition time) and stripped; the stripping time was short by an amount too large to be accounted for by the preceding

oxidation. Repetition of the plating/stripping process without cathodic transitions and with anodization to +1.0 V each time gave shorter and shorter anodic stripping times for the same cathodic deposition time (Curve 2, Fig. 3). Anodization of the electrode immediately following the last anodization, either in the test solution or in silver-free 1 *F* $HClO_4$, led to a rapid rise of the potential to +1.0 V.

Since the stripping times were so much shorter than the deposition times, the question then arose as to what had happened to the deposited silver. The following experiment showed that silver was still on the electrode after the anodic stripping. The electrode was removed, washed, cathodically reduced in 1 *F* $HClO_4$, and then anodized (Curve 3, Fig. 3). An anodic stripping wave at potentials characteristic of silver oxidation was obtained. Alternately, if the cathodic deposition was allowed to proceed through a transition (Curve 4, Fig. 3), an anodic stripping wave was obtained which was longer than would be expected from the cathodic wave. A spectrophotometric analysis for silver in a stripping solution which was initially silver-free showed that the additional anodic wave was indeed due to silver. A close correspondence between the amount of silver found spectrophotometrically and the amount calculated from the anodic wave($i\tau$) was obtained. A reduction wave at about −0.4 V corresponding to as much as 1 mC/cm^2 was obtained on both the cathodization wave of an oxidized electrode bearing retained silver (Curve 3, Fig. 3) and the complete deposition wave (Curve 4, Fig. 3). Only after reducing the electrode through this wave was the stripping of the retained silver possible. The amount of silver represented by the stripping wave in Curve 3, Fig. 3 is about 12 mC/cm^2, corresponding to at least sixty monatomic layers of silver on a smooth electrode.

A mechanism consistent with the observations is as follows. Deposition of silver from 1 *F* $HClO_4$ occurs before all of the PtO is reduced. Therefore, some silver is deposited on reduced portions of the electrode and some on oxidized sites. Upon anodization only silver on the reduced sites is stripped at the usual potentials, while silver on the oxidized sites is retained. Upon cathodization of the electrode, or when the chronopotentiometric deposition wave is carried through the second wave at −0.4 V, the underlying PtO is reduced. (The potential of −0.4 V is more negative than is usual for the reduction of PtO; the reason is probably the overlying silver). With the PtO reduced, the silver can be removed by anodization. This explanation imparts rectifying properties to the Pt–O–Ag junction. An alternative explanation[5] can be based on the reaction of PtO and silver metal on the electrode surface to form platinum metal and silver oxide (presumably Ag_2O). This silver could then not be removed upon anodization (*i.e.*, would be apparently retained). Cathodization would reduce the Ag_2O to silver metal, which could be removed by anodization. Two objections can be raised to this argument. First, Ag_2O is readily soluble in 1 *F* $HClO_4$. Also, the amount of retained silver recovered upon anodization following cathodization was much greater that that corresponding to the cathodic transition (Curve 3, Fig. 3) and was up to ten times the amount to be expected from the conversion of silver to silver oxide by a completely oxidized platinum surface. In order to show that the retention of silver is not due to entrapment in cracks between the electrode and its glass mounting[6], a series of experiments was performed with a platinum foil electrode attached to a platinum wire with no glass mounting. The cathodic wave at −0.4 V and the following anodic wave at 0.0 V were still observed.

Anodic chronopotentiograms for the stripping of silver from platinum into 1 *F*

$HClO_4$ show a wave at about +0.5 V. Oxidation of a bare platinum electrode in a silver-free solution of $HClO_4$ results in a wave in the same place, but the quantity of charge is smaller. The wave can amount to as much as 3 mC/cm² if the electrode is plated with silver and stripped to a potential of +0.5 V or less several times, and the wave is noticeably lenghtened by one such plating/stripping cycle. Thus the wave at +0.5 V is due partly to silver being dissolved; this dissolution is incomplete, however, since retained silver can be found after oxidation to +1.0 V. Immediate re-oxidation of the electrode gives a rapid rise to + 1.0 V, but if it is allowed to stand on open circuit for one minute, there is evidence of the wave at +0.5 V. Retention of silver deposited from 1 *F* KNO_3 (as evidenced by unusually long stripping waves) was also observed but was not studied in detail.

LEAD

Deposition

Lead deposits from 0.1 *F* $HClO_4$ at a potential very close to that for hydrogen ion reduction on platinum, and no clear wave is obtained (Curve 1, Fig. 4). Deposition of lead and reduction of hydrogen ion occur concurrently, since an anodic wave characteristic of lead appears upon reversal of the current after any cathodization, however short. Since the overvoltage for hydrogen evolution is greater on lead than on platinum[7], a clear wave for the deposition of lead was obtained on an electrode already covered with lead (Curve 2, Fig. 4).

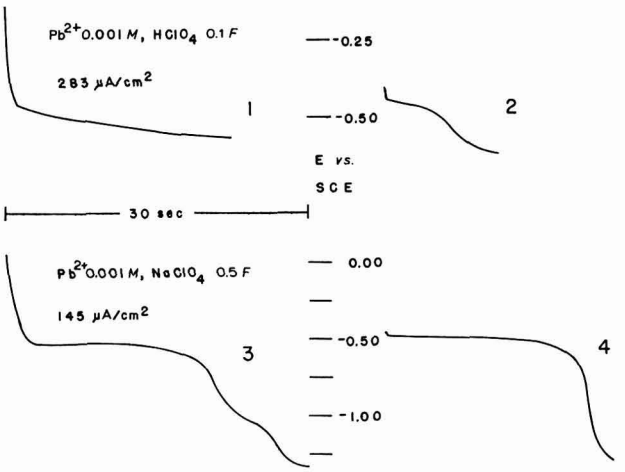

Fig. 4. Chronopotentiometric reduction waves of lead taken with weakly pre-oxidized electrodes and pre-plated electrodes.

The deposition of lead on-to a pre-oxidized electrode from 0.5 *N* $NaClO_4$ begins before all of the PtO has been reduced. A second more-or-less distinct wave at −1.0 V is found when an electrode which has been pre-oxidized to +0.25 V *vs.* S.C.E. is plated (Curve 3, Fig. 4); this wave is not found in a cathodic chronopotentiogram immediately following another one, nor is it found if the preceding anodic stripping is

stopped after the first anodic wave. This second cathodic wave is therefore apparently due to reduction of PtO underlying the deposited lead; the negative potential of this reduction as compared to the usual PtO reduction potential is caused by the overlying metal layer, as in the case of silver.

Anodic dissolution

A chronopotentiogram for the anodic dissolution of lead following deposition from 0.5 *F* $NaClO_4$ is shown in Fig. 5. Note that the final potential rise consists of three rather indistinct stages. Also shown in Fig. 5 are plots of anodization times measured to −0.38, +0.13, and +0.25 V *vs.* S.C.E. against the cathodization times preceding them. When the electrode is oxidized to +0.25 V, some oxidation of the platinum occurs. The following experiment shows that most of the anodic process up to +0.13 V is the dissolution of lead. A plated electrode was anodized to about −0.38 V; after the current was turned off, the solution was stirred and allowed to come to rest. The elec-

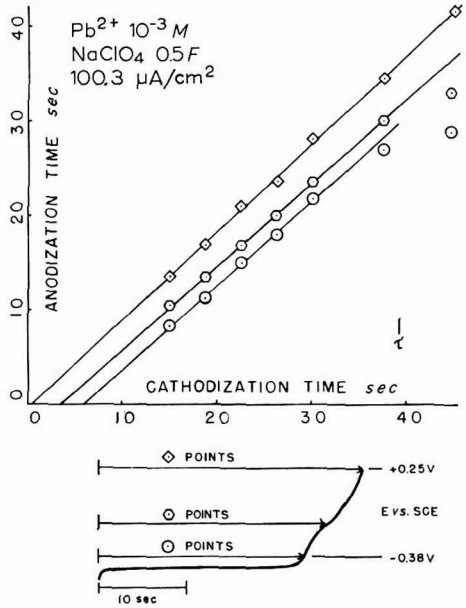

Fig. 5. Dissolution time of stripping of lead to various potentials, as a function of the preceding cathodization times, and dissolution chronopotentiogram of lead, showing potentials where measurements for data points were made.

trode was then anodized to +0.13 V, the current was reversed, and the cathodic transition time was measured. The cathodic process was the deposition of lead, part of which was dissolved from the electrode before the reversal of the current. The cathodic transition time was found to be lengthened by the same amount as that obtained by dissolving lead (during the first stripping stage) for the same length of time as was involved in the anodization to +0.13 V and then reversing the current. Therefore anodization to +0.13 V must predominantly involve stripping of lead.

The slopes of all three lines in Fig. 5 are less than unity, showing loss or retention

of deposited lead even upon anodization to +0.25 V *vs.* S.C.E. For short cathodization times, involving the deposition of lead on a bare or partially-covered platinum surface, the deposit strips only at potentials more positive than +0.13 V. Only after lead equivalent to about 0.6 mC/cm^2 has been deposited does stripping along the most cathodic plateau occur. The most cathodic plateau represents stripping of a deposit having the characteristics of bulk lead; the potential during this stage is nearly that calculated from the Nernst equation assuming unit activity of lead. Apparently lead plated on bare platinum metal is more difficult to remove than that plated on lead itself. Once the electrode is completely covered with lead, the electrode behaves as a massive lead electrode. A monatomic layer of lead on a perfectly smooth electrode would require 0.26 mC/cm^2 for its formation[8].

The top line is straight until some time after the cathodic transition time, probably because the process following the deposition of lead is the reduction of PtO, which is then re-oxidized during anodization. This explanation is also consistent with the fact that the stripping times of the later stages (between −0.38 and +0.25 V) are independent of the cathodization time for cathodization times less than the transition time, but increase for longer cathodization times. The middle and bottom lines remain straight only until the transition times. This is further evidence that the reverse of the second cathodic process (probably PtO reduction), occurs at potentials more positive than +0.13 V. The fact that the slopes are less than unity may be due to (i) retention of lead which would come off at more positive potentials, (ii) mechanical loss of deposited lead, or (iii) attack of the lead deposit by dissolved oxygen not removed by de-aeration.

No comparison of cathodic *vs.* anodic quantities of charge can be made for lead in acid solution, since hydrogen-ion reduction accompanies the deposition of lead until the electrode is extensively covered with lead, and since hydrogen ion attacks lead. The shape of the dissolution potential–time curve is similar to that obtained in neutral solution. Since PtO is reduced well before the deposition of lead in acidic solutions, the occurrence of several stages in the dissolution process in both acid and neutral solution is probably not due to deposition on top of PtO.

COPPER

Deposition

Cathodic chronopotentiograms for the deposition of copper at pre-oxidized and pre-plated electrodes are shown in Fig. 6. In general, waves obtained with copper are less reproducible than those of silver and lead. In 0.1 *N* H_2SO_4 a distinct wave for PtO reduction is obtained before the wave for copper deposition (Curve 1, Fig. 6). In a solution buffered at about pH 5 with 0.1 *F* acetic acid and 0.1 *F* potassium acetate, the PtO reduction wave occurs first, followed by a smeared wave which is probably due to concomitant copper deposition and PtO reduction. At a reduced or pre-plated electrode, on the other hand, a sharp transition is obtained in this medium. In 1 *F* KNO_3, copper deposition occurs first, followed by a distinct wave for PtO reduction. The constancy of $i\tau^{\frac{1}{2}}$ for this wave at different current densities and the appearance of a single wave at the same potential when the electrode is replated demonstrate that the first wave is due to copper deposition. In saturated K_2SO_4 the wave for PtO reduction precedes that for copper deposition, and the potential break at the end of the deposition is less steep than on a reduced electrode, probably because of some

PtO reduction also occurring after the deposition wave. Another difference between KNO_3 and K_2SO_4 media is the potential at which hydrogen evolution occurs. In KNO_3 (and also in the acetate buffer) evolution of hydrogen after copper deposition occurs at -1.0 V *vs.* S.M.S.E., while in K_2SO_4 the process occurs at -1.5 V.

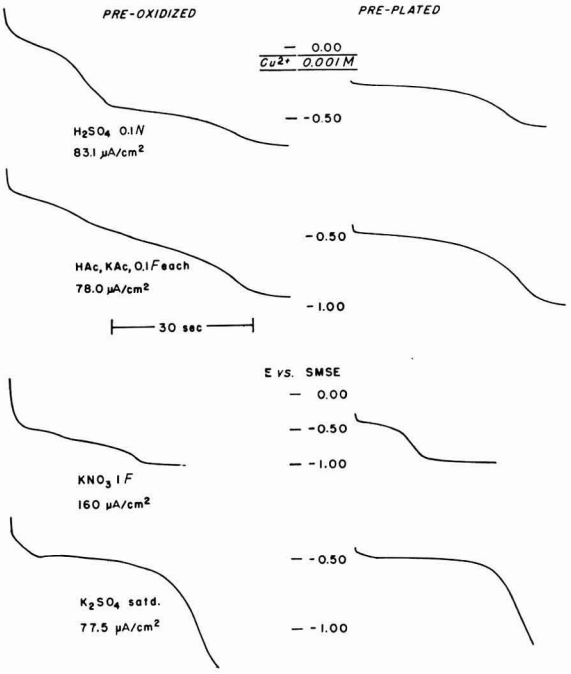

Fig. 6. Chronopotentiometric reduction waves for copper taken with strongly pre-oxidized electrodes and pre-plated electrodes.

Anodic dissolution

A chronopotentiogram for the anodic dissolution of copper after deposition from an acetate buffer solution is shown in Fig. 7. As with lead the final potential rise is characterized by rather indistinct stages. Also shown in Fig. 7 are plots of anodic transition times measured to -0.35, -0.31, and 0.00 V *vs.* S.M.S.E. against the cathodization times preceding them. The potential 0.00 V is the point of maximum slope of the curve before oxidation of the electrode begins. The top line has a slope of 0.95 and passes through the origin; thus the stripping time is 0.95 of the cathodization time preceding it. The middle and bottom lines have slopes of 0.93 and 0.85, respectively. As in the case of lead, the explanation of the small slope may involve concurrent reduction of residual oxygen, mechanical loss of deposited metal, or the retention of metal which would come off at more positive potentials. The slope of the bottom line is best explained as due to retention, since the other lines have larger slopes; oxidation of the electrode does not occur between -0.35 and -0.31 V.

The middle and lower lines have intercepts on the horizontal axis which are equi-

valent to 0.27 and 0.39 mC/cm², respectively. Therefore, the copper deposited on a bare or partly-covered electrode is oxidized only at more positive potentials. For comparison, 0.49 mC/cm² would be required for a monatomic layer of copper on a perfectly smooth electrode[8].

In 0.1 N H_2SO_4 a similar plot, for anodization to +0.25 V, yields a line with a slope of 1.00 and a horizontal intercept equivalent to 0.19 mC/cm². This intercept probably represents reduction of PtO formed during the anodization. A plot for a 0.5 F $KHSO_4$–0.5 F K_2SO_4 medium yields a horizontal intercept of as much as 2.5 mC/cm².

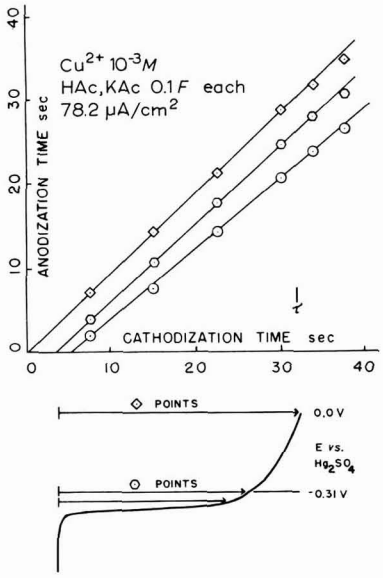

Fig. 7. Dissolution times, for stripping of copper to various potentials, as a function of the preceding cathodization times and dissolution chronopotentiogram for copper, showing potentials where measurements for data points were made.

DISCUSSION

The presence of a PtO film has been shown to hinder electro-reductions[9] and -oxidations at platinum electrodes[10]. The present work is consistent with these findings. In the cases in which the metal deposits before reduction of the PtO, the potential at which the metal deposits on the PtO-covered electrode is usually found to be slightly more cathodic than that for deposition at a reduced electrode.

A decrease in reversibility of the silver-dissolution reaction at an electrode bearing a PtO film was also suggested as an explanation of failure of some of the silver to dissolve at the potential for the oxidation of the bulk of silver. This explanation, however, cannot be used for copper and lead, since the electrode is completely reduced when their deposition starts from acidic solutions. A possible explanation in these cases is that it is more difficult to remove a lead or copper atom from a platinum surface than from the surface of the bulk metal itself. This explanation is in accord with the observation that incomplete layers of most metals on platinum have less than unit activity. The occurrence of several indistinct waves in the final potential rise during the

anodic stripping of lead and copper is perhaps suggestive of more than one kind of surface site on the platinum. Recent studies[4,11] have shown that some reactions occur with less overpotential at a platinized-platinum electrode than at an aged reduced electrode. This has led to speculation that edges, corners, and dislocations and other imperfections in crystals form more active sites than the crystal faces, in accord with ideas held for catalysts in heterogeneous kinetics. The differences in potential for removal of copper and lead might represent the differences in energy required to remove an atom from a face, a corner or imperfection of the platinum.

In this work, more or less pronounced negative maxima were found at the beginnings of plating curves when all or part of the electrode was still oxidized when deposition started (*e.g.*, Curve 3, Fig. 4). These maxima were quite pronounced in some cases and could be observed on a oscilloscope as well as with a graphic recorder. One explanation for these negative maxima is the same as that given by ANSON AND KING[4] for those found during the reduction of vanadate; reduction occurs less reversibly on PtO. The potential initially drops to a value characteristic either of PtO reduction or of deposition of the metal on PtO. When the PtO is reduced, or is covered with metal, the deposition occurs at a less negative potential, and thus the potential of the electrode rises. SCHOTTKY[12] interpreted the negative maxima at the beginnings of deposition curves as evidence of the onset of nucleation of the adsorbed atoms of the deposited metal. The observed retention of metals has implications in the anodic stripping of metal films for film-thickness determinations. A significant amount of the metal may not be removed from the base metal at the final potential rise especially for very thin films; for thicker films the amount of retained metal may be negligibly small compared to the total amount removed. This work may explain the findings of EHLERS AND SEASE[13], who constructed a coulometer in which the current to be integrated was made to deposit copper which was then redissolved at constant current; the quantity of charge was calculated from the constant current value and the dissolution time was measured to a sudden increase in the potential. They reported that the potential break was not sharp for current densities below 5 mA/cm^2 and that for current densities between 5 and 100 mA/cm^2 the efficiency, $Q_{\text{stripping}}/Q_{\text{passed}}$, was 0.997.

LORD *et al.*[14] deposited silver potentiostatically at 0.00 V *vs.* S.C.E. from 0.1 *N* acid and then redissolved it with a linear voltage scan from 0.00 to + 1.00 V; by this method they were able to recover only 80% of the silver placed in the solution. The deposition was continued for an hour, and the *shortage* was observed for solutions as concentrated as 10^{-3} *M*, with sufficient volume to give complete coverage of the electrode with silver. The equilibrium silver concentration at 0.00 V is 10^{-9} *M*, and certainly equilibrium was reached; hence incomplete deposition was not the reason. The authors suggest mechanical loss as the cause, but their observations are also compatible with the idea of retention of silver. No experiments using exactly their conditions were performed in this work, but the similarity of their conditions to those which led to the retention of large amounts of silver should be noted.

ACKNOWLEDGEMENT

The authors are grateful for financial support for this work from The ROBERT A. WELCH Foundation and also to the National Science Foundation, the Humble Oil and Refining Company, and the Socony Mobil Oil Company for graduate fellowships held by one of us (A.R.N.) at various times during the course of the work.

SUMMARY

The effect of pre-treatment (pre-oxidation, pre-plating, or platinization) of a platinum electrode on the chronopotentiometric deposition and stripping of silver, lead and copper in various media is considered. Depositions were found to occur less reversibly at a pre-oxidized electrode. Evidence for retention of some deposited metal, even at potentials considerably more positive than the reversible stripping potential is presented and possible mechanisms for this retention are suggested.

REFERENCES

1 A. J. BARD, *Anal. Chem.*, 33 (1961) 11.
2 W. H. REINMUTH, *ibid.*, 33 (1961) 485.
3 F. C. ANSON AND J. J. LINGANE, *J. Am. Chem. Soc.*, 79 (1957) 1015.
4 F. C. ANSON AND D. M. KING, *Anal. Chem.*, 34 (1962) 362.
5 S. BRUCKENSTEIN, private communication.
6 C. R. CHRISTENSEN AND F. C. ANSON, *Anal. Chem.*, 35 (1963) 205.
7 J. J. LINGANE, *Electroanalytical Chemistry*, Interscience Publishers, Inc., New York, 2nd ed., 1958, p. 209.
8 M. M. NICHOLSON, *J. Am. Chem. Soc.*, 79 (1957) 7.
9 F. C. ANSON, *J. Electrochem. Soc.*, 110 (1963) 436, and references given therein.
10 F. C. ANSON, *Anal. Chem.*, 33 (1961) 934.
11 A. J. BARD, *ibid.*, 35 (1963) 1602.
12 W. F. SCHOTTKY, *Z. Physik. Chem. (Frankfurt)*, 31 (1962) 40.
13 V. B. EHLERS AND J. W. SEASE, *Anal. Chem.*, 26 (1954) 513.
14 S. S. LORD, R. C. O'NEILL AND L. B. ROGERS, *ibid.*, 24 (1952) 209.

THE REDUCTION MECHANISM OF PERMANGANIC ION IN MINERAL ACID MEDIA

PIER GIORGIO DESIDERI

Institute of Analytical Chemistry, University of Florence (Italy)

(Received July 12th, 1963)

INTRODUCTION

The reduction mechanism of permanganic ion in sulphuric acid and caustic alkali media with a bubbling platinum electrode[2] was investigated in a previous study[1]. The results obtained in sulphuric acid suggested that the investigation should be extended also to perchloric and nitric acid media to obtain a wider view of MnO_4^- reduction mechanism in acid media. The influence of manganous ions on the permanganic ion reduction was studied using polarographic, coulometric and spectrophotometric methods. The results obtained have enabled us to explain the rôle of Mn(II) and Mn(III) ions in the permanganate reduction mechanism and to explain why the permanganate oxidation potential can decrease in the presence of large amounts of Mn(II) ions and strong ligands of Mn(III), as in the case of Fe(II) titrimetry according to ZIMMERMANN–REINHARDT[3].

EXPERIMENTAL

Apparatus and reagents

An AME polarograph was used for the polarographic measurements and an AMEL Corrograph potentiostat–amperostat with an electronic current integrator was used for the controlled potential reductions. The absorption measurements were made using 1 cm silica cells with a Beckmann DU spectrophotometer.

The standard permanganate solution was prepared according to BLUM[4], by dissolving weighed portions of recrystallized, pure potassium permanganate in water. The freshly prepared solution, after prolonged boiling, was filtered through sintered glass and standardized with sodium oxalate.

Sulphuric, nitric and perchloric acid solutions were prepared by diluting the concentrated reagents and were standardized by the usual analytical methods. The nitric and perchloric solutions of Mn(II) were prepared by dissolving portions of $MnCO_3$ in the respective acids. The solutions obtained were standardized potentiometrically with $KMnO_4$ in sodium pyrophosphate media. To prevent permanganic ion reduction by chloro-ions and agar-agar, expecially at high acid concentrations, a potassium/silica-gel bridge was used instead of a KCl/agar-agar bridge.

The half-wave potential values were referred to a S.C.E. A bubbling smooth platinum electrode was used. The platinum spherule was 2.0 mm in diameter.

RESULTS AND DISCUSSION

The permanganic ion is reduced irreversibly to Mn(II) on the bubbling smooth platinum electrode in mineral acid media. In sulphuric, nitric and perchloric acids the reduction occurs in the potential range +0.6 to +1.3 V *vs.* S.C.E. and the wave slope, calculated from the $\log[i/(i_d - i)]/E$ ratio is, for the three acids, from 60–100 mV (Table 1). Such a high value of the slope confirms that the permanganic ion reduction process

TABLE 1

POLAROGRAPHIC VALUES OF $1 \cdot 10^{-3}$ *N* MnO_4^- IN MINERAL ACID MEDIA, AT 25°

Concn. (equiv.)	H_2SO_4 I_d (μA)	$\log \frac{i/(i_d-i)}{E}$ (*mV*)	*Concn.* (equiv.)	HNO_3 I_d (μA)	$\log \frac{i/(i_d-i)}{E}$ (*mV*)	*Concn.* (equiv.)	$HClO_4$ I_d (μA)	$\log \frac{i/(i_d-i)}{E}$ (*mV*)
$1.0 \cdot 10^{-2}$	9.40	120	$1.0 \cdot 10^{-2}$	10.81	72	$1.0 \cdot 10^{-2}$	11.13	85
$2.5 \cdot 10^{-2}$	9.45	100	$2.5 \cdot 10^{-2}$	10.91	75	$2.5 \cdot 10^{-2}$	11.46	77
$5.0 \cdot 10^{-2}$	9.31	90	$5.0 \cdot 10^{-2}$	11.20	72	$5.0 \cdot 10^{-2}$	11.46	75
$7.5 \cdot 10^{-2}$	9.50	90	$7.5 \cdot 10^{-2}$	11.57	72	$7.5 \cdot 10^{-2}$	11.50	75
$1.0 \cdot 10^{-1}$	9.35	90	$1.0 \cdot 10^{-1}$	11.35	70	$1.0 \cdot 10^{-1}$	11.35	72
$2.5 \cdot 10^{-1}$	9.31	90	$2.5 \cdot 10^{-1}$	11.20 n	73	$2.5 \cdot 10^{-1}$	11.24	72
$5.0 \cdot 10^{-1}$	9.57	87	$5.0 \cdot 10^{-1}$	11.00	75	$5.0 \cdot 10^{-1}$	10.50	77
$7.5 \cdot 10^{-1}$	9.40	90	$7.5 \cdot 10^{-1}$	10.46	73	$7.5 \cdot 10^{-1}$	10.85	73
1.0	9.31	92	1.0	10.80	75	1.0	10.30	70
2.0	8.21	84	2.0	9.82	75	2.0	9.55	75
3.0	7.42	84	3.0	9.08	75	3.0	8.35	65
4.0	7.00	80	4.0	7.92	70	4.0	7.71	65
5.0	6.30	80	5.0	7.10	70	5.0	6.26	65
6.0	5.91	80	6.0	6.34	65	6.0	4.85	68
7.0	5.60	80	7.0	5.54	63	7.0	2.32	60
8.0	4.93	80	8.0	5.06	60	8.0	1.04	60
9.0	4.77	80	9.0	4.23	60			
10.0	4.54	80	10.0	4.01	60			
11.0	4.01	80						
12.0	3.77	78						
13.0	3.45	81						
14.0	2.95	82						
15.0	2.57	80						
16.0	2.09	80						

t = 3.64 sec.

is markedly irreversible. With increase in acid concentration the half-wave potential shifts to more positive potential values, as can be observed in Fig. 1. However $E_{\frac{1}{2}}$ has a quite different behaviour in the three acids especially at high acid concentrations. For low acid concentrations the half-wave potentials in perchloric acid are intermediate between the $E_{\frac{1}{2}}$ values in nitric and sulphuric acids, but as the acid concentration increases permanganate shows a greater oxidation potential in $HClO_4$ than in the other two acids. On the other hand, at high acid concentrations, the diffusion current intensity of MnO_4^- is lower in $HClO_4$ than in the other two acids (Table 1). The current decrease in more concentrated solutions of the three acids cannot be explained by the increase of ionic activity and the formation of associated permanganate–anion species (which may be found only in high H_2SO_4 concentrations) alone; it is evident

that $KMnO_4$ is partially decomposed with evolution of oxygen and formation of intermediate ionic species between permanganic and Mn(II) ions.

The polarographic waves for high acid concentrations, particularly sulphuric acid, are not well developed, because they critically depend upon increase in medium viscosity; coulometric and spectrophotometric methods of investigation have therefore been used. The electrolytic controlled-potential reductions were made on 50 ml of a

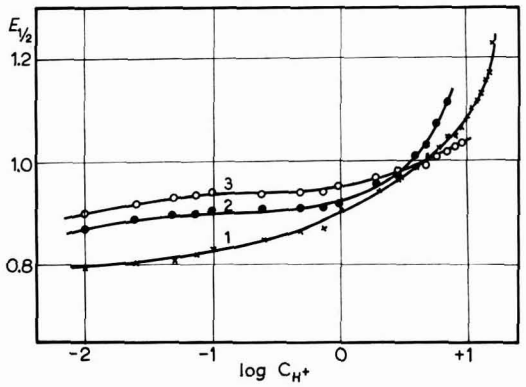

Fig. 1. Half-wave potential changes as acid concn. increases, for $1 \cdot 10^{-3}$ N MnO_4^-, at 25°: (1), in H_2SO_4; (2), in $HClO_4$; (3), in HNO_3.

TABLE 2

CONTROLLED-POTENTIAL COULOMETRY ON 50 ml OF 1 mM MnO_4^- IN H_2SO_4 MEDIA, AT 25°, AT A POTENTIAL OF +0.4 V *vs.* S.C.E.

H_2SO_4 concn. (M)	*Coulomb No.*
$1.0 \cdot 10^{-2}$	23.86
$5.0 \cdot 10^{-2}$	23.42
$1.0 \cdot 10^{-1}$	24.60
$5.0 \cdot 10^{-1}$	24.60
1.0	24.21
2.0	24.50
3.0	23.63
4.0	23.00
5.0	23.00
6.0	22.40
7.0	20.20
8.0	18.60
9.0	16.40
10.0	15.40
11.0	11.20
12.0	10.40
13.0	10.40
14.0	10.40
15.0	10.43
16.0	10.45
17.0	10.42
18.0	10.50

$1 \cdot 10^{-3}$ M $KMnO_4$ solution containing varying amounts of acid. These solutions were reduced at a controlled potential of +0.4 V *vs.* S.C.E. The results obtained in sulphuric media are shown in Table 2. It can be seen that for the acidity range $1 \cdot 10^{-2}$ M–4 M, about 24 C are used by the solution. This value is in very good agreement with the theoretical value of 24.2 C for a 5-electron reduction:

$$Mn(VII) + 5e \rightarrow Mn(II)$$

For acid concentrations greater than 4 M there is a marked increase in the half-wave potential and a large decrease in diffusion current; the number of the coulombs used begins to diminish until at acid concentrations greater than 12 M a constant value is reached. With the decrease in the amount of electricity used, the colour of the various solutions changes. For sulphuric acid concentrations greater than 10 M the solutions change colour from the red-violet characteristic of permanganic ion, to a reddish colour and then through yellow-brown, yellow-lemon finally to a green yellow colour in concentrated H_2SO_4. The spectra of several sulphuric solutions in the acidity range 10–18 M illustrated in Fig. 2 show that as the acidity increases the spectra charac-

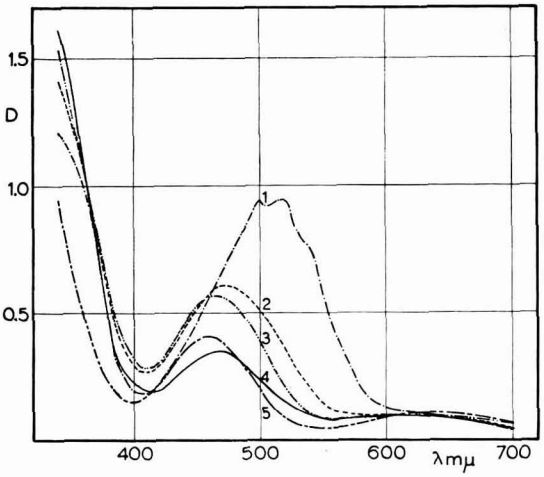

Fig. 2. Absorption spectra of $1 \cdot 10^{-3}$ M MnO_4^- in various concns. of H_2SO_4: (1), 10 M; (2), 12 M; (3), 14 M; (4), 16 M; (5), 18 M.

teristic of MnO_4^- ion disappear. All MnO_4^- solutions in H_2SO_4, including that in concentrated H_2SO_4, when diluted with water return to the original red-violet colour; it is evident however, that at high acid concentrations the permanganic ion is strongly associated with SO_4^{2-} ions to form complex ions. These complex ions have little ionic mobility and their spectral properties are quite different from the MnO_4^- ion.

The decrease in the concentration of oxidant as the sulphuric acidity changes, confirmed also by chemical methods, may be evidence for the relative stability of $KMnO_4$ in concentrated strong acids. In fact in these media $KMnO_4$ has a marked tendency to decompose with evolution of oxygen. This reaction is promoted by a temperatare increase, so that, to obtain reproducible titres for MnO_4^- solutions we

have had to operate constantly at a temperature of 0°. The values, (see Table 3), obtained in the reduction of a $1 \cdot 10^{-3}$ *M* MnO_4^- solution in nitric and perchloric acids are similar to the values obtained in H_2SO_4. The data for $HClO_4$ are obtained at a controlled-potential of +0.4 V *vs.* S.C.E. while those in HNO_3 are obtained at this potential only at acid concentrations lower than 3 *M*. For acid concentrations greater than 3 *M*, because of the discharge of the supporting electrolyte at this potential, the reduction wave has been carried out at more positive potentials, which are fixed for each acid concentration.

TABLE 3

CONTROLLED-POTENTIAL COULOMETRY ON 50 ml OF 1 m*M* MnO_4^- IN $HClO_4$ AND HNO_3 MEDIA, AT 25°

HNO_3 concn. (M)	*Coulomb No.*	*E vs. S.C.E. (V)*	*$HClO_4$ concn. (M)*	*Coulomb No.*	*E vs. S.C.E. (V)*
$1.0 \cdot 10^{-2}$	24.30	+0.4	$1.0 \cdot 10^{-2}$	24.25	+0.4
$5.0 \cdot 10^{-2}$	24.30	+0.4	$5.0 \cdot 10^{-2}$	24.45	+0.4
$1.0 \cdot 10^{-1}$	24.02	+0.4	$1.0 \cdot 10^{-1}$	24.15	+0.4
$5.0 \cdot 10^{-1}$	24.25	+0.4	$5.0 \cdot 10^{-1}$	24.30	+0.4
1.0	24.50	+0.4	1.0	24.50	+0.4
2.0	24.25	+0.4	2.0	24.25	+0.4
3.0	24.30	+0.4	3.0	24.00	+0.4
4.0	23.00	+0.4	4.0	23.00	+0.4
5.0	22.40	+0.9	5.0	22.00	+0.4
6.0	22.00	+0.9	6.0	21.00	+0.4
7.0	22.10	+0.9	7.0	19.15	+0.4
8.0	22.35	+0.9	8.0	15.00	+0.4
9.0	21.00	+1.0			
10.0	20.20	+1.0			
11.0	19.20	+1.0			
12.0	18.00	+1.02			

TABLE 4

I_d VALUES FOR $1 \cdot 10^{-3}$ *N* MnO_4^- IN 1 *N* H_2SO_4, $HClO_4$ AND HNO_3, AT 25°, FOR SEVERAL BUBBLE TIMES

t (sec)	I_{d_1} *(μA)*	I_{d_2} *(μA)*	I_{d_3} *(μA)*
3.30	9.73	10.80	11.20
3.70	9.20	10.22	10.60
4.12	8.70	9.75	10.10
4.60	8.25	9.35	9.65
5.11	8.00	8.95	9.30
5.55	7.82	8.62	9.01
5.95	7.60	8.40	8.70
6.30	7.48	8.20	8.55
6.58	7.35	8.05	8.40
7.00	7.20	7.90	8.28
7.62	6.98	7.65	8.00
8.14	6.75	7.40	7.82
8.90	6.35	7.10	7.46
9.45	6.20	6.90	7.35

I_{d_1} = H_2SO_4
I_{d_2} = $HClO_4$
I_{d_3} = HNO_3

The spectra of MnO_4^- solutions in nitric and perchloric media, show that the most absorbing species is still MnO_4^- for strong acid solutions.

The reduction of permanganic ion in the three mineral acids is a diffusion controlled process only, as shown by:

(1) the temperature coefficient of the numerical value of current which was found to be 1.3% in H_2SO_4, 1.38% in $HClO_4$ and 1.41% in HNO_3;

(2) the current changes in relation to the changes of the bubble time (Table 4) (*cf.* dropping time and bubble time change[5]).

As the acidity decreases, the half-wave potential shifts to less positive values, the wave changes its shape and the reduction process becomes more and more irreversible. In H_2SO_4, $HClO_4$ and HNO_3 media in very weakly acidic or neutral solutions, the polarographic wave divides itself into two or more steps, and at the same time a layer of MnO_2 is deposited on the platinum electrode.

The rôle of Mn(II) in the permanganate reduction

The stability of $KMnO_4$ aqueous solutions in presence of manganous ions is related to the Guyard reaction[6,7]

$$2MnO_4^- + 3Mn^{2+} + 2H_2O \rightleftarrows 5MnO_2 + 4H^+ \qquad (1)$$

The mechanism of the reaction, according to ADAMSON[8], involves a rapid pre-equilibrium between MnO_4^- and Mn(II) with formation of two intermediate species

$$MnO_4^- + 3Mn^{2+} + 6H^+ \rightleftarrows 3Mn^{3+} + MnO^{2+} + 3H_2O \qquad (2)$$

Reaction (1) is essentially instantaneous in neutral solution and its rate decreases markedly with increasing acidity. Reaction (2), on the other hand, should be promoted by strong acid conditions. The object of our investigation is to explain the mechanism of equilibrium (2) in terms other than acidity, anion type and concentration of Mn(II) ions.

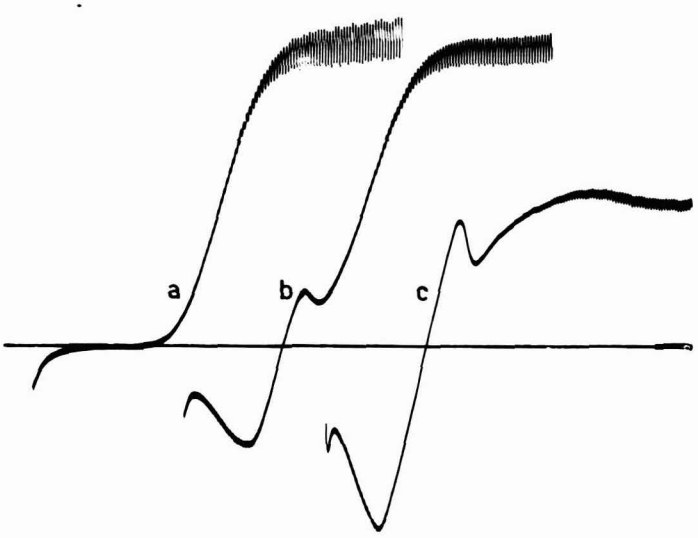

Fig. 3. Polarographic waves of MnO_4^- and Mn^{2+} in 1 *N* H_2SO_4: (a), 1 m*M* Mn^{2+}, 1 m*M* MnO_4^-; (b), 5 m*M* Mn^{2+}, 1 m*M* MnO_4^-; (c), 10 m*M* Mn^{2+}, 1 m*M* MnO_4^-.

Since for acid concentrations lower than 1 N a red-brown precipitate of MnO_2 forms immediately on the addition of manganous ions to MnO_4^- solutions, we have limited our researches to solutions of the three acids of acidity equal to or greater than 1 N. When manganous ions are added to a MnO_4^- solution 1 N in any of the three mineral acids, the permanganic ion reduction wave is not influenced until the amount of Mn(II) ions added to the solution is lower than a fixed value of the $Mn(II)/MnO_4^-$ molar ratio. In sulphuric and nitric acids this molar ratio is 2 : 1; in $HClO_4$ it is 5 : 1. For $Mn(II)/MnO_4^-$ ratios greater than these the permanganic ion reduction wave becomes notably modified. In fact it divides into three steps, one in the anodic region, and the other two in the cathodic region.

The first of these cathodic steps has a current maximum which is accentuated, as the concentration of Mn(II) ions in the solution is increased. It is also notably influenced by the acidity of the solution and by the anion type present in the solution. In the polarograms of Fig. 3 obtained from MnO_4^- sulphuric solution curve (a) is related to a $Mn(II)/MnO_4^-$ molar ratio lower than 2 : 1, while the others have been obtained from solutions having $Mn(II)/MnO_4^-$ ratios greater than 2 : 1.

It can be seen that the cathanodic wave becomes greater as the Mn(II) concentration increases. For the same $Mn(II)/MnO_4^-$ ratio and in solutions having equal acidity the phenomenon is more pronounced in HNO_3 but in $HClO_4$ is notably reduced. The cathanodic wave begins to be observed in perchloric media only for a $Mn(II)/MnO_4^-$ ratio equal to or greater than 10 : 1 (Fig. 4). Curves (a) and (b) are related to sulphuric and perchloric media respectively; curve (c) has been obtained in nitric acid.

As the acidity of the solutions increases the cathanodic wave is reduced, the second cathodic step is reduced until it disappears and in sulphuric and perchloric acids a

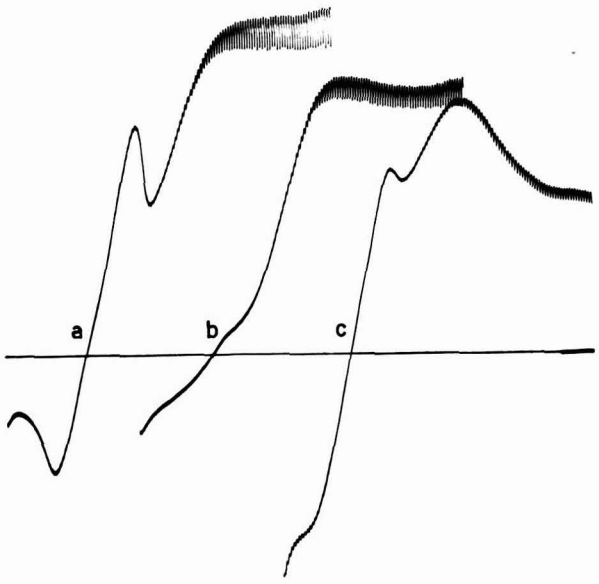

Fig. 4. Polarographic waves of 1 mM MnO_4^- and 10 mM Mn^{2+} in acid media: (a), in 1 N H_2SO_4; (b), in 1 N $HClO_4$; (c), in 1 N HNO_3.

third reduction wave appears at a potential of about +0.65 V *vs.* S.C.E. This third wave does not appear in nitric acid. At greater acid concentrations the permanganic ion reduction wave disappears almost completely while, in sulphuric and perchloric media, the reduction wave having $E_{\frac{1}{2}} = +0.65$ V *vs.* S.C.E. becomes increasingly greater and the cathodic part of the cathanodic wave is reduced. This can be seen in the polarograms, shown in Fig. 5, which have been obtained from solutions having

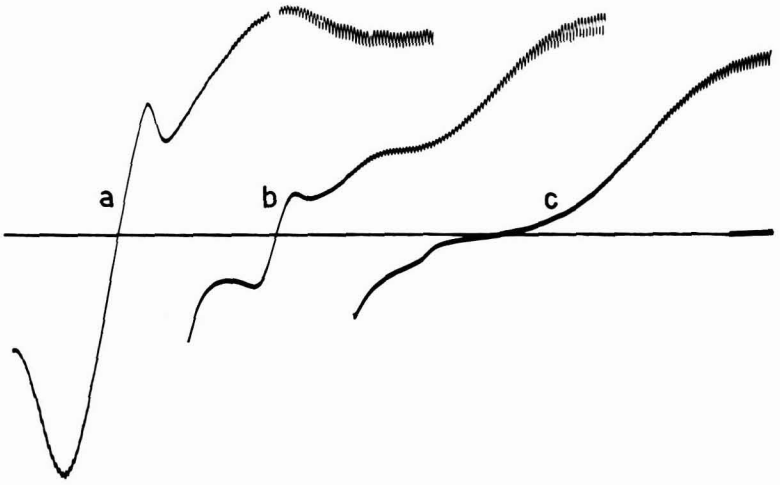

Fig. 5. Influence of H_2SO_4 concn. on the polarographic waves of 1 m*M* MnO_4^- and 10 m*M* Mn^{2+}: (a), 1 *N*; (b), 3 *N*; (c), 6 *N*.

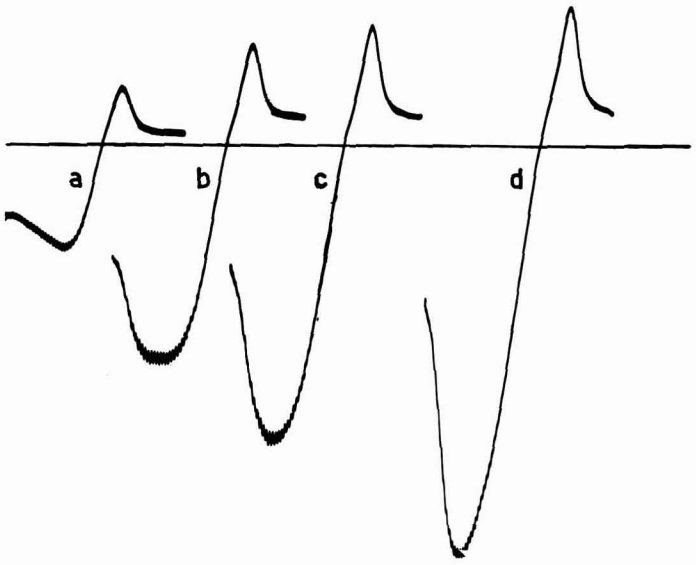

Fig. 6. Anodic waves of varying amounts of Mn^{2+} in 0.1 *M* H_2SO_4: (a), 1 m*M*; (b), 2 m*M*; (c), 3 m*M*; (d), 5 m*M*.

a constant $Mn(II)/MnO_4^-$ molar ratio but with different acidities. At the same time the colour of the solutions changes from the characteristic red-violet colour to rose in perchloric and sulphuric acids and to yellow-brown in nitric acid. It will be of interest to analyse each step to try to identify the ionic species present in the MnO_4^- strongly acid solutions of three mineral acids after the addition of Mn(II) ions.

The wave in the anodic region at a potential of +1.15 to +1.2 V *vs.* S.C.E. is supplied by oxidation of Mn(II) ions; in fact by polarographing Mn(II) solutions only, an oxidation wave which increases with increasing concentration manganous ions is obtained at the same potential. For high Mn(II) ion concentrations, (Fig. 6), a reduction wave with a current maximum appears at the same potential. The cathodic part of the cathanodic wave, identical to the one obtained from MnO_4^- solutions with added Mn(II) ions, is observed only if the polarographic curves are recorded passing from the anodic to the cathodic region. Only the anodic wave is observed when recording in the opposite direction, both in Mn(II) solutions and in Mn(II) solutions mixed with MnO_4^- (Fig. 7). The height of this unusual cathodic wave depends upon

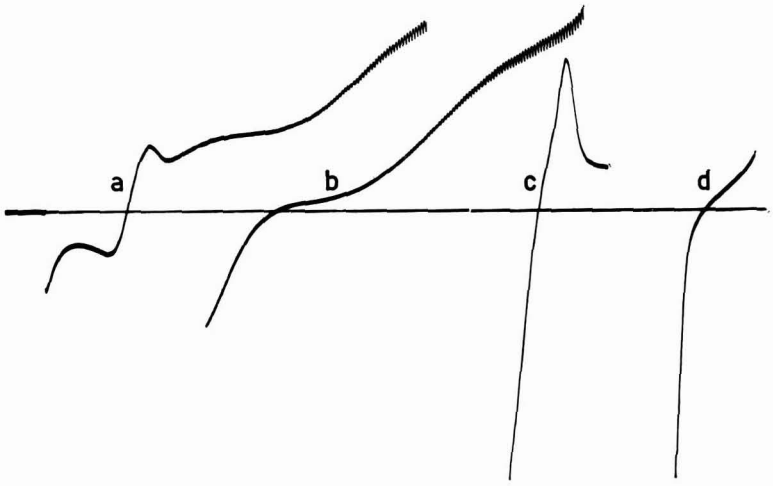

Fig. 7. Influence of polarographic recording direction on the waves of MnO_4^- and Mn^{2+} in acid media: (a), MnO_4^- 1 m*M*, Mn^{2+} 10 m*M*, H_2SO_4 3 *N*, forward recording; (b), as (a), backward recording; (c), Mn^{2+} 5 m*M*, H_2SO_4 0.1 *M*, forward recording; (d), as (c), backward recording.

the time during which the electrode potential is held at the diffusion-step potential of the anodic wave, *i.e.* upon polarogram recording rate, and upon solution acidity. In weakly acid solutions, at the step-potential of the anodic wave, a brown precipitate is deposited on the Pt electrode surface. It has oxidising properties and resembles MnO_2. If this electrode, after simple washing with distillated water is plunged into a sulphuric acid or other mineral acid solution, the oxidation wave disappears and a reduction wave with a current maximum, (although reduced in size) is formed (Fig. 8, curves (a) and (b)). Such behaviour is typical of polarographic waves due to the reduction of a surface film, which has been deposited on an electrode during a manganous ions oxidation process. The surface film can consist of H_2MnO_3 or even $MnMnO_3$; this last hypothesis is supported by the behaviour of the wave in presence of Mn(III)

ligands. It disappears on the addition of phosphoric acid to the solution as can be observed in Fig. 8, curves (c) and (d).

From experimental data it is evident however that the anodic wave corresponds to the Mn(II)–Mn(IV) oxidation process; the Mn(IV) which results, reacts with man-

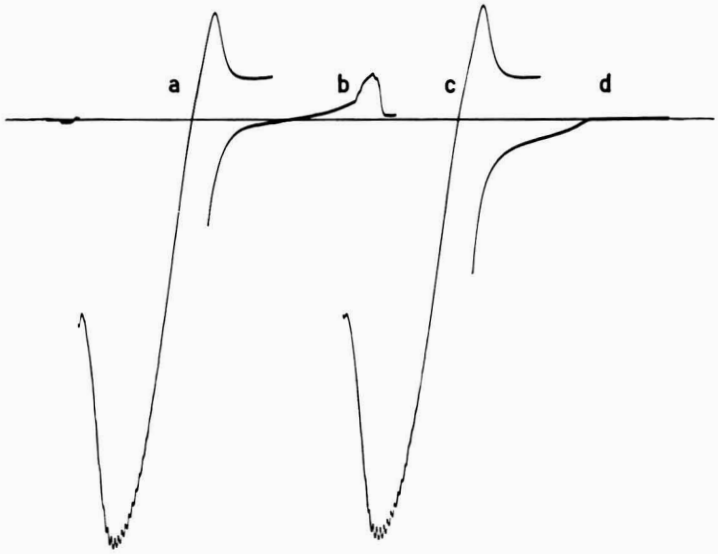

Fig. 8. Polarographic curves of $MnMnO_3$ superficial film: (a), anodic and cathodic waves of $2 \cdot 10^{-3}$ *M* Mn(II) in 0.1 *N* H_2SO_4; (b), cathodic wave obtained by plunging the platinum electrode in 0.1 *N* H_2SO_4 only; (c), Mn(II) $5 \cdot 10^{-3}$ *M*, H_2SO_4 0.3 *N*; (d), as (c), 0.1 *M* H_3PO_4.

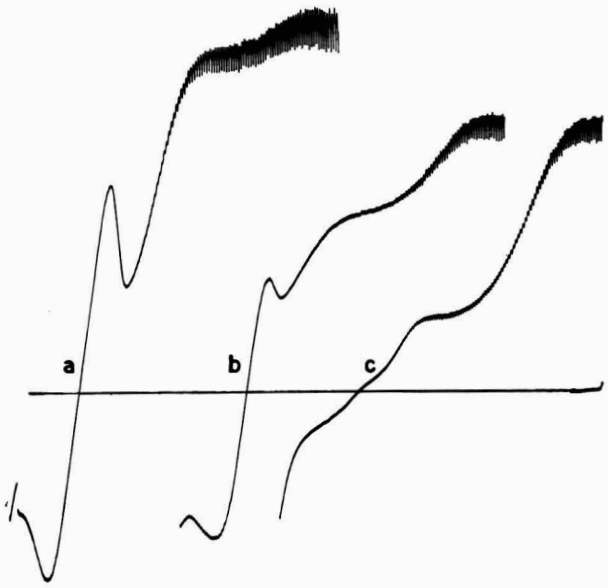

Fig. 9. Influence of the anion on the polarographic wave of $1 \cdot 10^{-3}$ *M* MnO_4^- and $10 \cdot 10^{-3}$ *M* Mn(II) in acid soln.: (a), in 3 *N* HNO_3; (b), in 3 *N* H_2SO_4; (c), in 3 *N* $HClO_4$.

ganous ions forming a superficial film the reduction of which corresponds to the cathodic part of the cathanodic wave. This explains why the cathanodic wave obtained from MnO_4^- solutions with added Mn(II) ions, depends not only upon the Mn(II)/MnO_4^- ratio and acidity but also upon the anion which is present in the solutions. In sulphuric and perchloric media the wave height is comparable but it is much greater in HNO_3 (Fig. 9). The size of the cathanodic wave depends, in fact, upon the complexing power of the acid with respect to Mn(III). This is zero for nitric acid and is of about equal value for the other two acids. The second cathodic step corresponds to the direct reduction of MnO_4^- ion to Mn(II) ion, while the third step, which appears at high acid concentrations (H_2SO_4 and $HClO_4$ only) is due to the reduction of Mn(III) ions which have been formed by direct reaction between MnO_4^- and manganous ions and which are bound in stable complexes. The presence of Mn(III) ions in sulphuric and perchloric acids has been confirmed by the following observations:

(1) In Fig. 10 are shown the absorption spectra obtained from sulphuric, perchloric and nitric solutions at equal acid concentration and with the same Mn(II)/MnO_4^-

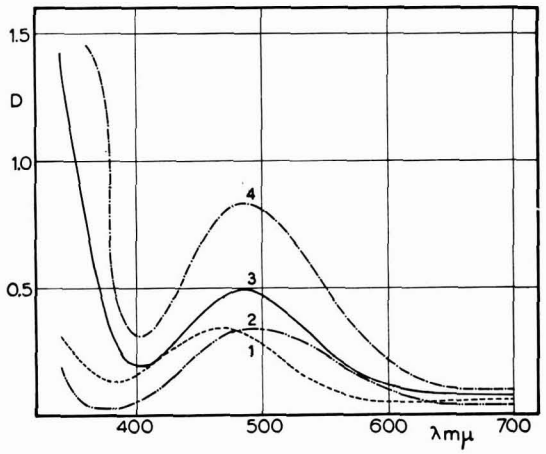

Fig. 10. Absorption spectra of $1 \cdot 10^{-3}$ *M* MnO_4^- and $10 \cdot 10^{-3}$ *M* Mn(II) in 6 *N* acid solns.: (1), in HNO_3; (2), in $HClO_4$; (3), in H_2SO_4; (4), Mn(II) $2 \cdot 10^{-2}$ *M* in H_2SO_4, electro-oxidised to Mn(III) for 30 min. $D = 3.98$ mA/cm^2.

molar ratio. The spectrum obtained in H_2SO_4 or $HClO_4$ is quite different from the spectrum of MnO_4^-; it is instead characteristic of Mn(III) and is identical to that obtained from concentrated solutions of Mn(II) of equal acidity and electro-oxidising power. The absorption spectra obtained in HNO_3 resemble those obtained in concentrated sulphuric acid medium.

(2) By polarographing electro-oxidised Mn(III) solutions a reduction wave having $E_{\frac{1}{2}} = +0.65$ V *vs.* S.C.E. is obtained which is identical with the one obtained from MnO_4^- solutions with added Mn(II) (Fig. 11).

(3) If a MnO_4^- solution with added Mn(II) is reduced at a controlled-potential of +0.4 V *vs.* S.C.E. a coulomb number (Tables 2 and 3) is obtained which agrees with a 5-electron reduction. If the potential is fixed at +0.8 V *vs.* S.C.E., *i.e.*, before the

Mn(III) reduction wave, the current corresponds to a reduction smaller than 5 electrons.

The Mn(III) formation reaction is notably influenced by acidity (optimum 6 N) and by the concentration of Mn(II) ions in the solution; the greater the Mn(II)/MnO_4^- ratio, the greater the amount of Mn(III) ions formed, at a fixed acidity. At high acid

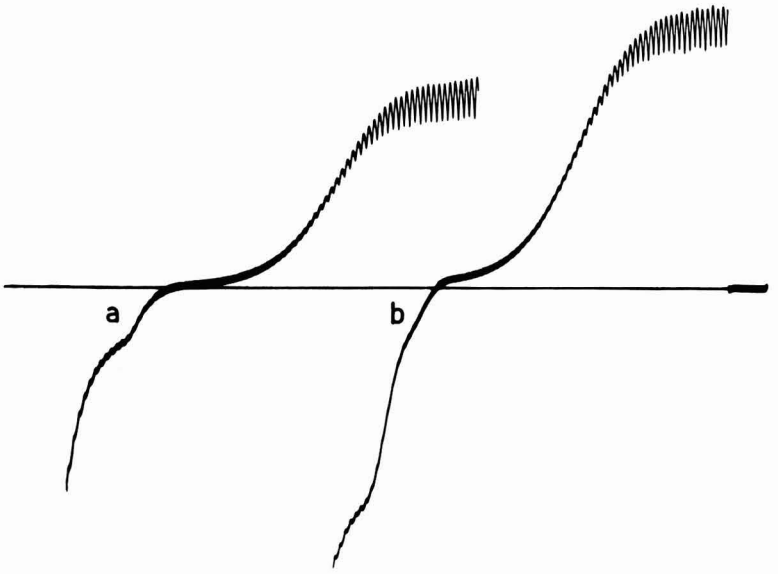

Fig. 11. Polarographic waves obtained from solns. of Mn(III) obtained by direct oxidation of Mn(II) with permanganate and by electro-oxidation of Mn(II): (a), MnO_4^- $1 \cdot 10^{-3}$ M, Mn(II) $10 \cdot 10^{-3}$ M, H_2SO_4 6 N; (b), Mn(II) $2 \cdot 10^{-2}$ M, electro-oxidised for 60 min. $D = 3.5$ mA/cm^2.

concentrations the Mn(III) ions which form are stable in sulphuric medium (in accordance with the complexing properties of this acid) and, what is surprising, also in perchloric medium. Perchloric acid is well known for its non-complexing properties, so that it is commonly used as inert supporting electrolyte in the study of ionic complexes. The complete instability of Mn(III) ions in nitric acid is also very strange, as nitric acid possesses more complexing properties than perchloric acid.

CONCLUSIONS

From experimental data we can draw the following conclusions on the reduction mechanism of permanganate ion in mineral acid media. The permanganic ion in acid medium and in absence of manganous ions is reduced irreversibly and very slowly to Mn(II). In the presence of Mn(II) permanganic ion reacts forming Mn(III) which is the active oxidising species in permanganate oxidation reactions. This explains (i) the MnO_4^- incubation period and its removal by the addition of Mn(II) ions in wet combustions and (ii) the permanganate oxidation-potential decrease in the oxidation of Fe(II) according to ZIMMERMANN–REINHARDT. The addition of Mn(II) ions does not decrease the oxidation potential of the MnO_4^-–Mn(II) couple below that of chloride–chlorine, as we had believed previously. An explanation of this type is inadequate

in view of the MnO_4^- → Mn(II) reduction which is completely irreversible. On the contrary it is clear that the rôle of Mn(II) ions is to react with permanganate so that it may form Mn(III) and so contribute to the lowering of the potential of the reversible couple Mn(III)–Mn(II), *i.e.*, the potential determining of the MnO_4^-–Mn(II) system. Phosphoric acid and, to a lesser extent, sulphuric acid (ZIMMERMANN–REINHARDT reagent) by complexing Mn(III) ions in stable ionic species, acts effectively together with the excess of Mn(II) ions to lower further the Mn(III)–Mn(II) system potential so that Mn(III) may be reduced by Fe(II) only and not by chloride.

SUMMARY

The reduction of MnO_4^- in nitric, perchloric and sulphuric acids on a bubbling platinum electrode and the influence of the acid anion on the behaviour of the permanganic ion in the presence of Mn(II) were studied. The rôle of Mn(II) and Mn(III) in the permanganate reduction process was fully investigated. Evidence is given for the formation of an Mn(III)–acid complex in sulphuric and perchloric acids. The presence of a surface film of $MnMnO_3$ on the platinum electrode and its reduction were observed and studied.

REFERENCES

1 P. G. DESIDERI, *J. Electroanal. Chem.*, 4 (1962) 359.
2 D. COZZI AND P. G. DESIDERI, *J. Electroanal. Chem.*, 1 (1959/1960) 301.
3 C. ZIMMERMANN, *Ber. Deut. Keram. Ges.*, 14 (1881) 779.
C. REINHARDT, *Stahl Eisen*, 4 (1884) 704.
4 W. BLUM, *J. Am. Chem. Soc.*, 34 (1912) 1379.
5 P. G. DESIDERI, *J. Electroanal. Chem.*, 2 (1961) 39.
6 M. J. POLISSAR, *J. Am. Chem. Soc.*, 58 (1936) 1372.
7 F. C. TOMPKINS, *Trans. Faraday Soc.*, 38 (1942) 131.
8 A. W. ADAMSON, *J. Phys. Colloid Chem.*, 55 (1951) 293.

POLAROGRAPHIC BEHAVIOUR OF HALIDE IONS

I. CHLORIDE

T. BIEGLER

*Section of Agricultural Chemistry, University of Sydney (Australia)**

(Received May 22nd, 1963)

Chloride, bromide and iodide ions belong to quite a large group of substances which depolarize the dropping mercury electrode with the formation of insoluble mercury salts. The resulting anodic polarographic steps have been described by simple equations[1] which indicate that the steps should begin steeply and discontinuously, should be asymmetric about the half-step potential and should shift to more negative potentials with increasing halide concentration. However, in no case has the polarographic behaviour been found to correspond precisely with this description and, further, there are clear differences between the three halide ions themselves. In following communications each ion will be examined in detail using the methods of d.c. and a.c. polarography which are complementary in assisting interpretation of the electrode processes.

VLCEK[2] investigated the d.c. polarographic behaviour of chloride ion and found several departures from that expected on the basis of the equations derived by KOLTHOFF AND MILLER[1], *viz.*,

$$E = E'^{\circ} - \frac{RT}{F} \ln [Cl^-]^{\circ} \tag{1}$$

$$= E'^{\circ} - \frac{RT}{F} \ln \frac{i_d - i}{k} \tag{2}$$

and

$$E_{1/2} = E'^{\circ} - \frac{RT}{F} \ln \frac{[Cl^-]}{2} \tag{3}$$

Here, E'° is the standard potential of the calomel electrode, $[Cl^-]^{\circ}$ indicates the surface concentration of chloride, k is the proportionality constant between the diffusion current and the bulk concentration of chloride ion and the other terms have their usual significance. In the first place, VLCEK found a small but distinct pre-step, the height of which did not vary with changing chloride concentration but increased in proportion to the mercury reservoir height (*cf.*, HAUL AND SCHOLZ[3]). The adsorption character of this pre-step was confirmed by the presence of characteristic current–time curves

* Present address: Department of Chemistry and Chemical Engineering, University of Illinois, Urbana, Illinois, U.S.A.

in the potential region of the pre-step. In addition, VLCEK noted that: (i) the beginning of the anodic step, although quite steep, was by no means discontinuous, (ii) both the potentials for the commencement of discharge and the $E_{1/2}$ values were some 50 mV more positive than the calculated values, (iii) the total limiting current was not a linear function of bulk chloride concentration and (iv) at concentrations above $2 \cdot 10^{-3} M$ the polarograms showed three or even four separate steps (including the above-mentioned pre-step).

VLCEK postulated that: (i) the initial product of the electrode reaction was a monolayer of adsorbed calomel in the form HgCl, (ii) at more positive potentials than the pre-step the reaction proceeded by way of an intermediary, Hg_2Cl^+, and (iii) the total limiting current was controlled, expecially at high chloride concentrations, by the rate of passage of mercurous ions through a relatively thick film of calomel which accumulated at the electrode surface.

The a.c. polarography of chloride ion was first examined by BREYER AND HACOBIAN[4] who found a sharp, well-defined a.c. wave corresponding to the anodic d.c. step. The wave was asymmetric, the base current was depressed on the positive side of the wave and the summit potential corresponded to the beginning of the d.c. step rather than to the half-step potential. These authors used the term *transition wave*[5] to describe the a.c. waves of the halide ions which were believed to be intermediate in their behavior between faradaic and tensammetric a.c. waves.

EXPERIMENTAL

A.c. and d.c. polarograms were obtained manually using a circuit of conventional design (*e.g.*, BAUER[6]). The superposed sinusoidal voltage was of mains frequency (50 c/sec) and the amplitude was adjusted by means of a voltage divider. Current readings for the polarograms were taken at the end of drop life. In several cases the form of the current–time curves for individual drops was also recorded; d.c. polarographic current–time curves were obtained by applying the voltage drop, across a decade resistance box in series with the cell, to the vertical plates of an oscilloscope (Tektronix type 502).

A saturated-calomel reference electrode was used, with a large electrolytic condenser (2,000 μF) providing a low impedance path between the reference electrode and a mercury pool in the polarographic cell. A salt bridge containing saturated potassium nitrate connected the cell solution with a beaker of saturated potassium chloride into which dipped a second bridge from the reference electrode. The bridge solution in contact with the cell was changed regularly to ensure that chloride from the beaker did not reach the cell.

Analytical grade reagents were used without further purification. Except where otherwise noted, experiments were carried out at 25°. Capillary characteristics were: mercury head, 38 cm; t, 4.3 sec (in air-free M Na_2SO_4 at zero applied potential); m, 1.60 mg/sec.

RESULTS

In agreement with previous workers[4,5,7] the chloride a.c. wave is found to be asymmetric when a superposed alternating voltage of 15 mV r.m.s. is used (Fig. 1a(ii)). The negative branch of the wave rises steeply to a sharp peak and then falls away more gradually on the positive side. Use of a comparatively small alternating voltage

(< 5 mV) gives an a.c. wave with a shape quite different from that found previously (Fig. 1a (iii), 1b (ii)). It appears that the use of a larger amplitude obscures changes in the electrode processes occurring over a small potential range. The current is seen to drop very sharply at potentials just more positive than the summit and then rise again to give a small peak at the positive foot of the wave.

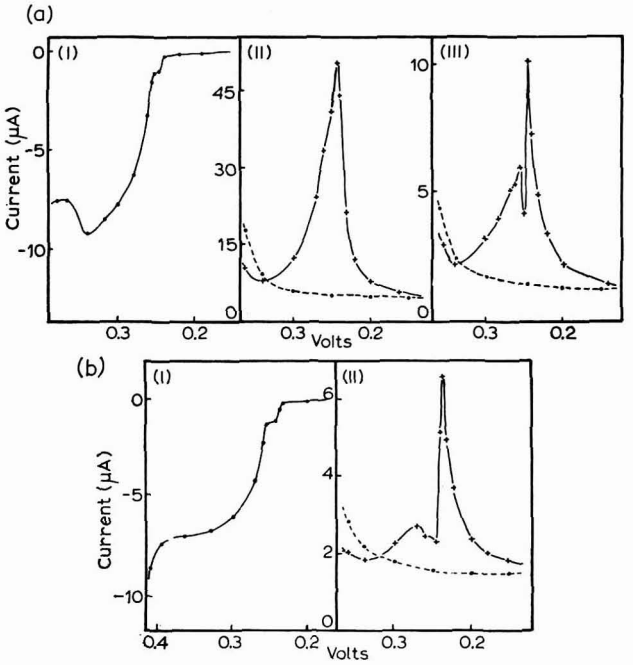

Fig. 1. (a), Polarograms for mM chloride ion in 1.0 M KNO_3: (i), d.c.; (ii), a.c. (alternating voltage 15 mV); (iii), a.c. (alternating voltage 4 mV).
(b), Polarograms for mM chloride ion in 1.0 M Na_2SO_4 + 0.001 N H_2SO_4: (i), d.c.; (ii), a.c. (alternating voltage 4 mV). Broken line indicates base current.

A feature of the d.c. polarograms is the sharpness of the start of anodic discharge; a potential change as small as 1 mV can be sufficient to shift from a region of no discharge to one where appreciable faradaic current flows. The sudden increase in current shown by the galvanometer is an adequate indication of the start of electron transfer. The shapes of the current–time curves in this potential region are useful in establishing the sharp change in the electrode process (Fig. 2). Thus, the curve at +0.240 V shows a continuous decrease in current with time, typical of a charging or condenser current (*e.g.*, McKENZIE[8]). At a potential only 2 mV more positive there is an increase in the anodic current during the later stages of the drop life; such an increase with increasing drop size strongly suggests that faradaic current is present.

By these means, it is possible to make very accurate determinations of the starting potential of the d.c. pre-step. Comparison of this value with the sharp summit potential of the d.c. wave shows agreement to within 2 mV in all cases. Because of the magnitude of this uncertainty it is not possible to state definitely whether or not the alternating current at the summit potential is accompanied by a faradaic direct current.

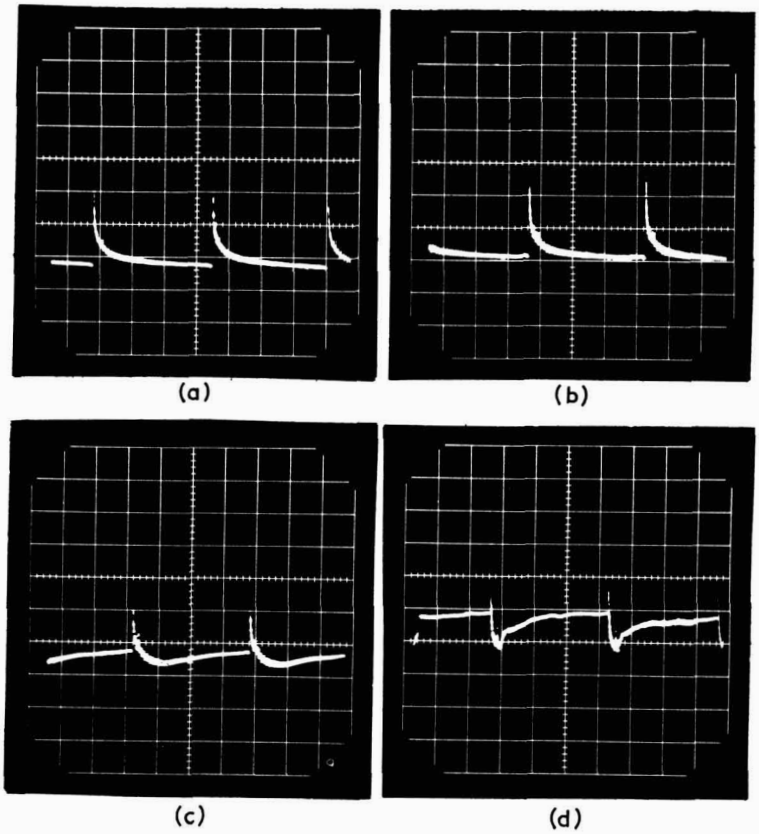

Fig. 2. Current–time curves (d.c.) for mM chloride ion in 1.0 M KNO_3 at following potentials: (a), 0.220 V (4.9); (b), 0.240 V (13.6); (c), 0.242 V (12.8); (d), 0.245 V (9.0). Figures in brackets indicate corresponding a.c. values (μA) with 5 mV alternating voltage.

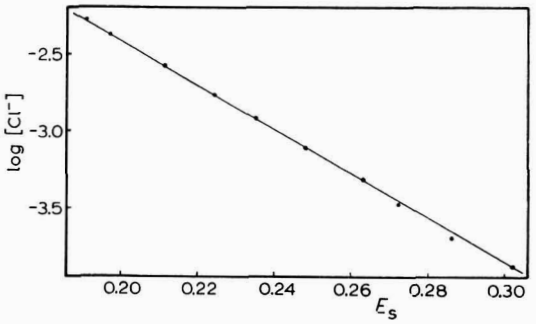

Fig. 3. Relationship between summit potential (E_s) and concn. for the chloride a.c. wave in 1.0 M KNO_3 at 25°.

Since the potential regions of faradaic and non-faradaic direct current are so sharply defined, it would seem desirable to use an alternating voltage no larger than 0.5 mV r.m.s. (1.4 mV peak-to-peak) in order to resolve this problem. The necessary sensitivity could not be attained with the equipment used in these experiments.

As expected from the d.c. polarographic behaviour, the summit potential of the chloride a.c. wave shifts to more negative values with increasing chloride concentration. The plot of summit potential against the logarithm of chloride ion concentration is a straight line of slope -71.5 mV (Fig. 3).

The composition of the supporting electrolyte has a specific influence on the height of the a.c. wave but not on the diffusion current (Table 1). Also shown in this table are the values of the base current for supporting electrolyte alone, at the potential of the peak of the chloride wave. It can be seen that the wave height increases as the corresponding base current decreases.

TABLE 1

A.C. WAVE HEIGHTS FOR CHLORIDE ION IN VARIOUS SUPPORTING ELECTROLYTES
Chloride concn. $5 \cdot 10^{-4}$ M; alternating voltage, 15 mV; $T = 25°$.

Supporting electrolyte	*Wave height* (μA)	*Base current at* E_s (μA)
1.0 M Na_2SO_4	16.6	7.4
0.1 M Na_2SO_4	18.6	6.6
1.0 M KNO_3	25.2	5.4
1.0 M $NaClO_4$	29.1	3.9

DISCUSSION

There is strong evidence to suggest that the start of anodic discharge of chloride ion occurs sharply and is discernible with a potential change of only 1–2 mV. Further, there is close agreement between this *starting potential* and the summit potential of the a.c. wave. It follows that at least the major part of the negative branch of the a.c. wave lies in a potential region where there is no charge transfer across the electrode solution interface and therefore this branch involves alternating currents which are non-faradaic in character. It should be noted that the above description for this part of the a.c. wave is directly supported by the experimental evidence only to within a few millivolts of the peak where the experimental difficulties mentioned earlier make interpretation uncertain. At this stage, the possibility cannot be excluded that the alternating current at the summit may contain a faradaic component.

The height of the chloride a.c. wave shows a strong dependence on the composition of the supporting electrolyte. For example, the effect of supporting electrolyte concentration is illustrated by the results for 1.0 M and 0.1 M sodium sulphate, the chloride wave being about 2 μA higher in the latter solution. The specific effect of the electrolyte concentration is emphasized by the fact that the additional resistance of the more dilute solution would tend to reduce rather than increase the a.c. wave height. The results in Table 1 indicate that the higher the supporting electrolyte base current, the lower is the chloride wave in that solution. It is generally believed that base current values at such positive polarizations are measures of the strength of bonding between mercury and the specifically adsorbed anions in the double layer[9]. On this assumption the present results suggest that the a.c. wave height becomes smaller as the adsorption of supporting electrolyte anions becomes stronger.

The non-faradaic nature of the cathodic side of this a.c. wave and the pronounced effect of double-layer structure on the height of the wave can both be readily explained by postulating that the negative branch of the wave is due to the high differential

capacity of the double-layer following upon intense specific adsorption of chloride ion (*cf.*, DIBBS *et al.*[10]). It is well known that chloride ion is specifically adsorbed on to mercury and that both the intensity of adsorption and the differential capacity increase as the potential is made more anodic[9]; this increase in capacity apparently becomes very steep at potentials just more negative than the starting potential of the discharge process. According to this view the a.c. wave height corresponds to a large differential capacity associated with a high surface concentration of adsorbed chloride ions. In the presence of other (*i.e.*, supporting electrolyte) anions in the double-layer, the approach of chloride ions into the inner Helmholtz plate is hindered because of a repulsion effect. Hence it is reasonable to expect that the extent of specific adsorption of chloride ions and therefore, the height of the a.c. wave, are greatest when the concentration of other anions within the double-layer is least. This is precisely the observed effect.

Because of the increasing double-layer capacity, the anodic d.c. residual current increases up to the point where discharge becomes evident. This feature has been confused with a gradual commencement of the discharge process itself[2], but current–time curves (Fig. 2) show convincingly that this process does start discontinuously, or nearly so, as predicted by KOLTHOFF AND MILLER[1].

The initial product of the charge transfer reaction seems to be a mono-layer of calomel having a fixed orientation related to the arrangement of the atoms in the underlying mercury surface[11–13]. The height of the d.c. pre-step is then a measure of the quantity of electricity required to form such a layer; a value of 125 μC/cm^2 is calculated from the present results (pre-step height of 0.96 μA). A value of this order (160 μC/cm^2) has previously been derived[11] on the assumption that one chlorine atom is attached to each mercury atom of the electrode surface. It is therefore likely that such a structure exists under polarographic conditions.

It should be stressed that the term *adsorption pre-step* is not strictly applicable here, at least in the same sense as used by BRDICKA[14]. True adsorption pre-steps are supposed to result from the fact that the initial layer of the adsorbable reduced species of a substance such as riboflavin or methylene blue is formed in a state of lowered activity and therefore the reduction is able to occur at a potential more positive than would be possible if the product were not adsorbed. It is hardly likely that the chloride pre-step is formed in the same way. In all probability, the complete surface layer of calomel (or chloromercury) acts as a barrier to the charge transfer reaction which therefore proceeds with an appreciable overvoltage in the presence of such a layer. Accordingly, the formation of this first layer can be observed as a separate step. Neither the current–time curves associated with this step nor the dependence of limiting current on the mercury head are satisfactory criteria for establishing the nature of such a pre-step because these properties behave similarly if either of the possible mechanisms is operating[15].

The fall in alternating current at potentials just more positive than the summit potential, corresponds to the plateau of the pre-step. At still more positive potentials the current rises again and a small a.c. wave, corresponding to the main portion of the d.c. step, is formed. The height of this wave, and the difference in its height in different media (Fig. 1), suggest that the discharge process is not completely reversible, probably because once the complete mono-layer is formed (*i.e.*, the initial phase of discharge) further passage of current takes place by migration of mercurous or chlor-

ide ions through the film. With a sufficiently thick calomel film there may be a further observable increase in the overvoltage of the electrode reaction. Thus, at high chloride concentrations the main step splits into two steps (*cf.*, VLCEK[2]), a phenomenon having essentially the same origin as the splitting of polarographic steps often observed in the presence of added surface active substances. In the case of chloride the surface film is composed of the insoluble product of the electrode reaction, and the behaviour of the first limiting current is in reasonable agreement with a theory developed for limiting currents due to such reaction product films[15].

The relationship between the starting potential (E_1) of chloride discharge and the concentration of chloride ion is given (from eqn. (1)) by

$$E_1 = E'^{\circ} - 0.0591 \log [Cl^-] \quad (4)$$

The derivation of eqns. (1)–(4) employs an over-simplified picture of the electrode process in that it is assumed that discharge starts when the solubility product of mercurous chloride is exceeded. Such a representation cannot be accurate[11] and, as noted previously[2], eqn. (4) does not correctly predict experimental values of E_1. Nevertheless, the relation between E_1 (which coincides with the more conveniently measured summit potential of the a.c. wave) and the logarithm of the chloride concentration is linear to a high precision (Fig. 3) and is given by

$$E_1 = \text{constant} - 0.0715 \log [Cl^-] \quad (5)$$

It is perhaps surprising that the value of the constant in this equation is found to be $+0.026 \pm 0.004$ V which is in very good agreement with a value recently quoted for the standard potential of the calomel electrode ($+0.026$ V on the molar concentration scale[16]).

ACKNOWLEDGEMENTS

The author wishes to thank Dr. B. BREYER and Dr. H. H. BAUER for many stimulating discussions. The award of a Studentship by the Commonwealth Scientific and Industrial Research Organization is gratefully acknowledged.

SUMMARY

The wave obtained in the a.c. polarography of chloride is attributed mainly to the adsorption of chloride ion which results in a high differential capacity of the electrical double-layer. The alternating current at potentials more negative than the summit of this a.c. wave is non-faradaic in character since no faradaic direct current can be detected in this potential region. D.c. polarographic current–time curves indicate that discharge of chloride ion begins almost discontinuously at a potential corresponding to the summit of the a.c. wave.

REFERENCES

1 I. M. KOLTHOFF AND C. S. MILLER, *J. Am. Chem. Soc.*, 63 (1941) 1405.
2 A. A. VLCEK, *Collection Czech. Chem. Commun.*, 19 (1954) 221.
3 R. HAUL AND E. SCHOLZ, *Z. Elektrochem.*, 52 (1948) 226.
4 B. BREYER AND S. HACOBIAN, *Australian J. Sci. Research*, A4 (1951) 610.
5 B. BREYER AND S. HACOBIAN, *Australian J. Chem.*, 6 (1953) 186.
6 H. H. BAUER, *J. Electroanal. Chem.*, 1 (1960) 363.
7 Y. TAKEMORI AND I. TACHI, *Bull. Chem. Soc. Japan*, 28 (1955) 151.

8 H. A. McKENZIE, *Australian J. Chem.*, 11 (1958) 383.
9 D. C. GRAHAME, M. A. POTH AND J. I. CUMMINGS, *J. Am. Chem. Soc.*, 74 (1952) 4122.
10 H. P. DIBBS, D. J. G. IVES AND R. W. PITTMAN, *J. Chem. Soc.*, (1957) 3370.
11 G. J. HILLS AND D. J. G. IVES, *J. Chem. Soc.*, (1951) 311.
12 H. R. THIRSK, *Proc. Phys. Soc., London*, B66 (1953) 129.
13 E. H. BOULT AND H. R. THIRSK, *Trans. Faraday Soc.*, 50 (1954) 404.
14 R. BRDICKA, *Z. Elektrochem.*, 48 (1942) 278.
15 T. BIEGLER, *J. Electroanal. Chem.*, 4 (1962) 317.
16 G. J. HILLS AND D. J. G. IVES, *J. Chem. Soc.*, (1951) 318.

POLAROGRAPHIC BEHAVIOUR OF HALIDE IONS

II. BROMIDE

T. BIEGLER

*Section of Agricultural Chemistry, University of Sydney (Australia)**

(Received May 22nd, 1963)

The polarographic behaviour of bromide ion has not previously been investigated in the same detail as that of chloride. The main facts already established are as follows. Since mercurous bromide is less soluble than calomel, the bromide d.c. step and a.c. wave occur at more negative potentials than those of chloride[1-3]. At concentrations above millimolar, the bromide step splits into two; the first limiting current remains constant with increasing bromide concentration and is attributed to the formation of a mercurous bromide film at the electrode surface[1]. This effect appears to be analogous to the splitting of the chloride step at high concentrations (*cf.*, Part I).

BREYER AND HACOBIAN[2] found that bromide gave a sharp, well-defined a.c. wave and, as with chloride, it was shown that the summit potential corresponded closely to the potential at which discharge of bromide commenced[2,3].

In the following communication, it will be shown that bromide passes through an initial phase of discharge similar to that of chloride, giving rise to a small pre-step. The accompanying a.c. polarographic phenomena are quite complex and reveal, among other things, a slow diffusion step in the adsorption of bromide ions and a reversible phase of the electron transfer reaction within a narrow potential region.

EXPERIMENTAL AND RESULTS

A.c.–time curves showing the time variation of the peak-to-peak value of the alternating current were obtained as described previously[4]. Other apparatus and experimental methods were the same as indicated in Part I of this series. Analytical grade potassium bromide was employed without purification. All potential values refer to the saturated calomel electrode.

Typical a.c. and d.c. polarograms for bromide ion are shown in Fig. 1. Two distinct sections are evident in the a.c. wave, firstly, a fairly steady rise in current from a potential around −0.2 V. (this becomes more cathodic at higher concentrations) to one corresponding closely to the beginning of the d.c. step and, secondly, a steep rise to a sharp peak which falls away steeply on the positive side to a current level somewhat lower than the base current. For convenience, these two sections will be referred to as the *hump* and *spike* respectively. It is noteworthy that the a.c. wave has essentially this shape even at the lowest concentrations at which the wave can be detected (*ca.* $5 \cdot 10^{-5}$ *M*). The heights of both portions of the wave increase linearly with concentra-

* Present address: Department of Chemistry and Chemical Engineering, University of Illinois, Urbana, Illinois, U.S.A.

tion up to around $5 \cdot 10^{-4}$ M; above this value the calibration graphs are curved. With the simple a.c. polarographic circuit used here it is not possible to detemine whether this curvature is real or is caused solely by the series resistance of the circuit[5].

The d.c. polarogram in Fig. 1 exhibits the general features of the bromide step. The initial anodic rise is more gradual than in the case of chloride and, as a result, the starting potential of electron transfer cannot be precisely determined from the d.c. polarogram alone (but see below). A well-developed pre-step with a height (0.91 μA) comparable to that of the chloride pre-step (0.96 μA using the same capillary and mercury head) is present. With concentrations above millimolar the main d.c. step splits

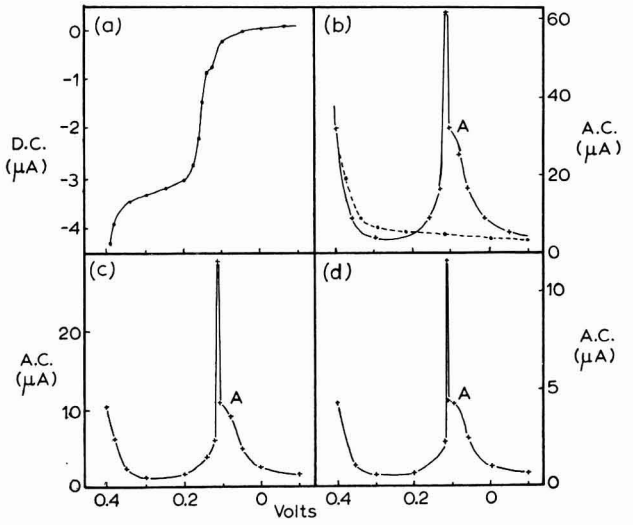

Fig. 1. Polarograms of $5 \cdot 10^{-4}$ M bromide ion in 1.0 M KNO_3: (a), d.c.; (b), a.c. (alternating voltage 15 mV), broken line is base current; (c), as (b), but alternating voltage 5 mV; (d), as (b), but alternating voltage 2 mV.

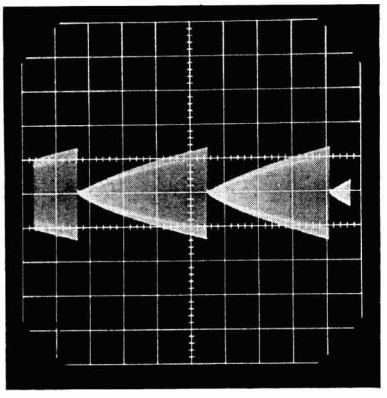

(a)i

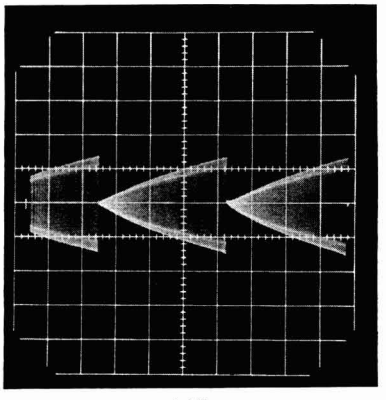

(a)ii

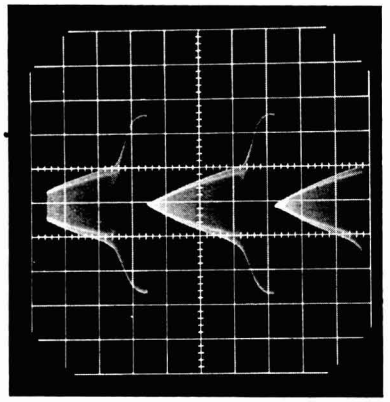

(a)iii

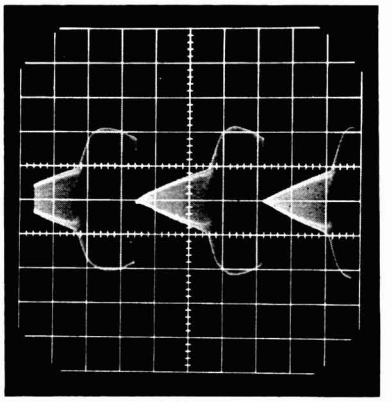

(a)iv

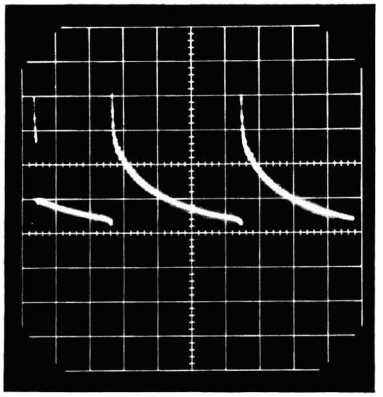

(b)i

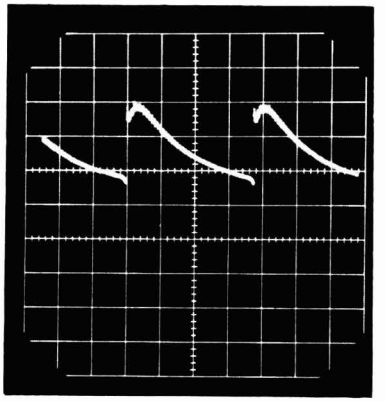

(b)ii

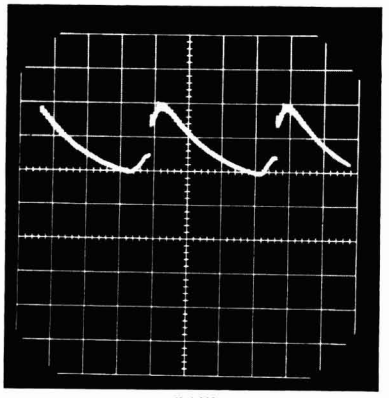

(b)iii

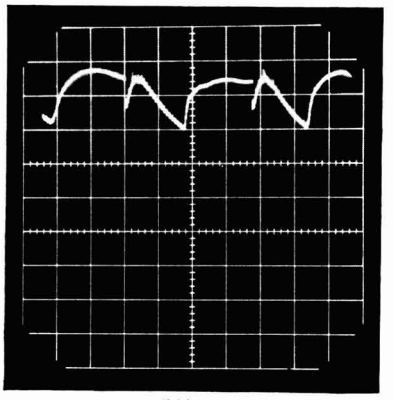

(b)iv

Fig. 2. (a), A.c.–time curves and (b), d.c.–time curves for $5 \cdot 10^{-4}$ *M* bromide ion in 1.0 *M* KNO_3 at following potentials: (i), 0.100 V; (ii), 0.113 V; (iii), 0.115 V; (iv), 0.116 V. Alternating voltage 2 mV.

into two; the first limiting current remains constant at about 4 μA while the total current is proportional to the bromide concentration.

With decreasing amplitude of the superposed alternating voltage the width of the spike becomes smaller. For example, with an alternating voltage of 15 mV r.m.s. the width, measured at point A (Fig. 1), is 20 mV; with 5 mV alternating voltage the width is 7 mV and decreases to only 4 mV when the alternating voltage is 2 mV r.m.s.

Comparison of a.c. and d.c. polarograms suggests that the a.c. hump is non-faradaic in origin and that the rise of the spike parallels the commencement of the electron transfer reaction. As with chloride (see Part I), current–time curves are useful in assisting interpretation of the polarograms and especially in deciding at what potential the discharge of bromide ion commences. A series of such curves is shown in Fig. 2. In this particular case the foot of the spike occurs at +0.115 V. At more negative potentials (*i.e.*, corresponding to the hump region) a.c.–time curves have their usual shape ($I \propto t^{2/3}$) and the d.c.–time curves show the decrease in current with time, typical of a capacity or charging current. The change in electrode process at +0.115 V is very sharp and is marked by a rise in both direct and alternating currents just before the end of drop life. This current rise marks the beginning of the spike in the a.c. polarogram and of the steep portion of the pre-step in the d.c. polarogram. An alteration in potential to +0.116 V causes the d.c. rise to shift to an earlier stage in the drop life but the current falls again towards the end of drop life. The a.c.–time curves reflect this behaviour and the alternating current reaches a maximum about halfway through drop life. At still more positive potentials the current rise and the maximum occur earlier in the drop life.

Some typical results showing the effects of supporting electrolyte composition and mercury head on the bromide hump are presented in Tables 1 and 2.

TABLE 1

HEIGHTS OF THE BROMIDE a.c. HUMP FOR 4.0×10^{-4} *M* BROMIDE IN VARIOUS SUPPORTING ELECTROLYTES
alternating voltage 4.0 mV r.m.s., $T = 25°$.

Supporting electrolyte	*Height of hump (μA)*
1.0 *M* Na_2SO_4	4.5
1.0 *M* KNO_3	5.5
1.0 *M* $NaClO_4$	5.3

TABLE 2

EFFECT OF MERCURY HEAD ON HEIGHT OF THE BROMIDE HUMP
4.0×10^{-4} *M* bromide in 1.0 *M* Na_2SO_4; alternating voltage 15 mV r.m.s., $T = 25°$.

h (cm)	*Wave height (μA)*
22	5.0
38	4.7
57	4.2

DISCUSSION

The most significant feature in the a.c. polarography of bromide ion is the appearance of two distinct sections in the a.c. wave, resulting, presumably, from different electrode processes. All the experimental evidence indicates that the hump is a feature which arises from the specific adsorption of bromide ions at the mercury surface. Faradaic current at potentials corresponding to the hump is absent; the gradual anodic increase of residual current in this potential region is due, as with chloride ion, to the increased surface charge density accompanying anion adosprtion. According to this view, the hump can be thought of as an exceptionally high base current resulting from a high differential capacity of the double-layer.

It is of interest to examine the influence of supporting electrolyte composition on the height of the hump, in view of the corresponding results and their interpretation in the case of chloride ion (see Part I). The heights in molar sodium perchlorate and potassium nitrate differ only slightly but in sodium sulphate the hump is significantly lower (Table 1). The same reasoning applies here as with chloride ion, namely, that the stronger adsorption of sulphate results in a lower surface concentration of bromide ion. It is possible that the smaller magnitude of the differences found with bromide, as compared to chloride, is a consequence of the greater strength of adsorption of the former which is therefore somewhat less affected by the presence of other anions in the double-layer than is the adsorption of chloride.

The height of the hump is significantly affected by altering the drop time (Table 2). These measurements were prompted by the idea that a system such as this, *i.e.*, one containing small bulk concentrations of a strongly adsorbed ion, should provide conditions favourable for observing diffusion-control of adsorption. The results shown in Table 2 seem to confirm this view; increasing the drop time causes an increase in wave height, probably due to a higher surface concentration of bromide ion at the end of drop life. This behaviour contrasts with the more commonly encountered case of an uncharged surfactant where diffusion-control of adsorption is manifested as a decrease in capacity (and alternating current) with increasing drop time. The existence of diffusion-control for ion adsorption has been predicted[6] but does not seem to have been detected previously for the reason that most measurements of double-layer capacity in electrolyte solutions are carried out using concentrations at which adsorption equilibrium is reached very rapidly.

The narrow and sharp appearance of the spike, especially when very small alternating voltages are employed, suggests that the underlying electrode process occurs only over a very narrow potential range. An a.c. wave corresponding to such a process can always be expected to increase in width when a larger alternating voltage is used because the periodically *alternating* potential can cover the region of the reversible process even when the *steady* applied potential is well removed from this region. This type of situation is not normally encountered for the reason that the alternating voltages commonly used are very small compared with the potential range within which a typical reversible electron transfer process occurs (*ca.* $240/n$ mV). With two different processes occurring close together, as with bromide, use of a large alternating voltage can completely obliterate the two regions of the a.c. wave (*e.g.*, TAKEMORI AND TACHI[3]).

If it is assumed that the spike arises from diffusion-controlled (faradaic process

involving one electron, it can be calculated that the height should be about 7 μA r.m.s. for a bromide concentration of $5 \cdot 10^{-4}$ M and 5 mV alternating voltage. This compares with an experimental value of about 25 μA so that the spike is abnormally high if in fact it is a faradaic a.c. wave.

One point of similarity in the polarographc behaviour of chloride and bromide stands out, namely, that we are dealing with electrode processes which are separated almost discontinuously by a narrow potential interval. On the basis of the results found with chloride, it is logical to infer that the spike is associated with the commencement of the electron transfer reaction, *i.e.*, the formation of mercurous bromide. This conclusion is supported by the shape of the d.c. polarograms which commence gradually (increase in residual current), show a sharp anodic rise (beginning of discharge) and then flatten out to give a pre-step of hight comparable with that of the chloride pre-step (formation of a mono-layer of mercurous bromide).

On the basis of the above considerations, two distinct mechanisms for the formation of the spike are possible. In the first, the current is considered to originate in the sudden decrease in surface charge density following formation of the mercurous salt. Thus, just before discharge begins the double-layer has a very high capacity which doubtless decreases when bromide ions are converted into mercurous bromide molecules. The fall in charge density would then result in a large differential capacity because of the large rate of variation of charge density with potential. If this interpretation is correct, the spike should be classified as a non-faradaic a.c. wave.

The second proposed mechanism consideres the current in the spike to be faradaic and produced by the reversible electron transfer reaction involved in the formation of mercurous bromide. Such a reaction is almost certainly not the classical one

$$2\ \mathrm{Hg} \rightleftharpoons \mathrm{Hg_2^{2+}} + 2\ \mathrm{e}$$

for reasons identical to those proposed for the discharge of chloride on mercury[7]. In analogy to the case of chloride, the initial phase of discharge of bromide ions is probably the formation of a mono-layer of bromine atoms covalently bonded to the mercury surface, giving a layer which could be named *bromomercury* (*cf.*, HILLS AND IVES[7]). Electron transfer occurs when a bromide ion loses its electron directly to the metallic mercury on to which it is specifically adsorbed; mercurous ions as such play no part. The a.c. wave is narrow because this reaction can occur reversibly only over the small potential range between the beginning of discharge and the formation of a complete mono-layer. The abnormal height of the wave could then be explained by the excess surface concentration, as compared with the bulk concentration (from which the theoretical height is calculated), due to adsorption of bromide. These last points account for the major objections to considering the spike as being faradaic in character.

There is insufficient experimental evidence to distinguish unequivocally between the alternatives presented above. However, the second mechanism is preferred, mainly on the grounds that it can be used to give a convincing explanation for the current–time curves found in the potential region of the spike. The specific conditions under which the current–time curves in Fig. 2 were obtained can be interpreted as follows.

At +0.100 V there is no faradaic current; the d.c.–time curve shows a continuous decay of current with time (typical residual current) while the alternating current increases with growth of the electrode area. At potentials up to +0.113 V, the picture

is very similar except for a small maximum which develops at the beginning of the d.c.–time curve. It seems likely that this maximum is connected with the slow formation of the electrical double-layer. Thus, the accepted form of the time dependence of the residual current[8],,

$$i_r = -\mathrm{d}q/\mathrm{d}t = kt^{-1/3},$$

is derived on the assumption that the double-layer reaches equilibrium instantaneously. When, as here, this assumption is not strictly valid, it is plausible that the term $\mathrm{d}q/\mathrm{d}t$ passes through a minimum at some time after the formation of a fresh drop, giving rise to a d.c.–time curve as found here.

At the next potential shown (+0.115 V), there is a pronounced change in the shapes of these curves, with a marked increase in current (both a.c. and d.c.) appearing shortly before the end of drop life. This increase is taken to represent the beginning of the electron transfer reaction and of the formation of the *bromomercury* layer. The reaction commences only towards the end of drop life because the adsorption of bromide is diffusion-controlled; the critical surface concentration required to bring about the electrochemical reaction is not reached until a late stage in the drop life. It is significant that when higher concentrations of bromide are used, the increase in current always appears quite early in the drop life because the double-layer reaches equilibrium more rapidly.

At the next potential shown, only 1 mV more positive, the alternating current at the end of drop life is already lower than at +0.115 V and a maximum appears in the a.c.–time curve. The d.c.–time curve can best be described by means of a schematic diagram (Fig. 3) which is divided into three sections.

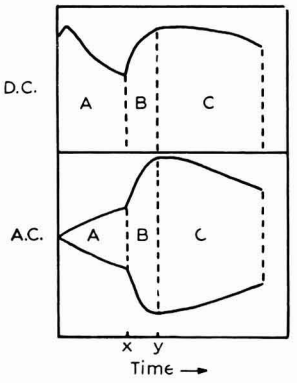

Fig. 3. Schematic representation of current–time curves at the start of discharge of bromide ion.

Section A represents the charging current, the maximum, as explained above, resulting from the slow formation of the double-layer. At x, the reversible formation of bromomercury begins and continues without limitation until all the available surface is covered (Section B). The available surface becomes limiting at point y and the reaction within Section C is controlled by the rate of formation of fresh surface, resulting in a decrease of current with time. The a.c.–time curve can be divided into three cor-

responding sections. Admittedly, this picture is idealized but it explains the essential features of the current–time curves.

The curves at still more positive potentials follow a similar pattern with both the rise in current (at x) and the maximum (at y) occurring earlier in the drop life. The reaction is no longer reversible at potentials more positive than the foot of the spike because the surface is very rapidly covered by the mono-layer of mercurous bromide; electron transfer then probably occurs, as with chloride, by the passage of mercurous ions through the surface layer.

ACKNOWLEDGEMENTS

The author wishes to thank Dr. B. BREYER and Dr. H. H. BAUER for many stimulating discussions and the Commonwealth Scientific and Industrial Research Organization for the award of a Studentship.

SUMMARY

The a.c. wave of bromide consists of two distinct portions, one, at more negative potentials, arising from the adsorption of bromide ion and the other resulting from the electron transfer process involved in the formation of mercurous bromide. Diffusion-control of adsorption of bromide ion can be detected at low concentrations. Evidence obtained from the shape of the a.c. wave and from current–time curves, both a.c. and d.c., for individual drops suggests that the faradaic process is reversible only over a narrow potential range corresponding to the formation of a mono-layer of mercurous bromide. Bromide ion gives a d.c. pre-step of origin similar to that of chloride.

REFERENCES

1 I. M. KOLTHOFF AND C. S. MILLER, *J. Am. Chem. Soc.*, 63 (1941) 1405.
2 B. BREYER AND S. HACOBIAN, *Australian J. Sci. Research*, A4 (1951) 151.
3 Y. TAKEMORI AND I. TACHI, *Bull. Chem. Soc. Japan*, 28 (1955) 151.
4 T. BIEGLER, *Australian J. Chem.*, 15 (1962) 34.
5 H. H. BAUER AND P. J. ELVING, *Australian J. Chem.*, 12 (1959) 335.
6 P. DELAHAY AND I. TRACHTENBERG, *J. Am. Chem. Soc.*, 79 (1957) 2355.
7 G. J. HILLS AND D. J. G. IVES, *J. Chem. Soc.*, (1951) 311.
8 I. M. KOLTHOFF AND J. J. LINGANE, *Polarography*, Vol. I, Interscience Publishers Inc., New York, 1952, Ch. IX.

POLAROGRAPHIC BEHAVIOUR OF HALIDE IONS

III. IODIDE

T. BIEGLER

*Section of Agricultural Chemistry, University of Sydney (Australia)**

(Received May 22nd, 1963)

The d.c. polarographic behaviour of iodide ion has been examined by KOLTHOFF AND MILLER[1] who found that the anodic limiting current became poorly defined at concentrations above $5 \cdot 10^{-4}$ *M*. They concluded that abnormalities in the diffusion plateau were caused by a film of mercurous iodide and were able to observe an irregular and pulsating growth of the mercury droplet. Recently, evidence has been presented[2] to indicate that iodide gives a pre-step corresponding to the formation of a monomolecular layer of mercurous iodide.

The a.c. polarographic behaviour has been reported by BREYER AND HACOBIAN[3] who found two separate a.c. waves and by TAKEMORI AND TACHI[4] who detected a single wave in the potential range of the d.c. step.

EXPERIMENTAL AND RESULTS

The apparatus used was the same as outlined earlier (Part I). Alternating current waveforms were obtained as described previously[5]. All potential values refer to the saturated calomel electrode.

Polarograms for three representative concentrations of iodide are shown in Fig. 1. At the highest of these concentrations three separate features are apparent in the a.c. polarograms (Fig. 1c). Proceeding from right to left (cathodic to anodic potentials), these are:

(i) A wave (Wave 1) whose summit corresponds to the most negative part of the d.c. step. This wave appears at concentrations lower than the other waves (Fig. 1a) and is a continuation of a rise in alternating current which begins around −0.6 V.

(ii) A second wave (Wave 2) which begins to appear on the positive shoulder of the first wave at concentrations in excess of $4 \cdot 10^{-4}$ *M*. This is the same concentration at which marked irregularities in the d.c. readings commence; these are indicated in the diagram by a broken line. The a.c. readings for this wave are also somewhat irregular but do not fluctuate to nearly the same extent as do the d.c. values.

(iii) A narrow wave (Wave 3) occurring at concentrations above 10^{-4} *M* and at a quite positive potential. As the iodide concentration is increased, the summit potential of Wave 3 shifts to slightly more positive values and the wave becomes smaller and

* Present address: Department of Chemistry and Chemical Engineering, University of Illinois, Urbana, Illinois, U.S.A.

less sharp (*cf.* Figs. 1b and 1c). Comparing a.c. and d.c. polarograms for iodide concentrations greater than about $4 \cdot 10^{-4}$ *M* (*e.g.*, Fig. 1c) it is found that Wave 3 occurs close to the positive end of the potential range in which fluctuation of the d.c. readings are evident. At lower concentrations, *i.e.*, between 10^{-4} *M* and $4 \cdot 10^{-4}$ *M*, Wave 3 is accompanied by a small kink in the diffusion current plateau.

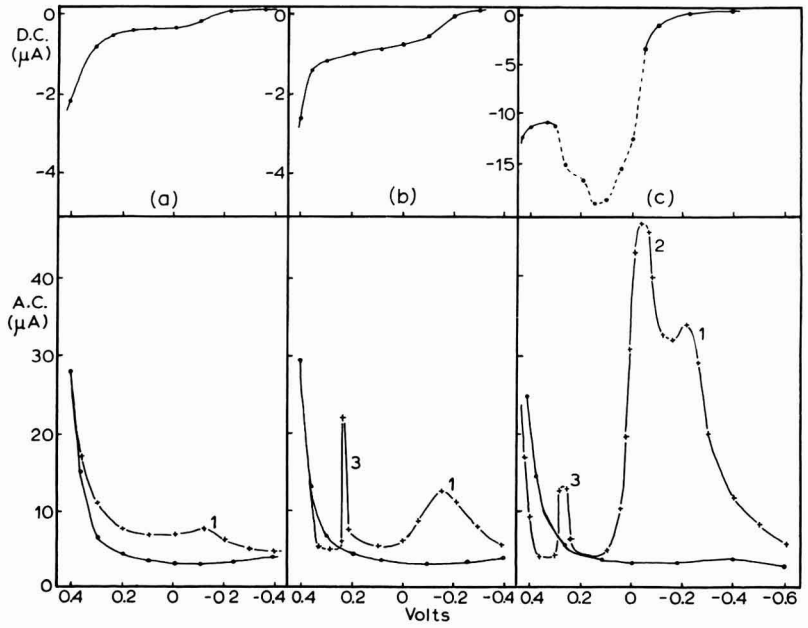

Fig. 1. A.c. and d.c. polarograms for iodide ion in 0.1 *M* KNO_3 at the following concns: (a), 9.8×10^{-5} *M*; (b), 1.9×10^{-4} *M*; (c), 1.67×10^{-3} *M*. A.c. base currents are shown. Broken curve indicates irreproducible d.c. readings.

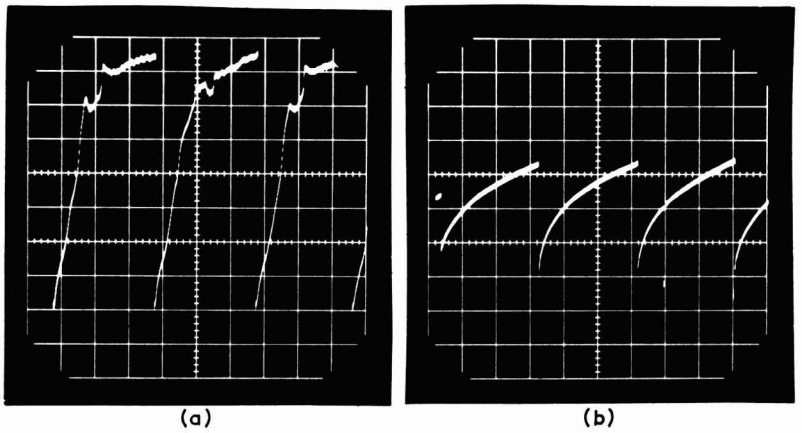

Fig. 2. Current–time curves (d.c.) for 1.67×10^{-3} *M* iodide ion in 1.0 *M* KNO_3 at: (a), 0.24 V; (b), 0.36 V.

As pointed out above, the limiting current of the iodide d.c. step is irreproducible at concentrations greater than $4 \cdot 10^{-4}$ *M*. However the fluctuations disappear at potentials more positive than +0.32 V. Between this point and the beginning of *free* mercury dissolution, a constant and reproducible limiting current is attained which is proportional to the iodide concentration at least up to 2.5×10^{-3} *M* and is of magnitude comparable to the diffusion currents of chloride and bromide obtained with the same

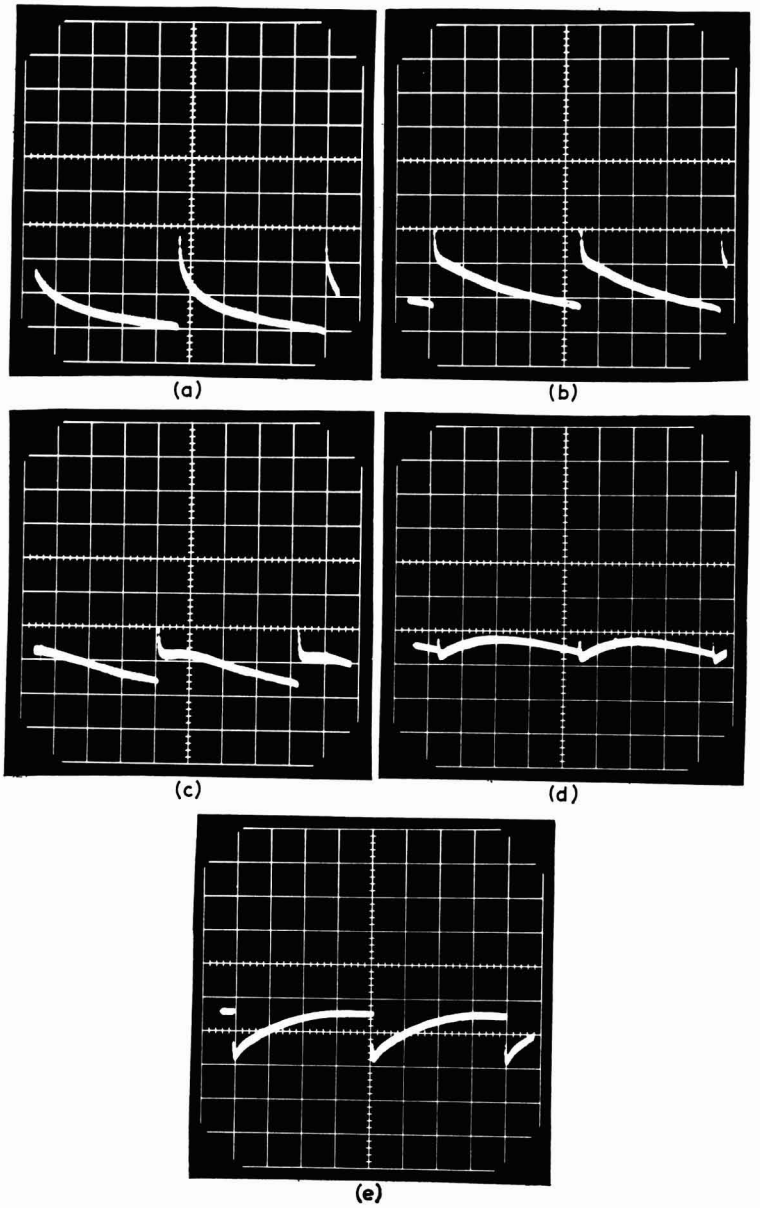

Fig. 3. Current–time curves (d.c.) at the beginning of the iodide d.c. step for 1.5×10^{-4} *M* iodide ion in 0.5 *M* H_2SO_4: (a), −0.30 V; (b), −0.22 V; (c), −0.18 V; (d), −0.14 V; (e), −0.10 V.

capillary and mercury head. It is therefore likely that this reproducible portion of the limiting current represents the true diffusion current. It is of interest to note that current–time curves corresponding to the reproducible current readings at these very positive potentials are normal in shape whereas those for the fluctuating readings show that the current varies irregularly with time and that curves at a given potential are not reproducible (Fig. 2).

In the d.c. polarograms the start of the charge transfer reaction is not at all sharply defined because of a large residual current at potentials negative to the region of discharge. Current–time curves near the start of the d.c. step (Fig. 3) change shape steadily as the potential is made more anodic, in contrast to the behaviour found with chloride and bromide where discontinuous changes are observed (*cf.* Parts I and II). There is no indication of any sudden change in the nature of the electrode process such as found for the other two halides.

Some other significant aspects of the a.c. polarographic behaviour of iodide are presented below. The concentration of iodide chosen for studying the influence of these factors is in the range where only Waves 1 and 3 appear. Under these conditions Wave 3 is best developed and the polarograms are quite reproducible.

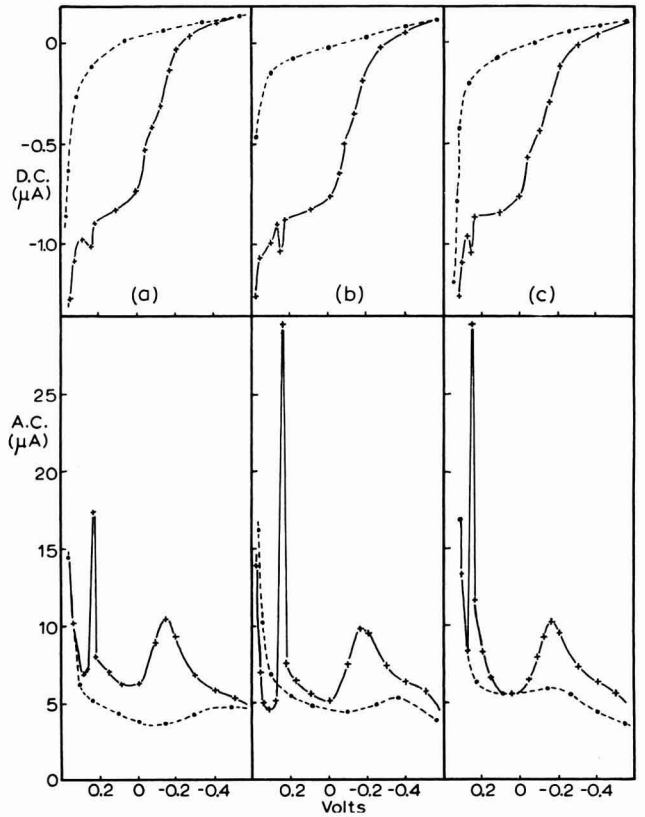

Fig. 4. A.c. and d.c. polarograms for 1.48×10^{-4} *M* iodide ion in: (a), 1.0 *M* KNO_3; (b), 0.5 *M* H_2SO_4; (c), 0.5 *M* K_2SO_4. Base and residual currents shown as broken curves. Alternating voltage 15 mV.

Supporting electrolyte effects

At an iodide concentration of 1.48×10^{-4} *M* the height and shape of both a.c. waves depends on the supporting electrolyte used (Fig. 4). However, the minimum base current between Waves 1 and 3 is fairly constant (in the range 5–6 μA under the existing conditions) in a variety of electrolytes despite the fact that at the same potential (*i.e.*, at the potential of minimum base current) the base current for the pure supporting electrolytes tested ranges from 3.5 μA in molar perchloric acid to 8 μA in phosphate buffer pH 6.8. As a result, depending on the supporting electrolyte used, the base current in this region may appear to be depressed (*e.g.*, in phosphate buffer), unchanged (*e.g.*, in half-molar potassium sulphate) or elevated to a greater or less extent (*e.g.*, in molar potassium nitrate or perchloric acid.)

Effect of mercury head

Changing the mercury head affects Waves 1 and 3, the latter to quite a marked extent can be seen from Table 1.

TABLE 1

EFFECT OF MERCURY HEAD ON WAVES 1 AND 3
1.48×10^{-4} *M* iodide in *M* $HClO_4$; alternating voltage 15 mV; $T = 25°$.

h (cm)	*Wave 1* (μA)	*Wave 3* (μA)
22	7.7	21.7
38	6.8	18.0
57	5.9	6.2

Effect of temperature

Increase in temperature raises the height of Wave 1 by about 0.5% per degree but causes a substantial lowering of Wave 3; at 60° the latter is completely eliminated (Table 2).

TABLE 2

EFFECT OF TEMPERATURE ON THE HEIGHTS OF WAVES 1 AND 3
1.48×10^{-4} *M* iodide in *M* $HClO_4$; alternating voltage 15 mV.

T (°C)	*Wave 1* (μA)	*Wave 3* (μA)
25	6.8	18.0
40	7.4	9.0
60	8.0	—

Alternating current waveforms for Wave 3

Under certain circumstances, the waveform of the alternating current is useful in interpreting the electrode process giving rise to an a.c. wave[5]. The current waveforms found with iodide, Wave 3 (Fig. 5) are seen to contain a large degree of harmonic distortion, with the implication that the a.c. wave is tensammetric in origin.

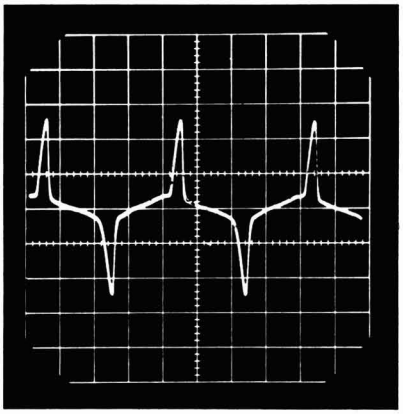

Fig. 5. Alternating current waveform for Wave 3 of iodide ion at 0.254 V (E_s).

DISCUSSION

It is evident that the polarographic behaviour of iodide ion is in many respects different from that reported for the other two halides (Parts I and II). Two quite separate a.c. waves are found, in contrast to the single chloride wave and the composite bromide wave. It is perhaps tempting to suggest that the iodide waves correspond, respectively, to the two processes postulated in the discharge of bromide ion but with a larger potential difference interposed between them. However, this idea is not supported by the experimental evidence; the sharp, more positive iodide wave, for example, corresponds to the limiting current plateau of the d.c. step rather than to the commencement of discharge as is the case with bromide. A different scheme of electrode processes is needed to account for the iodide a.c. waves.

Wave 1

The case of low concentrations of iodide, for which only Waves 1 and 3 appear will be considered first. Qualitatively, the peak of Wave 1 represents the highest point of a steady increase in current which begins at quite cathodic potentials, around −0.6 V for 1.5×10^{-4} M iodide. This current rise is wholly due to the increasing specific adsorption of iodide ions, and the consequent increase of the double-layer capacity, as the potential is made more positive[6,7]. Near the summit itself and towards more positive potentials, the start of the d.c. step is in evidence (Figs. 1 and 4), introducing the possibility that the alternating current at these potentials contains a faradaic component. However, logarithmic analysis of the iodide anodic step indicates that the charge transfer reaction is quite irreversible[2] and is therefore unlikely to give a faradaic alternating current. The whole of Wave 1 is probably non-faradaic in origin and can be considered analogous to the bromide hump, with the difference that at potentials more positive than that corresponding to the maximum capacity the surface charge density of iodide ions decreases steadily as these ions are removed by reaction with mercury. Just as in the case of the bromide hump, the height of iodide Wave 1 increases with decreasing h, indicating that adsorption equilibrium for iodide at these concentrations is also diffusion-controlled.

There is no evidence comparable with that discussed for the other halides, to indicate

that a coherent mono-layer of mercurous iodide is formed at the electrode surface. Iodide gives a very poorly defined pre-step (ref. [2] and Fig. 4) which is about half the height of the pre steps found with chloride and bromide using the same capillary. If a mono-layer is in fact formed it is not likely to possess the compact, crystalline structure envisaged for calomel and mercurous bromide films. This conclusion gains support from results obtained in electron microscope and diffraction studies[8] which show that the anodic film of mercurous iodide exists as a rather loosely organized deposit rather than as a specifically oriented layer.

The alternating current in the region between Waves 1 and 3 depends very little on the supporting electrolyte used and may be higher or lower than the base current in the absence of iodide. It seems that the interface capacity is determined wholly by the presence of the film of mercurous salt, as it is independent of the capacity found with supporting electrolyte alone. In this respect mercurous iodide does not behave as a simple uncharged surfactant which would lower the base current under all circumstances. The suggestion[2] that the iodide end of the mercury salt is oriented away from the metal surface and that, as a result, the salt behaves like an anionic surface active substance could possibly explain these results but the matter needs further investigation.

Wave 2

Wave 2 is associated with the appearance of irregular fluctuations in the d.c. readings. The presence of a mercurous iodide film is doubtless responsible for these irregularities[1] which seem to result from convective disturbances at the electrode surface and/or in the surrounding solution. It is known that the mercurous iodide film produces a marked lowering in the interfacial tension[2] and disturbances at the interface probably arise when the film does not crystallise uniformly over the electrode surface. If this is so, the portion of the d.c. step where these irregularities occur is a kind of polarographic maximum; this conclusion is borne out by comparing current–voltage curves in the presence and absence of gelatin[1] or by recognising that the lowered current at very positive potentials corresponds to the true diffusion current.

A connection between a.c. waves and d.c. maxima has been noted previously[9]. It is also known that, even when the electrode process appears to be irreversible, a.c. waves can occur together with d.c. maxima, *e.g.*, in the reduction of hexammine cobalt(III) ion and in the oxidation of ascorbic acid (unpublished results obtained in this laboratory). Wave 2 of iodide appears to be an example of this effect and its presence cannot be taken to indicate the occurrence of a reversible charge transfer process.

Wave 3

This a.c. wave is almost certainly tensammetric in nature, *i.e.*, it arises from a sharp change in surface charge density brought about by an adsorption/desorption process. The evidence for this view is as follows:

(a) The wave is sharp, narrow and very high, at least for low iodide concentrations.

(b) There is no corresponding d.c. step, only a small kink in the iodide diffusion current (Fig. 4).

(c) The base current between Waves 1 and 3 differs from that for supporting electrolyte alone but on the positive side of Wave 3 the two base currents correspond fairly closely.

(d) The amount of distortion in the alternating current waveforms is comparable with that found for waves of known tensammetric origin[5].

(e) The wave decreases in height with increasing temperature and is completely eliminated at a sufficiently high temperature (*cf.* BREYER AND HACOBIAN[10]).

(f) Wave 3 is clearly associated with the disappeareance of irregularities in the iodide limiting current at concentrations above *ca.* $4 \cdot 10^{-4}$ *M*. Since these irregularities are presumably due to a film of mercurous iodide on the electrode surface, it is reasonable to suppose that wave 3 represents the desorption of this film, or at least a severe change in its structure. KOLTHOFF AND OKINAKA[2] have presented electrocapillary curves which support this conclusion; the curves show a break at about +0.3 V which is interpreted by these authors to indicate that the mercurous iodide film breaks down at this potential.

ACKNOWLEDGEMENTS

The author wishes to thank Dr. B. BREYER AND Dr. H. H. BAUER for many stimulating discussions and the Commonwealth Scientific and Industrial Research Organization for the award of a Studentship.

SUMMARY

A.c. polarograms of iodide ion at concentrations less than $4 \cdot 10^{-4}$ *M* show two separate waves, one of which occurs near the potential region of the anodic d.c. step and is probably due to adsorption of iodide ion and the other at a considerably more positive potential, resulting from desorption of mercurous iodide from the electrode surface. At higher iodide concentrations a third a.c. wave is evident and is connected with the occurrence of convection phenomena at the electrode surface.

REFERENCES

1 I. M. KOLTHOFF AND C. S. MILLER, *J. Am. Chem. Soc.*, 63 (1941) 1405.
2 I. M. KOLTHOFF AND Y. OKINAKA, *J. Am. Chem. Soc.*, 83 (1961) 47.
3 B. BREYER AND S. HACOBIAN, *Australian J. Sci. Research*, A4 (1951) 610.
4 Y. TAKEMORI AND I. TACHI, *Bull. Chem. Soc. Japan*, 28 (1955) 151.
5 T. BIEGLER, *Australian J. Chem.*, 15 (1962) 34.
6 D. C. GRAHAME, *Chem. Rev.*, 41 (1947) 441.
7 D. C. GRAHAME, M. A. POTH AND J. I. CUMMINGS, *J. Am. Chem. Soc.*, 74 (1952) 4122.
8 E. H. BOULT AND H. R. THIRSK, *Trans. Faraday Soc.*, 50 (1954) 404.
9 B. BREYER AND H. H. BAUER, *Australian J. Chem.*, 9 (1956) 425.
10 B. BREYER AND S. HACOBIAN, *Australian J. Sci. Research*, A5 (1952) 500.

APPLICATION OF OSCILLOGRAPHIC POLAROGRAPHY IN QUANTITATIVE CHEMICAL ANALYSIS*

XX.* THE OSCILLOGRAPHIC DETERMINATION OF TRACE AMOUNTS OF HEAVY METALS IN HYDROCHLORIC ACID, PURE ALUMINIUM AND ZIRCONIUM.

PŘEMYSL BERAN, JAN DOLEŽAL AND DUŠAN MRÁZEK

Department of Analytical Chemistry, Charles University, Praha (Czechoslovakia)

(Received March 2nd, 1963)

The present rapid development of semi-conductor devices, powder metallurgy and other branches of technology requires the preparation of very pure substances, especially metals, since slight amounts of impurities often cause large changes in the properties of many materials. Spectrographic, photometric, radiochemical and certain other methods have already been used for some time for the determination of trace amounts of metals; the method of oscillopolarographic microanalysis has lately been developed[1]. This method is based on a preliminary concentration and separation of a metal into the mercury cathode by electrolytical means; an oscillopolarographic analysis is made on the amalgam thus formed. Electrolysis is usually carried out by means of a superimposed current, for the sake of speed and convenience, although procedures with superimposed voltage have also been proposed[2]. The mercury cathodes which have been employed are:

(i) a cup-shaped mercury electrode[3];

(ii) a hanging drop electrode obtained by (a) pressing mercury out of a capillary[4], (b) precipitating mercury on to a platinum wire[5], or (c) hanging a drop of mercury on a silver wire.

The electrode (c), proposed by MICKA[6], is the most suitable one for oscillopolarographic measurements.

REAGENTS AND APPARATUS

Analytical grade reagents were unsuitable in some instances and required further purification before use, since the impurities contained in them gave rise to high blank values. Doubly-distilled water was further purified by repeated distillation in a silica apparatus. Hydrochloric acid, AR, was purified by double distillation of the azeotropic mixture in a silica distillation apparatus, or by saturating doubly-distilled water with gaseous hydrogen chloride, obtained from hydrochloric acid by the addition of sulphuric acid. Dilute sulphuric acid (5 *M*, analytical grade product of the Lachema Company) was purified by continuous electrolysis with a direct current of 100–200 mA by the following method. A special covered electrolyser of about 400-ml capacity

* XIX, *Collection Czech. Chem. Commun.*, 27 (1962) 2365.

was provided with a layer of mercury on the bottom, to serve as cathode, the anode was a platinum net electrode. Agitation was provided by energetic evolution of hydrogen. The purified acid could be removed from the electrolyser without interruption of the current but the contaminated mercury at the bottom had to be replaced after some time. This method allowed the purification of about 400 ml of 5 *M* sulphuric acid per week.

A standard aluminium chloride solution, 1 *M*, was prepared by first dissolving Merck aluminium chloride, purissimum grade, in concentrated hydrochloric acid. The solution was purified electrolytically using the following method. The cathode was a larger cup-shaped mercury electrode, of volume 0.5 –1.0 ml and the anode a platinum wire of area about 1 cm^2, or a spectroscopic carbon. Since the anode was corroded extensively by the chlorine evolved during electrolysis, the anodic space was separated by a glass tube with a sealed-in sintered glass plate, type S3-Sial. 100 ml of the solution was electrolysed for a period of 10 h, by a current of 200 mA, the mercury in the cup-shaped electrode being replaced every half hour. The purified solution was mixed by an electromagnetic stirrer. The hydrochloric acid concentration in the unpurified aluminium chloride solution was purposely higher than the required strength (1 *M*), since the acid concentration decreases in the course of electrolysis. In order to prepare an aluminium chloride solution of definite acid molarity, an aliquot of the purified solution (100 ml) was concentrated by gradual evaporation in a silica crucible to a syrup-like consistency. The required amount of doubly-distilled hydrochloric acid was added and the solution was transferred into a volumetric flask and made up to the initial volume. The same procedure was used for the dissolution of aluminium samples for analysis, *i.e.*, an aluminium chloride solution prepared in this way could be used in the analysis of samples by means of the dilution method.

The technique of ion exchange chromatography[7,8] was also employed for the purification of the aluminium chloride solution. Aluminium chloride was dissolved in dilute HCl (1 : 1) to obtain a solution 1 *M* with respect to $AlCl_3$. This solution was passed twice through a column of the strongly basic anion exchange Wofatit L 150 (flow rate 100 ml/h, column height 25 cm). An aliquot of the resulting solution, from which most of the copper and all but minute traces of iron had been removed, was evaporated in a beaker until crystals of aluminium chloride appeared. The evaporated solution was transferred quantitatively into a volumetric flask and made up to the initial volume. This solution was again passed twice through the ion exchange column, which had previously been regenerated by 100 ml of distilled water. At the hydrochloric acid concentration then pertaining in the solution lead, zinc and cadmium were removed practically quantitatively. This purification procedure required only one-third of the time necessary for electrolytical purification.

A 0.25 *M* $ZrOCl_2$ solution in 1 *M* hydrochloric acid was prepared by dissolving 2.28 g of pure zirconium (product of Johnson, Matthey and Co., London) in a mixture of 40 ml of doubly-distilled hydrochloric acid and 2 ml of concentrated hydrofluoric acid, and making up to 100 ml. The procedure for the purification of zirconyl chloride is similar to that for the purification of aluminium chloride, although the possibility of hydrolysis in the course of the electrolysis or evaporation of zirconyl chloride solutions is far more acute, because of the chemical character of zirconium.

0.01 *M* solutions of copper, cadmium, lead and zinc were prepared from the pure metals (product of Soyuzkhimexport, Moscow, extra purissimum grade); more dilute

solutions were obtained by precise dilution of these solutions. Solutions of other depolarisers were prepared by dissolving analytical reagent grade salts.

All measurements were carried out with the Type P 576 Polaroscope. Perfect synchronisation of the switching from electrolysis to alternating current polarisation was ensured by using the arrangement proposed by BERAN[9], which permits adjustment to delayed exposure. The delayed exposure is necessary, because the first oscillopolarographic curves, formed after switching from electrolysis to alternating current polarisation, develop badly. The synchronisation mechanism connected with the electromotor of the photographic camera Praktina (manufactured by Kamerawerke, Dresden) permits a fully automatic registration. The exposure time used was 1/30 sec; the diaphragm, f 2; the film, Afga Isopan Rapid and the exposure delay, 1/5 sec. The polarisable electrode was a stationary electrode as described by MICKA[6]. In order to ensure perfect reproducibility of the oscillopolarographic curves, it was necessary to keep the volume of the hanging mercury drop constant. This was done by using a polarographic capillary with mercury reservoir[2], from which the mercury drop, after separation by means of an electromagnetic hammer was caught up on a glass spoon and hung on to a silver wire by contact only. The weight of the mercury drop was 0.0085 g. The capillary was not submerged in water, so that it was unnecessary to dry the mercury and the droplet was caught up on to the wire more easily. A platinum wire spiral, of surface area about 2 cm^2, or a carbon electrode was used as the non-polarisable electrode. Since electrolysis was carried out in hydrochloric acid medium, chlorine was liberated in the course of electrolysis and interfered to a very considerable extent. The comparison electrode was therefore separated from the solution by means of a glass tube with a sintered glass plate, Type S3, sealed into it. The electrolyte in the separated space was 1 N sulphuric acid, electrolytically purified. The solutions were agitated by an electromagnetic stirrer of high output; agitation was interrupted for about 5 sec before the end of electrolysis and the ensueing registration of the curve.

EXPERIMENTAL

In order to test the suitability of hydrochloric acid as solvent for the determination of impurities in aluminium and zirconium, it was necessary to study the suitability of this acid as supporting electrolyte by means of the conventional oscillopolarographic method, and to apply the results obtained to oscillopolarographic microanalysis. The results of these measurements are given in Tables 1–3. Quotients, Q; depolarisation potentials, E_{dep}, and sensitivities of the detection of individual depolarisers, pD, were measured in 1 M, 2 M and 8 M hydrochloric acid.

The results show, that about 10^{-2} % copper, lead, cadmium, zinc and bismuth in aluminium may be determined by means of conventional oscillopolarography, using the method of comparative titration or of standard additions. The optimum hydrochloric acid concentration for the detection or simultaneous determination of these depolarisers is 1–2 M. At lower concentrations the bismuth incision shifts to the left-hand edge of the curve; at higher hydrochloric acid concentrations the sensitivity of the detection and determination of zinc decreases and in 8 M hydrochloric acid the zinc incision is lost.

In 1 M $AlCl_3$ (1 M HCl) it has been found possible to detect as little as: 0.033% Cd, 0.019% Cu, 0.061% Pb, 0.062% Bi and 0.019% Zn (calculated as a percentage of the aluminium metal content) see Fig. 1.

TABLE 1

DEPOLARISATION POTENTIALS, Q-QUOTIENTS AND DETECTION LIMITS OF INORGANIC DEPOLARISERS IN HYDROCHLORIC ACID SOLUTIONS

1 M HCl					*2 M HCl*					*8 M HCl*				
Metal	*Incision*	E_{dep} *(V)*	*Q*	*pD*	*Metal*	*Incision*	E_{dep} *(V)*	*Q*	*pD*	*Metal*	*Incision*	E_{dep} *(V)*	*Q*	*pD*
Bi	C	−0.09	0.10	6.4	Bi	C	−0.09	0.10	6.4	Bi	C	−0.22	0.13	5.4
	A	−0.09	0.10			A	−0.09	0.10			A	−0.22	0.13	
Cu	C	−0.27	0.21	6.13	Cu	C	−0.27	0.21	6.42	Cu	C	−0.42	0.28	6.4
	A	−0.27	0.21			A	−0.27	0.21			A	−0.42	0.28	
Pb	C	−0.39	0.33	5.54	Pb	C	−0.44	0.34	5.73	Pb	C	−0.59	0.40	5.8
	A	−0.39	0.33			A	−0.44	0.34			A	−0.59	0.40	
Cd	C	−0.61	0.47	5.87	Cd	C	−0.62	0.48	5.9	Cd	C	−0.75	0.60	6.06
	A	−0.61	0.47			A	−0.62	0.48			A	−0.75	0.60	
Zn	A	−0.87	0.69	6.04	Zn	A	−0.88	0.70	5.77	Tl	C	−0.67	0.54	4.7
Tl	C	−0.48	0.38	5.1	Tl	C	−0.49	0.38	5.0		A	−0.67	0.54	
	A	−0.48	0.38			A	−0.49	0.38		In	C	−0.67	0.55	
In	C	−0.59	0.44		In	C	−0.58	0.44			A	−0.67	0.55	5.94
	A	−0.56	0.42	5.64		A	−0.58	0.44	5.94	As	C	−0.45	0.31	5.8
As	C_1	−0.25	0.20	6.12	As	C_1	−0.17	0.13	5.98	Sb	C	−0.28	0.17	5.57
	C_2	−0.9	0.69	5.8		C_2	−0.87	0.67	5.42		A	−0.28	0.17	
	A	−0.25	0.20			A	−0.13	0.11		Sn	C	−0.59	0.41	6.45
Sb	C_1	−0.15	0.11	6.44	Sb	C_1	−0.16	0.13	6.6		A	−0.59	0.41	5.45
	C_2	−0.22	0.20	6.22		C_2	−0.23	0.20	6.31					
	C_3	−1.07	0.80	5.54		C_3	−1.04	0.79	5.53					
	A	−0.15	0.11			A_1	−0.16	0.13						
Sn	C	−0.48	0.38	6.23		A_2	−0.23	0.20						
	A	−0.48	0.38		Sn	C	−0.48	0.36	6.15					
						A	−0.48	0.36	6.02					

C; cathodic incision
A; anodic incision

The depolarisation potentials E_{dep}, have been measured in the conventional manner[10] against a saturated calomel electrode.

Since the incisions of the depolarisers in 1 *M* hydrochloric acid are sufficiently mutually distinguished by their potentials, acid of this strength was used as the supporting

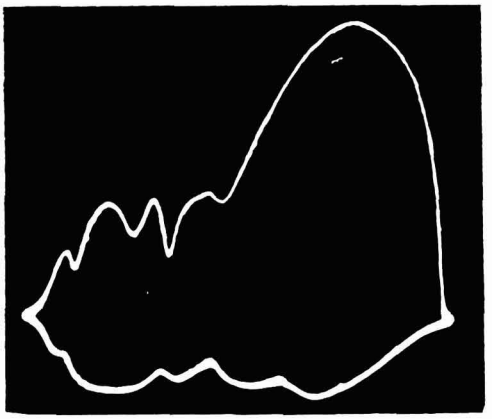

Fig. 1. $dE/dt = f(E)$, curve for mixture of Bi, Cu, Pb, Cd, Zn, each at concn. 10^{-4} *M*, in 1 *M* $AlCl_3$ (1 *M* HCl); dropping electrode.

electrolyte for the determination of impurities in hydrochloric acid, aluminium and zirconium by the method of oscillopolarographic microanalysis. There are, however, certain limitations because oscillopolarographic curves obtained on the hanging-drop mercury electrode are not developed perfectly in the vicinity of the edge points. For instance, it is impossible to use analytically the cathodic bismuth incision at −0.09 V.

DETERMINATION OF IMPURITIES IN HYDROCHLORIC ACID

Copper, lead, cadmium and zinc at concentrations of about 10^{-7} *M* have been determined in 1 *M* hydrochloric acid by means of the calibration curve method, with a mean relative error of 9%. At low concentrations it was possible to use doubly-distilled hydrochloric acid diluted with doubly-distilled water as the pure standard.

Electrolysis was carried out for 2 min by a direct current of 12.5 mA; after switching over to alternating current polarisation, the photographic registration was carried out, using an alternating current component of 1.7 mA (exposure delay 1/5 sec). As long as the cathode was not replaced, the amalgam formed had to be dissolved by an alternating current of 2 min duration. The behaviour of several depolarisers which are currently present in hydrochloric acid, aluminium and zirconium was studied under the described conditions.

The influence of bi- and tri-valent iron, cobalt, nickel and chromium was investigated. These metals, with the exception of chromium, do not give oscillopolarograms in hydrochloric acid but they do influence the depth of incisions, especially those of copper and zinc, and at high concentrations (from 10^{-4} *M* upward) they make the determination of these depolarisers impossible. KALVODA[3] explains the influence of Fe^{2+} on the depth of zinc incisions by postulating the formation of inter-metallic compounds

TABLE 2

INFLUENCE OF SOME IONS ON THE DETERMINATION OF Cu, Pb, Cd AND Zn IN HYDROCHLORIC ACID SOLUTIONS

Metal	*Concn. taken* ($\times 10^{-7}$ *M*)	*Concn. of accompanying element*	*Concn. found* ($\times 10^{-7}$ *M*)	*Deviation* ($\times 10^{-7}$ *M*)	*Rel. deviation* (%)
		Fe^{2+}			
Cu	3.20	0	3.15	−0.05	−1.6
Pb	6.05		6.40	0.35	5.8
Cd	4.25		4.40	0.15	3.5
Zn	6.65		7.40	0.75	11.3
Cu	3.20	8.5×10^{-6} *M*	2.95	−0.25	−7.8
Pb	6.05		6.40	0.35	5.8
Cd	4.25		4.45	0.20	4.7
Zn	6.65		6.45	−0.20	−3.0
Cu	3.15	6.75×10^{-5} *M*	2.25	−0.90	−28.6
Pb	6.05		6.15	0.10	1.7
Cd	4.25		4.20	−0.05	−1.2
Zn	6.60		3.45	−3.15	−47.7
		Fe^{3+}			
Cu	2.15	0	2.10	−0.05	−2.3
Pb	4.25		4.90	0.65	15.3
Cd	4.25		3.95	−0.30	−7.1
Zn	6.40		7.25	0.85	11.7
Cu	2.15	2.55×10^{-5} *M*	2.05	−0.10	−4.6
Pb	4.25		4.65	0.40	9.4
Cd	4.25		3.90	−0.35	−8.2
Zn	6.40		5.05	−1.35	−21.1
Cu	2.10	1.70×10^{-4} *M*	1.30	−0.80	−38.1
Pb	4.20		4.65	0.45	10.7
Cd	4.20		3.00	−1.20	−28.5
Zn	6.30		×	×	×
		Co^{2+}			
Cu	4.90	0	4.70	−0.20	−4.1
Pb	1.45		1.70	0.25	17.2
Cd	4.15		3.70	−0.45	−10.9
Zn	6.15		6.60	0.45	7.3
Cu	4.90	9.85×10^{-6} *M*	4.35	−0.55	−11.2
Pb	1.45		1.40	−0.05	−3.5
Cd	4.15		3.00	−0.15	−27.7
Zn	6.15		3.45	−2.70	−43.9
Cu	4.85	7.80×10^{-5} *M*	2.30	−2.55	−100
Pb	1.45		1.65	0.20	13.8
Cd	4.15		3.95	−0.20	−4.8
Zn	6.10		×	×	×
		Ni^{2+}			
Cu	3.65	0	3.45	−0.20	−5.5
Pb	1.20		0.80	−0.40	−33.3
Cd	4.90		4.95	0.05	1.0
Zn	11.0		9.05	−1.95	−17.6
Cu	3.65	9.80×10^{-6} *M*	3.30	−0.35	−9.6
Pb	1.20		0.75	−0.45	−37.5
Cd	4.90		4.85	−0.05	−1.0
Zn	11.0		3.20	−7.80	−100
Cu	3.65	7.80×10^{-5} *M*	0.10	−3.55	−100
Pb	1.20		0.70	−0.50	−41.7
Cd	4.90		4.60	−0.30	−6.1
Zn	11.0		×	×	×

Metal	*Concn. taken* ($\times 10^{-7}$ *M*)	*Concn. of accompanying element*	*Concn. found* ($\times 10^{-7}$ *M*)	*Deviation* ($\times 10^{-7}$ *M*)	*Rel. deviation* (%)
		Cr^{3+}			
Cu	8.55	0	7.40	−1.15	−11.5
Pb	0.75		0.60	−0.14	−18.9
Cd	6.10		5.50	−0.60	−9.8
Zn	2.45		2.55	0.10	4.1
Cu	8.55	9.80×10^{-6} *M*	6.25	−2.30	−26.9
Pb	0.74		−5.20	−0.22	−29.7
Cd	6.10		5.50	−0.60	−9.8
Zn	2.45		2.35	−0.10	−4.1
Cu	8.55	2.95×10^{-5} *M*	4.45	−4.10	−48.0
Pb	0.74		0.55	−0.19	−25.7
Cd	6.10		5.65	−0.45	−7.4
Zn	2.45		×	×	×
		Co^{2+}			
Cu	1.30	2.40×10^{-4} *M*	×	×	×
Pb	2.85		2.20	−0.65	−22.8
Cd	7.15		4.95	−2.20	−30.8
Zn	7.15		×	×	×
		Ni^{2+}			
Cu	1.85	2.35×10^{-4} *M*	×	×	×
Pb	9.35		10.15	0.80	8.6
Cd	9.36		9.10	−0.25	−2.7

× ; no measurable incision formed

of the type $Zn_xFe_yHg_z$[11,12], which dissociate very slowly. The metals mentioned are chemically very much alike and it is therefore possible to make a similar assumption also for Co^{2+}, Ni^{2+}, Fe^{3+} and Cr^{3+}.

Copper cannot be determined accurately at high concentrations because of the low solubility of copper in mercury. As a result, mercury loses the properties of a fluid when copper is present in excess because of the influence of the precipitated metal.

The results of this study are presented in Table 2 and it can be seen that at Fe^{2+}, Fe^{3+}, Co^{2+}, Ni^{2+} and Cr^{3+} concentrations of 10^{-5} *M*, copper and zinc incisions are already substantially influenced (errors reach 100%) and that at concentrations of 10^{-4} *M* determination of copper and zinc often becomes completely impossible. The depolarisers mentioned have less influence on the depth of lead and cadmium incisions.

In the course of the analysis of hydrochloric acid, incisions which did not correspond to the presence of any of the depolarisers studied, sometimes appeared on the oscillopolarographic curves. They were therefore of adsorptive character. In these cases it was necessary to renew the electrode by cutting off the end of the silver wire and hanging on a fresh mercury drop. It has also been found, that after prolonged electrolysis on to one mercury drop, the drop is partially dissolved and the oscillogram increases in the vertical direction. For these reasons, the mercury drop on the stationary electrode should be replaced frequently.

In order to determine these metals at very low concentrations, corresponding to the impurity contents of "pure", "analytical grade" and doubly-distilled hydrochloric acid, the value of the blank experiment must be decreased, *i.e.*, it is impossible to use

doubly-distilled hydrochloric acid diluted with doubly-distilled water as the pure standard. Another method for quantitative evaluation was therefore proposed.

The incision depth is proportional to the amalgam concentration ($h = fC_a$); furthermore, the amalgam concentration is a function of the duration of electrolysis (t) and the concentration of the depolariser in the solution analysed (C_r)[3].

$$C_a = K\frac{C_r t}{V_{Hg}} = kC_r t$$

Since equal incision depths must correspond to equal amalgam concentrations, the following relation must also be valid:

$$h \sim C_a = kC_r' t' = kC_r'' t''$$

The validity of this relation has been proved experimentally by means of the oscillographic analysis of a 0.99×10^{-7} M Cu^{2+} solution for various times of electrolysis. The dependence of the incision depth obtained, on the time of electrolysis has been plotted in equal units, and compared with a calibration curve for copper, measured at a constant time of electrolysis, $t = 2$ min. The two curves are in reasonable agreement.

Let us assume, that a solution is electrolysed for a time t_x, until well-developed incisions form. After oscillopolarographic analysis with photographic registration the time of electrolysis is shortened to t. Three standard additions of the corresponding depolariser are then added, selected in such away that, after the third addition, incisions formed are a little deeper than in the initial solution (with longer duration of electrolysis). A calibration curve is prepared by plotting incision depth against the concentration of depolariser added. The initial concentration C_x in the solution studied is calculated thus:

$$(C_x + C)t = C_x t_x$$

$$C_x = C\frac{t/t_x}{1 - t/t_x} = C\frac{t}{t_x - t}$$

When the time of electrolysis is, for instance, shortened to half its original value, *i.e.*, $t = t_x/2$, the relation $C_x = C$ is valid, meaning that the depolariser concentration read from the calibration curve is in this case directly the concentration required.

The precision of the proposed method has been tested for short times of electrolysis *i.e.*, 2 min and 5 min (Table 3). The mean relative error at $t = 2$ min was 17%. At $t = 5$ min, it was 20% as positive errors were prevalent, since the influence of impurities in the doubly-distilled hydrochloric acid used as the pure standard, became manifest.

The method described has also been used for determining impurities in pure, analytical-grade and doubly-distilled hydrochloric acid at longer electrolysis times. Before adding the standard additions the duration of electrolysis was always shortened by one-half. In all cases the acid analysed was diluted in such a way, as to make the solution 1 M with respect to hydrochloric acid. Using electrolysis times of 30 and 15 min the authors have succeeded in determining 4.9×10^{-7}% Cu, 9.0×10^{-7}% Pb and 4.2×10^{-7}% Zn in doubly-distilled hydrochloric acid (Table 4), corresponding to concentra-

TABLE 3

THE DETERMINATION OF Cu, Pb, Cd AND Zn IN SYNTHETIC HYDROCHLORIC ACID SAMPLES
Duration of electrolysis: Nos. 1 to 4, t = 2 and 1 min; Nos. 5 to 8, t = 5 and 2.5 min.

No.	*Metal*	*Incision*	*Concn. taken* ($\times 10^{-7}$ *M*)	*Concn. found* ($\times 10^{-7}$ *M*)	*Deviation* ($\times 10^{-7}$ *M*)	*Rel. deviation* (%)
1	Cu	C	9.62	10.7	1.08	11.2
	Pb	C	4.81	5.37	0.56	11.7
	Cd	A	9.62	8.95	−0.67	−7.0
	Zn	A	14.4	17.3	2.9	20.1
2	Cu	C	4.86	5.10	0.24	4.9
	Pb	C	3.65	5.36	1.71	46.7
	Cd	A	9.62	8.30	−1.32	−13.7
	Zn	A	9.62	7.31	−2.31	−24.1
3	Cu	C	7.23	8.20	0.97	13.4
	Pb	C	2.70	3.16	0.46	17.0
	Cd	A	14.4	14.1	−0.3	−2.1
	Zn	A	12.1	14.1	2.0	16.5
4	Cu	C	12.0	11.7	−0.3	−2.5
	Pb	C	6.02	8.15	2.13	35.4
	Cd	A	12.0	11.7	−0.3	−2.5
	Zn	A	7.22	5.57	−1.65	−22.8
5	Cu	C	2.62	2.51	−0.11	−4.2
	Pb	C	2.10	3.02	0.92	43.8
	Cd	A	4.74	5.43	0.69	14.2
	Zn	A	5.04	5.86	0.82	16.3
6	Cu	C	1.66	1.90	0.24	14.5
	Pb	C	1.81	2.12	0.31	−17.1
	Cd	A	2.31	1.77	−0.54	−23.3
	Zn	A	2.61	2.94	0.33	12.7
7	Cu	C	1.92	2.32	0.40	20.8
	Pb	C	1.63	1.61	−0.02	−1.2
	Cd	A	1.91	1.37	−0.54	−28.3
	Zn	A	2.44	2.66	0.22	9.0
8	Cu	C	2.11	2.26	0.15	7.1
	Pb	C	1.36	1.57	0.21	15.5
	Cd	A	2.32	1.89	−0.43	−18.5
	Zn	A	2.16	1.61	−0.55	−25.4

C; cathodic incision
A; anodic incision

tions of 1.4×10^{-8} *M* Cu, 7.9×10^{-9} *M* Pb and 1.1×10^{-8} *M* Zn in 1 *M* hydrochloric acid obtained by dilution of doubly-distilled hydrochloric acid. Doubly-distilled water, purified by further electrolysing for 15 h, was always used to dilute the acid.

DETERMINATION OF HEAVY METAL TRACES IN PURE ALUMINIUM

The simultaneous determination of traces of copper, lead, cadmium and zinc in very pure alumium has been studied by using so-called "synthetic" samples. These were prepared having regard to the usual levels of impurities in aluminium of 99.99%–99.999%

TABLE 4

THE DETERMINATION OF IMPURITIES IN HYDROCHLORIC ACID

(a) Content of impurities in "pure" hydrochloric acid (Duration of electrolysis, t = 10 and 5 min.)

No.	$\times 10^{-6}\%$ *Cu*	$\times 10^{-6}\%$ *Pb*	$\times 10^{-6}\%$ *Zn*
1	4.4	6.7	8.8
2	3.2	6.9	6.7
3	4.2	6.1	11.1
4	3.2	6.5	6.4
5	3.8	5.7	10.1
mean	3.8	6.4	8.6

(b) Content of impurities in "analytical-grade" hydrochloric acid (Duration of electrolysis, t = 12 and 6 min.)

No.	$\times 10^{-6}\%$ *Cu*	$\times 10^{-6}\%$ *Pb*	$\times 10^{-6}\%$ *Zn*
1	6.3	6.9	5.7
2	5.8	3.8	5.8
3	5.2	4.6	5.2
4	5.1	5.5	4.1
5	6.8	4.2	5.4
mean	5.8	5.0	5.2

(c) Content of impurities in doubly-distilled hydrochloric acid (Duration of electrolysis, t = 30 and 15 min.)

No.	$\times 10^{-6}\%$ *Cu*	$\times 10^{-6}\%$ *Pb*	$\times 10^{-6}\%$ *Zn*
1	5.3	7.1	4.3
2	4.6	8.4	4.1
3	4.9	8.8	4.1
4	4.2	11.1	4.7
5	5.3	9.8	3.6
mean	4.9	9.0	4.2

purity. 40 ml of a purified 1 *M* $AlCl_3$ solution in 1 *M* hydrochloric acid (aluminium is not precipitated on the mercury electrode; its potential is more negative than the evolution potential of hydrogen) was pipetted into the electrolytic vessel (a 50-ml beaker). The required amounts of 10^{-4} *M*–10^{-5} *M* standard solutions of the depolarisers to be determined were added successively. The dilution method was used for the analysis, in order to eliminate any possible interference by impurities. Individual synthetic samples were electrolysed for 2–5 min depending on the content of depolarisers, by a direct current of 12.5 mA under constant agitation. The amalgam was then analysed oscillopolarographically with photographic registration. Agitation was always stopped 4 sec before the exposure, in order to achieve a stable picture. After dilution of the solution of the sample at a ratio of 1 : 1 by a purified aluminium chloride solution, three standard additions of the individual depolarisers were made. These were selected so that the incisions obtained after the third addition were slightly deeper than for the initial solution. The corresponding oscillopolarographic curves were registered twice, in order to eliminate any possible interference. Calibration curves were plotted from the results obtained. The depolariser concentration in the solution in-

TABLE 5

THE DETERMINATION OF IMPURITIES IN SYNTHETIC ALUMINIUM SAMPLES

Sample no.	*Metal*	*Concn. taken* ($\times 10^{-4}$%)	*Concn. found* ($\times 10^{-4}$%)	*Rel. deviation* (%)	*Sample no.*	*Metal*	*Concn. taken* ($\times 10^{-4}$%)	*Concn. found* ($\times 10^{-4}$%)	*Rel. deviation* (%)
1	Cu C	2.75	3.06	11.3	8	Cu	0.33	0.33	0
	Pb C	10.8	11.2	3.7		Pb	12.5	11.0	−12.3
	Cd A	7.79	7.34	−5.8		Cd	8.71	7.87	−9.6
	Zn A	4.52	4.26	−5.8		Zn	4.50	3.72	−17.2
2	Cu C	4.44	4.09	−7.9	9	Cu	3.55	3.74	5.3
	Pb C	5.46	5.53	1.3		Pb	13.5	13.6	0.6
	Cd A	6.88	5.84	−15.1		Cd	7.75	6.83	−11.8
	Zn A	3.14	2.55	−18.8		Zn	0.44	0.38	−15.3
3	Cu C	5.15	4.49	−12.9	10	Cu	3.88	4.07	4.7
	Pb C	12.4	13.5	9.1		Pb	12.7	13.7	7.9
	Cd A	7.67	6.97	−9.2		Cd	0.20	0.21	7.4
	Zn A	5.30	4.72	−10.9		Zn	5.34	5.80	8.6
4	Cu C	1.69	1.36	−20.2	11	Cu	2.25	2.47	9.4
	Pb C	6.46	6.92	7.1		Pb	0.64	0.72	13.3
	Cd A	3.00	2.87	−4.3		Cd	5.96	4.78	−19.6
	Zn A	2.90	3.12	7.6		Zn	3.75	4.30	14.8
5	Cu C	0.55	0.52	5.5	12	Cu	2.25	2.11	−6.3
	Pb C	10.8	10.2	−5.3		Pb	0.64	0.69	8.4
	Cd A	6.79	6.33	−6.8		Cd	5.96	5.20	−12.6
	Zn C	3.94	3.66	−32.5		Zn	3.75	3.92	4.5
6	Cu	0.54	0.66	20.8	13	Cu	1.98	1.93	−2.4
	Pb	13.3	13.8	3.9		Pb	10.2	10.3	1.5
	Cd	7.71	7.08	−8.1		Cd	5.5	7.16	30.3
	Zn	3.92	3.75	−4.3		Zn	0.20	0.12	−40.5
7	Cu	4.33	4.68	8.2					
	Pb	13.3	13.9	4.6					
	Cd	9.08	8.78	−3.2					
	Zn	0.53	0.51	−3.7					

C; cathodic incision
A; anodic incision

vestigated was obtained by multiplying the concentration read from the curves, by a factor of 2.

The mean relative error in the determination of copper, lead, cadmium and zinc in 1 *M* $AlCl_3$ (1 *M* HCl) at concentrations of 10^{-6}–10^{-7} *M* (10^{-3}–10^{-5}% of these metals in aluminium metal) is about 10%. The deviations of individual determinations depend to a large extent on the way, in which the incisions are measured. Deviations of the results are least, when the depths of the larger incisions are measured whereas for small incisions it is better to measure their distance from the potential axis. This manner of measurement greatly increases the ratio of individual depolariser concentrations, which may be measured in the same solution. Copper, lead, cadmium and zinc may be determined in the presence of each other even in ratios of 1 : 15. This

ratio may be further increased by prolonging the time of electrolysis. Incisions of depolarisers, present in larger concentrations, have been measured at shorter times of electrolysis; incisions of depolarisers which are present in lower concentrations are measured using longer times of electrolysis. By increasing the time from 2 to 5 min, it was possible to determine the investigated depolarisers at ratios of 1 : 25. When the time of electrolysis was increased, it was necessary to decrease the value of the direct component of the current, in order to permit the mercury electrode to polarise to positive potential values. Results of the measurements are given in Table 5.

Adsorptive incisions are formed to a far less degree in the analysis of aluminium than in the analysis of hydrochloric acid. This is evidently due to the buffering effect of the high ionic strength of the solution.

Procedure

2.7 g of pure aluminium in the form of fine filings were gradually dissolved in 50 ml of doubly-distilled hydrochloric acid and 0.5 ml of hydrogen peroxide. A silica beaker was used for the dissolving operation, since platinum dissolves in the presence of hydrogen peroxide. Both the hydrochloric acid and the 30% hydrogen peroxide were added in small portions; after reacting, the portions of the solution were poured off and concentrated in a silica dish. The dissolution was catalysed by the addition of a drop of 0.01 *M* H_2PtCl_6. Using these conditions, 2.7 g of 99.999% aluminium were dissolved in 6 h. The solution was carefully evaporated to a syrupy consistency and on cooling solidified into a crystalline mass. After the addition of 16.4 ml of 6.1 *M* doubly-distilled hydrochloric acid the solution was transferred quantitatively into a 100-ml volumetric flask, and made up to volume with doubly-distilled water. The solution thus obtained was analysed in the same way as the synthetic samples. Purified aluminium chloride solution was used to dilute the solutions.

When using the dilution method, it is unnecessary to keep precisely to the prescribed hydrochloric acid concentration. On dissolving a sample for analysis, it is possible to proceed so that the solution is evaporated only partially, and is transferred to a 100-ml volumetric flask and made up to volume directly with doubly-distilled water. In this case, the same sample solution is used for dilution, after the impurities have been removed by electrolysis.

Since the content of impurities in the hydrochloric acid used to dissolve the aluminium samples was known, no blank tests were necessary; a correction was made for the impurities contained in the amount of acid used.

In the simultaneous determination of copper, lead, cadmium and zinc, the presence of larger amounts of alkaline metals, alkaline earths, magnesium and rare earths caused no interference. The influence of cobalt, nickel, chromium etc., when present in the amounts usually encountered in pure aluminium, is largely eliminated by the method employed.

Arsenic and antimony do not interfere as they largely evaporate, when the aluminium chloride solution is evaporated, and any traces that remain are oxidised to the pentavalent state.

The method described has been used to analyse aluminium of 99.99% purity (Johnson-Matthey Co. London) and aluminium of 99.999% purity (Light and Co., Colnbrook). The results, and a comparison with the analyses given by the manufacturer are given in Table 6.

TABLE 6

THE ANALYSES OF VERY PURE ALUMINIUM SAMPLES

Sample		*Cu*	*Pb*	*Cd*	*Zn*
99.99% Al, product of Johnson and Mattney, London	mean of three determinations	1.26×10^{-7} *M*	1.53×10^{-7} *M*	2.9×10^{-7} *M*	5.85×10^{-6} *M*
	correction for impurity in HCl	-0.42×10^{-7} *M*	-0.24×10^{-7} *M*	0	-0.03×10^{-6} *M*
	impurity content of sample alone	0.84×10^{-7} *M*	1.29×10^{-7} *M*	2.9×10^{-7} *M*	5.82×10^{-6} *M*
	impurity content related to Al	1.98×10^{-5}%	9.9×10^{-5}%	1.21×10^{-4}%	1.41×10^{-3}%
	manufacturer's analysis	—	—	1.00×10^{-4}%	1.5×10^{-3}%
99.999% Al, product of L. Light and Co., England	mean of three determinations	1.06×10^{-7} *M*	2.63×10^{-7} *M*	—	1.46×10^{-7} *M*
	correction for impurity in HCl	-0.42×10^{-7} *M*	-0.24×10^{-7} *M*	—	-0.33×10^{-7} *M*
	impurity content of sample alone	0.64×10^{-7} *M*	2.39×10^{-7} *M*	—	1.13×10^{-7} *M*
	impurity content related to Al	1.5×10^{-5}%	1.85×10^{-4}%	—	2.75×10^{-5}%
	manufacturer's analysis	—	1.5×10^{-4}%	—	—

TABLE 7

THE DETERMINATION OF IMPURITIES IN SYNTHETIC ZIRCONIUM SAMPLES

Sample no.	*Metal*	*Concn. taken* ($\times10^{-4}$%)	*Concn. found* ($\times10^{-4}$%)	*Relative deviation* (%)
1	Cu C	0.86	0.84	−2.9
	Pb C	2.14	1.92	−10.6
	Cd A	5.8	6.4	18.6
	Zn A	1.08	1.0	−7.4
2	Cu C	0.65	0.64	−2.1
	Pb C	3.18	2.54	−20.3
	Cd A	5.8	5.36	−7.6
	Zn A	1.2	1.08	−10.5
3	Cu C	0.33	0.38	16.9
	Pb C	1.50	1.64	9.1
	Cd A	5.8	5.27	−9.3
	Zn A	0.54	0.37	−30.8
4	Cu C	0.27	0.28	6.2
	Pb C	3.04	3.68	20.9
	Cd A	4.53	3.94	−11.0
	Zn A	0.47	0.55	15.8

C; cathodic incision
A; anodic incision

DETERMINATION OF HEAVY METAL TRACES IN PURE ZIRCONIUM

The determination of impurities in zirconium was carried out in the same manner as for aluminium. The zirconium concentration was modified to 0.25 *M* $ZrOCl_2$ in 1 *M*

hydrochloric acid. Copper, lead, cadmium and zinc were determined in concentrations of 10^{-6}–10^{-7} M, corresponding to a content of 10^{-4}–10^{-5}% of these metals in zirconium metal. Since no sufficiently pure zirconium sample was available, the following procedure was tested only on synthetic samples, using a purified zirconium solution.

Procedure: 2.28 g pure zirconium, in the form of a fine foil were dissolved carefully during one hour in 40 ml of doubly-distilled hydrochloric acid and 2 ml of concentrated hydrofluoric acid in a platinum dish. The resulting solution was then evaporated for 3 h over a small flame, until the solution solidified into a crystalline mass. 16.4 ml of 6.1 M hydrochloric acid were added to the residue on evaporation, and the solution was transferred into a 100-ml volumetric flask and made up to volume with doubly-distilled water. The slight turbidity, which sometimes formed as a result of hydrolysis, always redissolved in 6–10 h. The solution thus prepared was subjected to oscillopolarographic analysis. The time of electrolysis was 2–5 min; the electrolysis was carried out using a direct current of 12.5 mA and the optimum intensity of the alternating current component was 1.7 mA. The direct current component should be adjusted according to the time of electrolysis selected.

The precision of the determination of impurities in zirconium was usually about 10% (relative error), see Table 7 and Fig. 2.

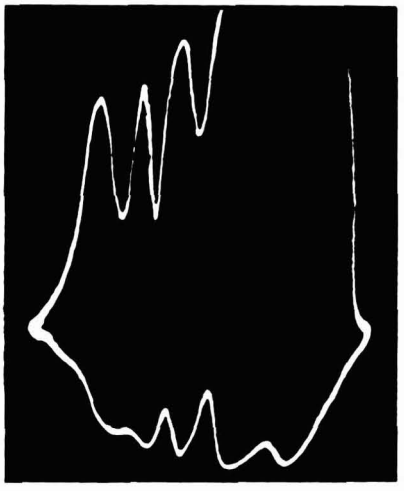

Fig. 2. $dE/dt = f(E)$, curve for mixture of Cu, Pb, Cd, Zn in 1 M $AlCl_3$ (1 M HCl); Cu 1.8; Pb 1.7; Cd 2.2; Zn 0.2×10^{-6} M. Curve registered after 2 min of electrolysis by direct current of 12.5 mA; hanging-drop mercury electrode.

DISCUSSION

The minimum amount of an element, which may be determined using a given method, is governed by the value and the reproducibility of the blank. The only methods which are not subject to this limitation are radioactivation, mass spectrographic and emission spectrographic methods. To assure the reliability of the results obtained it is therefore necessary to eliminate the possibility of secondary contamination in the course of analysis and to decrease the value of the blank to a minimum.

The main principles for the analysis of very pure substances are given by POHL[13]: (i) employment of the simplest methods, (ii) employment of especially pure reagent acids and solvents, (iii) elimination of the use of inorganic reagents and (iv) careful cleaning of vessels and the laboratory bench. It is also advantageous to work in a closed system, and to use vessels of specified material (polyethylene is the most suitable).

The orders of magnitude of the sensitivity and precision of other currently employed methods, are presented below to permit an evaluation of the proposed method.

Polarographic analysis permits a determination of depolarisers in concentrations down to 10^{-6} *M*. Concentrations of 10^{-4}–10^{-5} *M* are, however, used ordinarily, the deviations being in this case in the region of 1–3%. The sensitivity of polarographic analysis is increased by chemical or physico-chemical separation and concentration of the depolarisers to be determined[14] but in this way the method loses its simplicity and precision and the problem of the blank test is aggravated. The polarographic method, in conjunction with various methods of separation, may be used to determine amounts of the order of magnitude of 10^{-5}% copper, lead, cadmium and zinc[14], with a precision of 5–15%. The conventional method of oscillopolarographic analysis reaches a sensitivity which is lower by about two orders of magnitude than polarography, *i.e.*, it is possible to determine depolarisers in minimum concentrations of 10^{-5} *M*. At the beginning of this paper the possibility of the simultaneous determination of amounts of the order of 10^{-2}% of copper, lead, cadmium zinc and bismuth, using 1–2 *M* hydrochloric acid as electrolyte, was mentioned.

Spectrographic methods permit the determination of 10^{-4}% of impurities in pure aluminium[15] and zirconium[15,16] with a precision of 20%. Chemical methods of separating impurities using organic reagents (dithizone, quinoline), are used in these methods also. Impurities in specially purified hydrochloric acid are determined by a spectrographic analysis of the residue on evaporation[17]. A disadvantage of spectrographic methods is the high cost of equipment, and it can be seen that no simple procedure is possible even with these methods.

The method of oscillopolarographic microanalysis permits the determination of concentrations down to 10^{-9} *M*. In order to keep the method sufficiently rapid, and to avoid prolonged electrolysis, it is better to work in the concentration range of 10^{-6}–10^{-7} *M*, and to select the amount of sample accordingly. Using the method described, copper, lead, cadmium and zinc have been determined in concentrations of 10^{-6}–10^{-8} *M* with a relative error of 10–20%. A certain disadvantage is the use of relatively large volumes. This may, however, be avoided by using precise micro-pipettes, but this again decreases the limit of detection, although the amount of sample to be weighed and the consumption of chemicals, are both decreased and this is important if the purification of the reagents has been a lengthy process.

Summarising, it can be said that the method of oscillopolarographic microanalysis has advantages of simplicity, sensitivity, rapidity and precision, which are comparable with the sensitivity and precision of spectrographic analysis. The limitation that only those metals may be determined which are capable of forming amalgams, is outweighed by the low cost of the equipment, since a polaroscope is today available in every analytical laboratory and its adaptation to this method is not very expensive.

SUMMARY

A method has been developed for the oscillopolarographic determination of trace

amounts of copper, lead, cadmium and zinc in hydrochloric acid. This method has also been applied to the simultaneous determination of these metals at concentrations of 10^{-4}–10^{-5}% in pure aluminium and zirconium. A new method for the quantitative evaluation of the results has been proposed.

REFERENCES

1 J. HEYROVSKÝ AND R. KALVODA, *Oszillographische Polarographie mit Wechselstrom*, Akademie–Verlag, Berlin, 1960, p. 113.
2 R. KALVODA AND CH. STOCKMANNOVÁ, *Chem. Listy*, 55 (1961) 477.
3 R. KALVODA, *Chem. Listy*, 51 (1957) 696.
4 W. KEMULA AND Z. KUBLIK, *Anal. Chim. Acta*, 18 (1958) 104.
5 L. JENŠOVSKÝ, *Chem. Tech. (Berlin)*, 13 (1961) 519.
6 K. MICKA, *Chem. Listy*, 55 (1961) 474.
7 K. A. KRAUS, *J. Am. Chem. Soc.*, 77 (1955) 3974.
8 K. A. KRAUS AND G. E. MOORE, *J. Am. Chem. Soc.*, 72 (1950) 4293.
9 P. BERAN, *Chem. Zvesti*, 16 (1962) 258.
10 J. HEYROVSKÝ AND R. KALVODA, *Oszillographische Polarographie mit Wechselstrom*, Akademie–Verlag, Berlin, 1960, pp. 14, 22, 90.
11 A. S. RUSSELL, P. V. F. CARALET AND N. M. IRVIN, *J. Chem. Soc.*, (1932) 841.
12 A. S. RUSSELL AND H. A. M. LYONS, *J. Chem. Soc.*, (1932) 857.
13 F. A. POHL, *Chem. Ing. Tech.*, 30 (1958) 347.
14 M. SPÁLENKA, *Příručka anorganické polarografické analyzy (Handbook of Inorganic Polarographic Analysis)* SNTL, Praha, 1961, pp. 191, 233, 339.
15 A. G. KARABASH *et al.*, *Fiz. Sb. L'vovsk. Gos. Univ.*, 4 (1958) 556.
16 N. P. SOTNIKOVA *et al.*, *Tr. Komis. po Analit. Khim., Akad. Nauk SSSR, Inst. Geokhim. i Analit. Khim.*, 12 (1960) 366.
17 J. H. OLDFIELD AND E. P. BRIDGE, *Analyst*, 85 (1960) 97.

AN IMPROVED TECHNIQUE IN IMPEDANCE TITRATION

U. H. NARAYANAN AND K. SUNDARARAJAN

Central Electrochemical Research Institute, Karaikudi 3 (India)

(Received August 12th, 1963)

When a constant alternating current is applied between two platinum electrodes (one of them a polarisable electrode and the other a non-polarisable electrode such as a platinum gauze) immersed in a titrant, the impedance of the cell changes during the course of the titration. A sudden change in the impedance of the titration cell, as indicated by the large change in the a.c. voltage across the cell, denotes the end-point of the titration. This titration is termed an *impedance titration*[1,2]. In this paper, a technique has been described by which the alternating voltage at the commencement of the titration is compensated and only the changes in the alternating voltage during the course of the titration are recorded.

EXPERIMENTAL

The titration set-up is given in Fig. 1. The a.c. source (i) provides *constant* alternating current and the current can be varied with the help of a variable resistance connected in series with the titration cell. The alternating voltage across the cell is fed to one set of input terminals of the difference amplifier. The compensating voltage which can be adjusted to any required value is fed to the other set of input terminals of the difference amplifier.

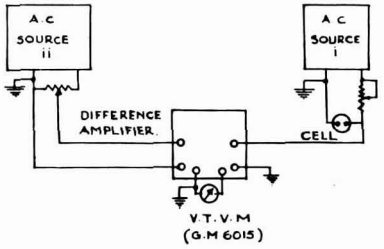

Fig. 1. Set-up for the improved technique in impedance titration.

At first, before any titrant is added from the burette, the two signals, one from the titration cell and the other from the second a.c. source are made equal so that the output of the difference amplifier is very nearly equal to zero. In the course of the titration the alternating current is kept at a constant value and the alternating voltage across the cell changes from the initial value because of changes in the impedance of

the cell. At the end-point there is a sudden change in the alternating potential which also indicates the change in the impedance.

Difference amplifier[3]

In this amplifier, (see Fig. 2) the right-hand half of the twin triode (V_2) forms the cathode load of the other triode (V_1) and the output is taken at the plate of this tube. If a signal (A) is injected at the grid of V_1, the resulting current flowing in the potentio-

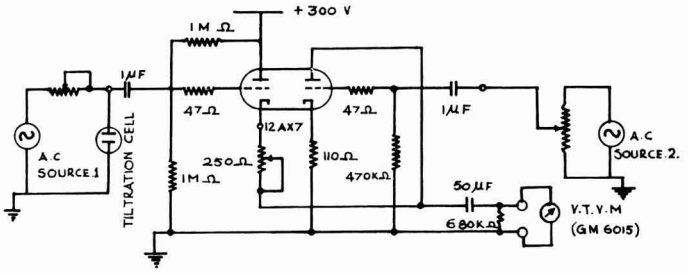

Fig. 2. Circuit diagram of the difference amplifier used in the set-up.

meter (250 Ω) is in the same phase. The signal at the second triode (B) is 180° out of phase and opposes the current due to the first signal. Thus the output is the difference between the two signals. The whole circuit can be considered as a cathode follower of practically unity gain. Thus the output is exactly the difference of the two signals fed to the two grids of the twin triode.

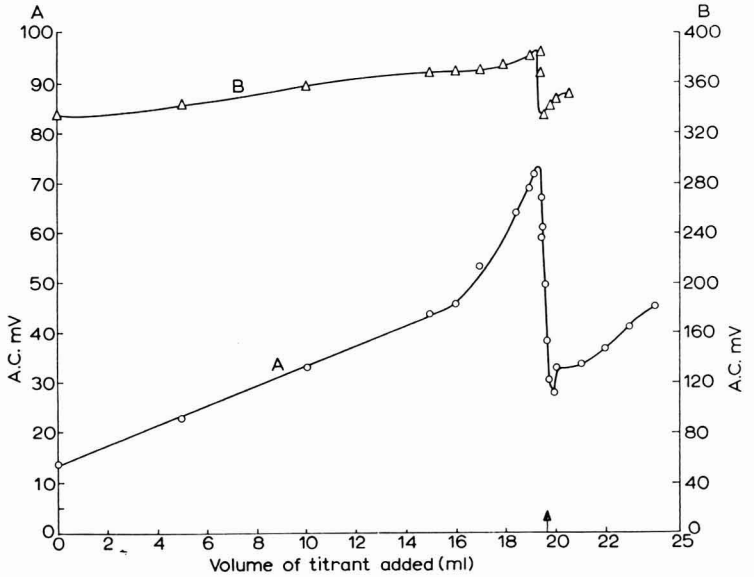

Fig. 3. Titration of ferrous ammonium sulphate with ammonium meta-vanadate: point ○, with compensation; point △, without compensation.

I. Titration of ferrous ammonium sulphate with ammonium meta-vanadate

(*a*) *Solution in the beaker*: 25 ml of ferrous ammonium sulphate solution and 75 ml of 1.5–2 *M* H_2SO_4 (supporting electrolyte).

(*b*) *Solution in the burette*: About 3 g of ammonium meta-vanadate was dissolved in 100 ml of hot 1.8 *N* H_2SO_4 and the volume made up to 250 ml. This was diluted 10 times to give a solution approximately 0.0104 *N* with respect to vanadate.

II. Titration of ferrous ammonium sulphate with ceric sulphate

(*a*) *Solution in the beaker*: 25 ml of 0.0084 *M* ferrous ammonium sulphate and 100 ml of *N*/10 sulphuric acid (supporting electrolyte).

(*b*) *Solution in the burette*: Approximately 0.0168 *M* ceric sulphate in 1.8 *N* sulphuric acid.

Analytical grade chemicals were used for the preparation of all solutions.

Typical values of changes of cell impedance during the course of the titrations are presented in Figs. 3 and 4.

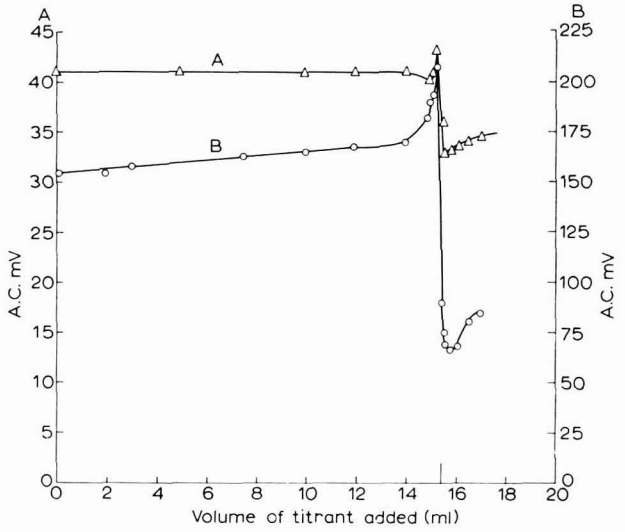

Fig. 4. Titration of ferrous ammonium sulphate with ceric sulphate: point ○, with compensation; point △, without compensation.

DISCUSSION

This technique has potentialities for detecting the end-points of several systems which may not be determined with reasonable accuracy by other electroanalytical or purely chemical techniques. It is possible to improve the precision of the end-point by providing compensating alternating voltage just before the end-point. The output voltage of the difference amplifier will not be much affected by parameters such as mains fluctuations and temperature effects, as both the inputs will be affected equally. The loading effects due to the compensatory circuit will be minimal as the cell circuit has been isolated from it by employing a vacuum tube circuit. This impedance titration

method has been found to be satisfactory for dilute solutions for which the ordinary potentiometric titration fails[4].

ACKNOWLEDGEMENT

The authors are grateful to Prof. K. S. G. Doss, Director Central Electrochemical Research Institute, for suggesting the idea and for helpful discussions during the course of the work.

SUMMARY

The precision of the end-point of the impedance titration can be improved by compensating the alternating voltage of the titration cell with that from an external alternating voltage with the help of a difference amplifier. The output signal of the difference amplifier is A-B if the input signals are A and B. There will be a sharp jump in the output of the difference amplifier at the end-point of the titration.

REFERENCES

1 U. H. NARAYANAN AND K. SUNDARARAJAN, unpublished work.
2 K. S. NARAYANAN AND H. C. GAUR, *J. Electroanal. Chem.*, 2 (1961) 161.
3 K. E. MULLENGER AND R. H. MCMANN JR., *Electronics*, 29 (1956) 130.
4 K. S. NARAYANAN AND C. P. NAMBUDRIPAD, in course of publication.

STUDIES OF THE MECHANISM OF THE ANODIC OXIDATION OF ETHYLENE IN ACID AND ALKALINE MEDIA

HALINA WROBLOWA*, BERNARD J. PIERSMA AND JOHN O'M. BOCKRIS

The Electrochemistry Laboratory, The University of Pennsylvania, Philadelphia 4, (Penna, U.S.A.)

(Received August 28th, 1963)

Ethylene oxidation in alkaline solution has recently been studied by DRAZIC, GREEN AND WEBER[1]. Their results were interpreted[2] in terms of OH^- ion discharge as the rate-determining step. The primary object of this paper is the study of ethylene oxidation on platinum in acid solution. However, a thorough study of the pH and pressure dependence of the reaction rate necessary for establishing the reaction mechanism led to investigation over a wide pH range.

EXPERIMENTAL

(i) The cell

A conventional electrolytic cell of Pyrex glass with anodic and cathodic compartments separated by fritted glass discs and stopcock (which was closed for galvanostatic and open for potentiostatic experiments**) was used. The anode compartment was thermostated at 80° ± 0.5°C.

The anodes were platinum gauze, 0.1 mm wire thickness, 52 mesh size, and were used as both bright and platinized Pt electrodes. The smooth Pt electrodes were large (1000 cm^2) pieces of folded gauze, the platinized electrodes were gauzes in planar form. The procedure for platinization has been reported elsewhere[1]. Before each experiment the electrodes were activated in 20% H_2SO_4 in the following manner: the electrode was placed in acid solution with another Pt electrode and cycled*** at 0.1 A cm^{-2} (geom.****) from oxygen evolution to hydrogen evolution at one second intervals about 10 times. The electrode was then polarized for about 100 seconds† cathodically at the same current density.

The cathodes also consisted of Pt gauze, platinized, and wound around glass rods to give a low c.d. for hydrogen evolution and hence to avoid the production of H_2 bubbles. Prepuritied nitrogen (see below) was passed through the cathode compartment throughout the experiment.

* On leave of absence, *Academy of Sciences, Warsaw, Poland.*

** In potentiostatic runs the stopcock had to be opened to prevent a high resistance between the auxiliary and test electrodes. The diffusion of H_2 to the anode compartment was proved by special tests to be fully prevented by the fritted disc and the stream of nitrogen.

*** *cf.* BOCKRIS, AMMAR AND HUQ[3] who described and discussed the effects of pulsing in activating Pt electrodes. The same technique as that described here was used by DRAZIC, WEBER AND GREEN[1].

**** Geometric area

† The electrode was activated in one cell and transferred immediately thereafter to the reaction vessel. Activation in a closed system gave identical parameters.

Reference electrodes used were mercury-mercurous sulfate, containing the same solution as that in the cell for the pH range 0–6 and saturated calomel electrodes in the more alkaline solutions.

(ii) Reagents

Sulfuric acid – "Baker Analyzed" reagent; sodium sulfate – Fisher Certified Reagent; sodium hydroxide — "Baker Analyzed" reagent; ethylene – Matheson, C.P. grade (99.5% min. purity)*; nitrogen – Matheson, pre-purified (99.996% purity); water – distilled and conductivity water (specific conductance approximately 5×10^{-7} ohm^{-1} cm^{-1}); gas mixtures of ethylene and pre-purified nitrogen for several partial pressures of ethylene were supplied in cylinders with analysis (Matheson).

(iii) Electrical accessories

The "Wenking" electronic potentiostat coupled with an "Esterline Angus" graphic ammeter were used to record current at constant potential. Potential was measured by a Kintel 203 vacuum tube voltmeter.

(iv) Determination of faradaic efficiency

The consumption of ethylene and the production of CO_2, were measured by techniques described elsewhere[4].

RESULTS

(i) Faradaic efficiency of oxidation to carbon dioxide

The amount of carbon dioxide evolved during the anodic oxidation of ethylene in 1 *N* H_2SO_4 solution for 18 hours with a current strength of 40 mA was found to be $N_{CO_2} = (4.47 \pm 0.01) \times 10^{-3}$ moles. The calculated value for complete oxidation according to the reaction:

$$C_2H_4 + 4H_2O \rightarrow 2CO_2 + 12H^+ + 12\,e$$

$$N_{CO_2} = \frac{2it}{12F} = 4.477 \times 10^{-3} \text{ moles.}$$

In 1 *N* NaOH solution the consumption of ethylene during the anodic oxidation for 12 h with a current strength of 30 mA was found to be $1.23 \pm 0.06 \times 10^{-3}$ moles. The calculated value for complete oxidation according to the reaction

$$C_2H_4 + 12OH^- \rightarrow 2CO_2 + 8H_2O + 12e$$

$$N_{C_2H_4} = \frac{it}{12F} = 1.12 \times 10^{-3} \text{ moles.}$$

(ii) Rest potential

All potentials are given on the normal hydrogen scale unless otherwise indicated and refer to the scale in which the normal potential of the hydrogen electrode $e^{o}_{H_2} = 0$ at 80°C.

Since the test and reference electrodes were at different temperature, measurements of correction of the thermo-junction effect and temperature coefficient of the hydrogen and mercury-mercurous sulfate electrodes were made. The difference between

* The only contaminants are relatively inactive saturated hydrocarbons.

the anode potential measured in isothermal arrangement at 80°C and in that used throughout experiments (*i*) was 13 mV. The potentials reported are corrected by this experimentally obtained value.

The rest potential of Pt in 1 *N* H_2SO_4 in nitrogen atmosphere of 1 atm, was 0.23 V. Upon introduction of ethylene, the rest potential shifted to 0.25 V.* This value was decreased by 70 mV per unit of increasing pH (Fig. 1), and was independent of the partial pressure of ethylene (P_E) in the range $10^{-4} \leqslant P_E \leqslant 1$ atm.

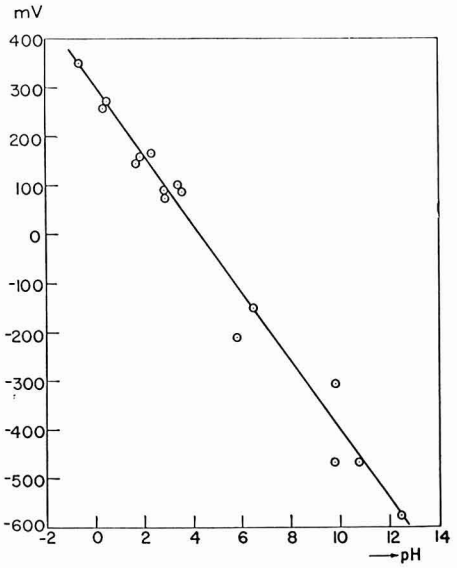

Fig. 1. Rest potential (NHE) as a function of pH.

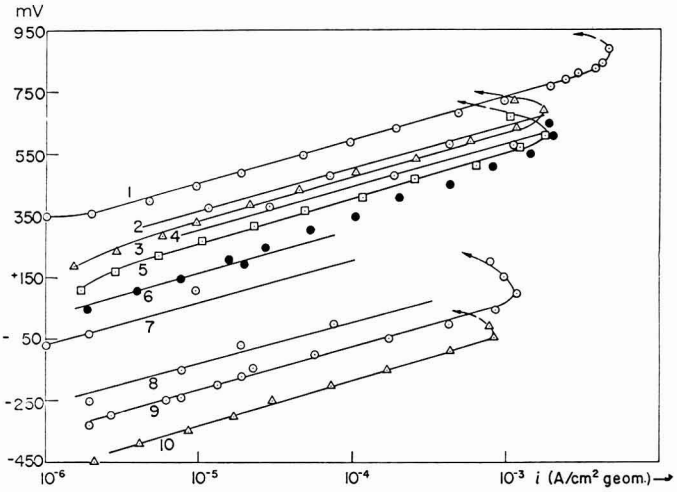

Fig. 2. Current-potential relation (P_E = 1 atm) as a function of pH: (1) 0.5, (2) 1.9, (3) 2.3, (4) 2.9, (5) 3.45, (6) 5.6, (7) 6.5, (8) 9.8, (9) 10.8, (10) 12.5.

* The small change of the rest potential upon introduction of ethylene exemplifies the danger of deducing information concerning reactivity at an electrode from effects on the rest potential.

(iii) Current-potential relation

Polarization curves obtained potentiostatically at a series of pH values for platinized Pt in solutions containing excess neutral salt (Na_2SO_4) to maintain a constant ionic strength I = 1.5 moles l^{-1} are shown in Fig. 2. The reproducibility of the current values at constant potential is within 10%. Four regions may be distinguished on the potential log current curves:

(a) A potential range close to the rest potential, where no steady states could be obtained, the current at constant potential decreased for several hours.

(b) A linear Tafel region with a slope (b) of 140–160 mV in the pH range 0.3 to 12.5,

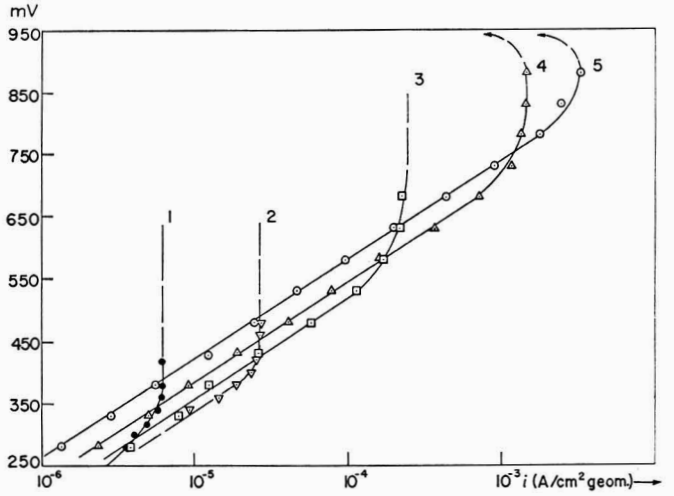

Fig. 3. Current-potential relation (pH ~ .5) as a function of ethylene partial pressure: (1) P_E = 10^{-4} atm, (2) 10^{-3} atm, (3) 10^{-2} atm, (4) 10^{-1} atm, (5) 1 atm.

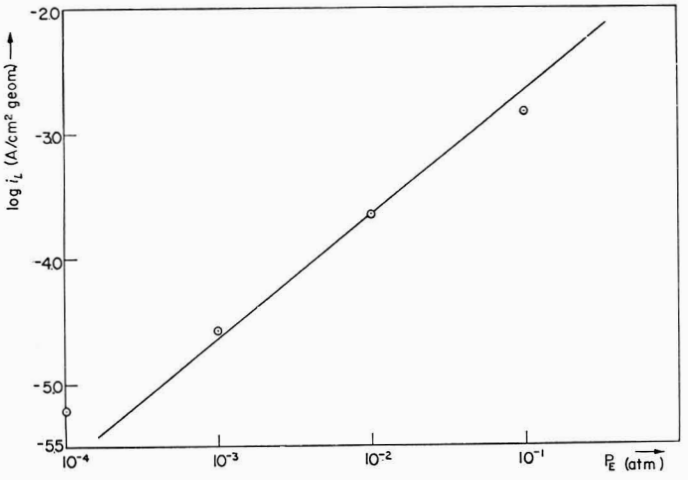

Fig. 4. Limiting current as a function of ethylene partial pressure.

and about 200 mV in 10 N H_2SO_4. At a pressure $P_E = 1$ atm and pH close to 0, the c.d. range for this region is 3×10^{-6} to 3×10^{-3} A cm^{-2} (geom.).

(c) A region where the line curves upward and becomes independent of potential (Fig. 3). The current increases here roughly proportionally to ethylene pressure (Fig. 4) and increases with increased rate of stirring.

(d) At about 0.9 V (reversible hydrogen electrode), the current rapidly decreases to negligible values.

Galvanostatic determinations yielded the same results except for region (d), where, in this case, the current remained independent of potential until the potential of oxygen evolution was reached.

Essentially the same behavior was observed on smooth Pt anodes, where the slope of the Tafel region was also about 150 mV, except at pH $\approx$ 0.3, where it increased to about 170 mV, and in 10 N H_2SO_4 was about 220 mV. The reproducibility of results for smooth Pt was somewhat less than for platinized Pt.

(iv) Exchange current densities

From the thermodynamic data, the free energy and the entropy of the reaction

$$2CO_2 + 12H^+ + 12e \rightleftharpoons C_2H_4 + 4H_2O \qquad (1)$$

are: $\Delta G^\circ_{25^\circ} = 21.96$ kcal, $\Delta S_{25^\circ} = 17.3$ cal deg^{-1} mole^{-1}. The temperature coefficient $(\partial E^\circ/\partial T)_{25^\circ} = 10^{-4}$ V deg^{-1}.

The thermodynamic reversible potential of reaction (1) at 80°C is

$$E^\circ_{80^\circ} = -\frac{(\Delta G^\circ_{25^\circ} - \Delta S(80 - 25))}{12F} = 0.082 \text{ V}$$

where

$$\Delta S = \frac{\Delta S_{25^\circ} + \Delta S_{80^\circ}}{2}.$$

Under experimental conditions, the activity of carbon dioxide dissolved in the vicinity of the electrode may be lower than that in equilibrium with 1 atm pressure of CO_2 ($\sim 10^{-2}$ moles l^{-1}). The values of exchange currents are obtained by extrapolation of the linear section of the polarization curve to the reversible potential. The current density observed in the middle range of Tafel section at $P_E = 1$ atm and pH = 0.5 is $i \sim 10^{-4}$ A cm^{-2} (geom.). In the steady state,

$$i = zF\frac{D}{\delta}(C_E - C_B) \qquad (2)$$

where F = 96500 coulombs; z=6; D $\sim 2 \times 10^{-5}$ cm^2 sec^{-1}; C_E = concentration of CO_2 at the electrode in moles cm^{-3}; C_B = concentration in the bulk $\sim$ 0; δ = thickness of diffusion layer $\simeq$ 0.01 cm.

From eqn. (2)

$$C_E \approx 2 \times 10^{-4} \text{ moles/l}$$

Thus, the reversible potential may be estimated at a value of about 0.03 V (R.H.E.) for purposes of extrapolating the Tafel section to obtain the values of the exchange current, i_0. The values of i_0 at $P_E = 1$ atm are $\sim 10^{-10}$ and 10^{-8} A cm^{-2} (geom.) for smooth and platinized Pt, respectively. The highest probable value for roughness factor of platinized Pt is thus R $\sim$ 100.

(v) Current-pressure relation

The dependence of current on ethylene pressure was studied on platinized Pt for ethylene partial pressures from 1 atm to 10^{-4} atm in two ways:

(a) Polarization curves were determined potentiostatically at constant pressure (Fig. 3). The range of the Tafel sections depends on P_E, decreasing roughly by one decade per tenfold decrease of ethylene partial pressure. The potential range of region (c) expands in the negative direction with decreasing P_E, but always ends on the positive side with a potential of V $\approx$ 0.9 V (reversible hydrogen electrode).

(b) The current was recorded at constant potential as a function of ethylene partial pressure.

Experimental points obtained by both methods are shown in Figs. 5 and 5a for

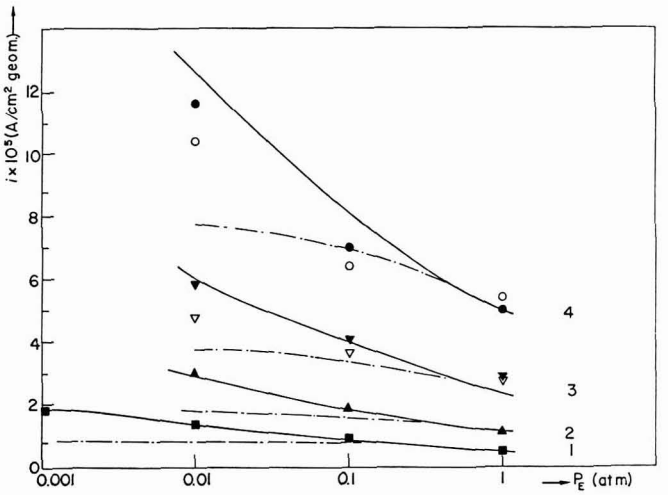

Fig. 5. Current as a function of ethylene partial pressure at constant potential: (1) 0.38 V, (2) 0.43 V, (3) 0.48 V, (4) 0.53 V.

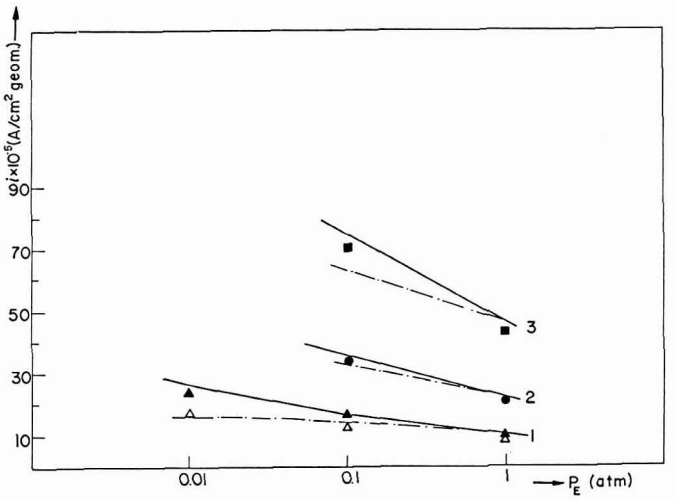

Fig. 5a. Same as 5: (1) 0.58 V, (2) 0.63 V, (3) 0.68 V.

1 N H_2SO_4 solution (shaded points – method a; unshaded points – method b). The current decreases roughly logarithmically with increasing partial pressure of ethylene. The value of $|di/d \log p|_V$ increases with increasing positive potential and is slightly higher in acid than in alkaline solutions.

(vi) Current-pH relation

The pH dependence of current is shown in Figs. 2 and 6. The following relations were found:

$$\left(\frac{d \log i}{d \log c_{H+}}\right)_V = -0.45$$

$$\frac{d\eta}{d \log c_{H+}} \approx 0$$

$$\frac{d \log i_0}{d \log c_{H+}} \approx 0$$

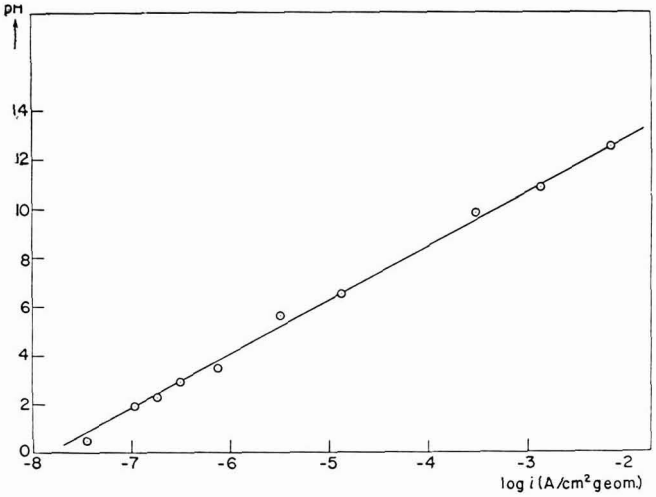

Fig. 6. Current (V = 0.100 V) as a function of pH.

(vii) Current-temperature relation

The dependence of current on temperature for 1 N H_2SO_4 and P_E = 1 atm is given in Fig. 7 for several potentials. The apparent activation energy A = (20.5 ± 1) kcal mole^{-1} at 0.380 V and was not found to change systematically with potential. This is attributed to the experimental error arising from the limited scope of temperature and potentials over which the measurements could be carried out.

The activation energy at the reversible potential calculated as $\Delta H^\circ = A_{0.38V} - x\eta F \sim 17 \pm 2$ kcals. ($\partial e^\circ_{Ethylene}/\partial T$ is negligible (*cf. Results iv*), α is assumed to be constant with temperature, thermojunction potential is assumed to be negligible).

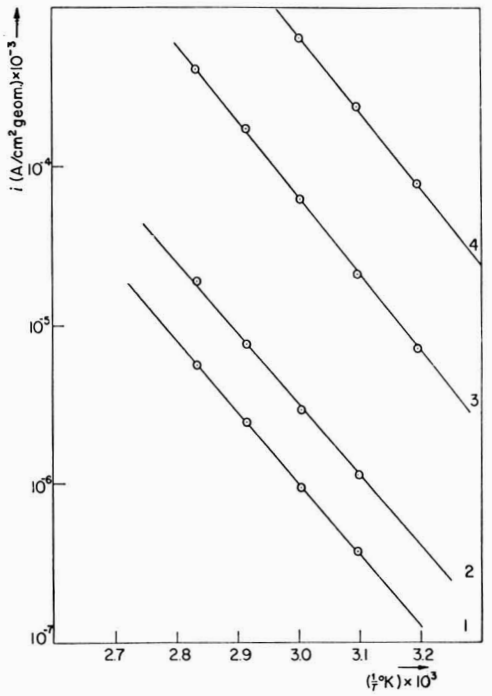

Fig. 7. Current as a function of temperature at constant potential: (1) 0.38 V, (2) 0.48 V, (3) 0.68 V, (4) 0.88 V.

(viii) Effect of purification

Use of conductivity water, Teflon cells for NaOH solutions and extensive pre-electrolysis of solution under nitrogen atmosphere (12 h at −0.5 V and 12 h at

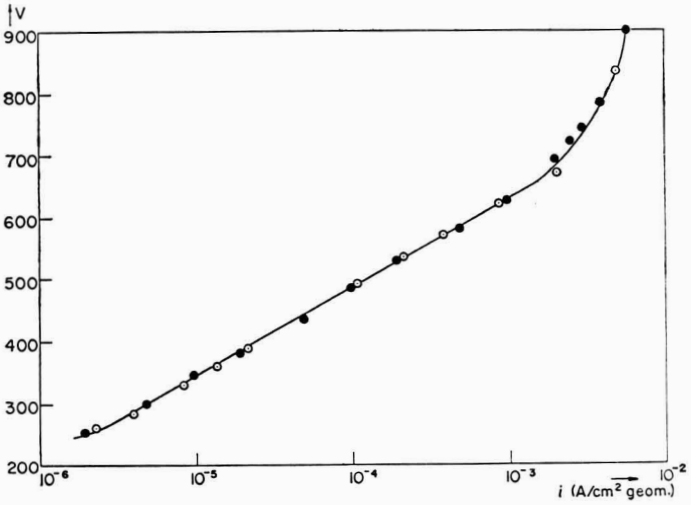

Fig. 8. Effect of pre-electrolysis on current-potential curve: (⊙) distilled water, (●) pre-electrolysis using conductivity water.

+ 1.8 V) on separate platinized Pt electrodes made no significant changes in the polarization curves (Fig. 8).

DISCUSSION

(i) Adsorption of ethylene

The two most probable modes of ethylene adsorption are:

$$C_2H_{4(g)} \rightarrow \begin{matrix} H_2C{-}CH_2 \\ | \quad | \\ Me \quad Me \end{matrix} \qquad (A)$$

$$C_2H_{4(g)} \rightarrow \begin{matrix} HC{=}CH \\ | \quad | \\ Me \quad Me \end{matrix} + 2MeH \qquad (B)$$

Mechanism (A) has been postulated for the gas phase by TWIGG AND RIDEAL[5] on the basis of their results on ethylene hydrogenation and hydrogen-deuterium exchange. Subsequent work by CONN AND TWIGG[6] and BEECK, SMITH AND WHEELER[7] seemed to confirm this result. Later work by BEECK *et al.*[8] and TRAPNELL[9] favors mechanism (B) on the basis of studies of the ethane production in hydrogenation of ethylene.

The energetics of adsorption from the gas phase favors mechanism A, only by ~35 kcal mole^{-1}, assuming the bond energies to be[10]: C=C (breaking of one bond in a double bond) 63 kcal mole^{-1}; C–H 106 kcals mole^{-1}; Pt–H 62 kcals mole^{-1} (calculated with Pauling formula). Under conditions of adsorption from aqueous solution and at anodic potentials three other factors must be taken into account: (a) the extra energy needed in mechanism (B) to desorb two additional water molecules replaced; (b) the ionization of the adsorbed H atoms to form solvated protons under charge-free conditions; and (c) the energy of the charge-transfer process. The heat of desorption of a water molecule from the Pt surface is an endothermic process. The heat of the reaction

$$Pt\text{-}H \rightarrow H^+_{(solv)} + Pt + e$$

at the potential of zero charge is ~112 kcals mole^{-1}. The middle of the potential range of the measurements is about 0.2 V positive to the point of zero charge, so that the energy of the reaction

$$C_2H_4 \rightarrow \begin{matrix} HC{=}CH \\ | \quad | \\ Me \quad Me \end{matrix} + 2H^+_{solv} + 2e$$

would be by ~240 kcals mole^{-1} higher than that corresponding to mechanism A (assuming ionization energy of hydrogen I = 313 kcals mole^{-1} and energy of solvation S = — 263 kcals/mole[11]).

Hence mechanism (A) under conditions of anodic oxidation is much more probable. In this model adsorption of ethylene molecules (both on the basis of steric considerations as well as taking into account the covalence with d-band as responsible for ethylene chemisorption) involves four surface sites of Pt per one molecule of ethylene[12] The adsorption isotherm is then of the form

$$\frac{\theta}{(1-\theta)^4} = K_e c, \quad \text{or} \qquad (3)$$

$$\frac{\theta}{(1-\theta)^4} = K_p P_E \tag{3a}$$

where $\theta = \Gamma/\Gamma_{max}$ — fractional coverage with ethylene, K_c = equilibrium constant ($cm^3\,mole^{-1}$), K_p = equilibrium constant (atm^{-1}), c = concentration of ethylene in solution (mole cm^{-3}).

It is of importance to the following mechanistic consideration to attempt to calculate the degree of coverage of the Pt catalyst with ethylene* An estimate can be made using data of DAHMS, GREEN AND WEBER[13] who, using radiochemical method, found that for concentrations of $\sim 4 \times 10^{-8}$ moles cm^{-3}, $\Gamma_{ethylene}$ per apparent cm^2 at the maximum of coverage-potential curve is about 2.5×10^{-9} moles cm^{-2}. For a four site attachment model

$$\theta = \frac{\Gamma}{\Gamma_{max} R} = \frac{2.5 \times 10^{-9}}{0.6 \times 10^{-9} R} \approx \frac{4}{R}$$

where R is the roughness factor. The above authors stated the roughness factor of 14, which they considered low. The results of this paper (*iv*) show as a probable highest value $R = 100$. It will be assumed here that the roughness factor is between 10 and 100. Hence for $c = 4 \times 10^{-8}$ moles cm^{-3}, the coverage θ is between 0.04 and 0.4. The concentration (at 1 atm ethylene partial pressure) in the present work is $\sim 2 \times 10^{-6}$ moles cm^{-3}, *i.e.* 50 times higher than that of the above quoted measurements. The coverage calculated from eqn. (3) gives for $c = 2 \times 10^{-6}$ moles cm^{-3}, $0.37 \leqslant \theta \leqslant 0.73$ for $R = 100$ and 10 respectively. The corresponding K_p values are $2.3 \leqslant K_p \leqslant 150$.

Another way of obtaining an approximate estimate of θ is as follows: it is known[14] that time, τ, to reach steady state adsorption when θ is in the linear section of the isotherm

$$\tau = 1.1 \times 10^3 \frac{K_1^2}{\pi D} \tag{4}$$

where D — diffusion constant ($= 5 \times 10^{-6}$ cm^2 sec^{-1})[15]; $K_1 = K_c\,\Gamma_{max}$. From experimental data[16], when $\theta < 0.1$, $\tau \sim 600$ sec. Introducing the relevant values into eqn. (4)

$$K_c \simeq 5 \times 10^6 cm^3\,mole^{-1}$$

$$K_p \simeq 10\ atm^{-1}$$

When introducing this value of K_c into eqn. (3), for $c = 2 \times 10^{-6}$ moles cm^{-3}, $\theta \simeq 0.5$.

Thus estimates derived from radiochemical method and the above calculation agree reasonably well** and suggest a surface coverage at maximum (with respect to potential)for $P_E = 1$ atm of $\theta = 0.55 \pm 0.2$.

* A study of this phenomenon is in progress in the Electrochemistry Laboratory at the University of Pennsylvania.

** The consistence of the two methods for obtaining an approximate value of θ_E is less significant than appears for eqn. (4) applies only in the linear range of a Langmuir isotherm with one point attachment. Although eqn. (4) might have an approximate applicability at $\theta = 0.5$ for one point attachment it would seem to be a very poor approximation for four point attachment at this coverage.

No data are as yet available for the coverage-potential relation at the concentration corresponding to that of $P_E = 1$ atm. However, for concentration corresponding to about 10^{-3} atm, the coverage is invariant ($\pm 10\%$) over the potential range + 200 to + 500 mV[13]. According to the measurements of BLOMGREN, BOCKRIS AND JESCH[14], the potential invariant portion of θ–V curves for organic compounds is expanded as the concentration increases. For an increase of about 10^3 in concentration, the flat ($\theta = \pm 10\%$) portion increases by some 3–4 times. Hence, an estimate of the potential invariant section for this concentration would be for about — 100 to + 800 mV.

(ii) State of adsorbed hydroxyl

In the ensuing discussion of the mechanism of the ethylene oxidation, the adsorbed hydroxyl radical will play an essential part of the suggested mechanism. It is hence necessary to discuss the probable state of the electrode with respect to adsorbed hydroxyl in the potential range under consideration. The experimental results must be considered in which the adsorption of the oxygen containing species has been examined upon the electrode in the absence of significant quantities of dissolved oxygen in the solution. Such measurements have been carried out by DAHMS AND BOCKRIS[17], and are shown in Fig. 9. The coverage below V ~ 0.9 V is very low. At

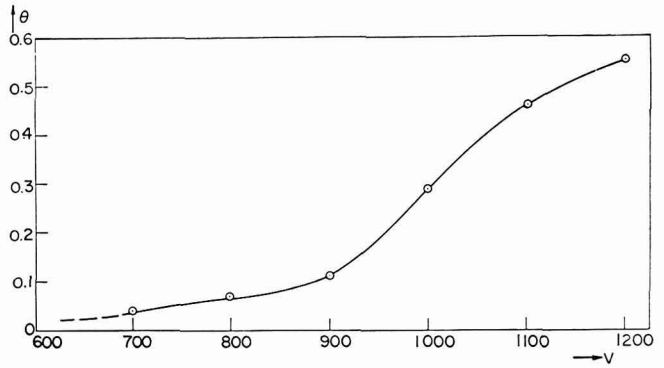

Fig. 9. Oxygen atom coverage on Pt as a function of potential (mV).

0.9 V, an inflection in the curve is observed after which the coverage steeply rises with potential. A probable interpretation of this behavior is that below V ~ 0.9 V, the species adsorbed is OH radical resulting from water discharge onto platinum electrode. In absence of any species capable of removing OH radicals from the surface an equilibrium is set up between water and Pt–OH. At potentials V $\geqslant$ 0.9 V Pt–O, or $Pt(OH_2)$ starts forming, leading to a high coverage of the electrode with an oxide. This interpretation is in conformity with the "passivation" of the electrode occurring in the vicinity of 0.9 V (see *iii*, 4, p. 415).

The question remains concerning the number of metal sites covered by one adsorbed OH. There is no evidence for d-band adsorption of O on metals[12]. Hence a one site attachment mechanism may be assumed.

(iii) The reaction mechanism

(1) General nature. (a) The overall reaction yields CO_2 with 100 $\pm$ 1% efficiency in acid and 90 $\pm$ 5% efficiency in alkaline solution (*Results, i*). Thus it is assumed that

no branching leading to other products than CO_2 and water (or protons) occurs to an appreciable extent.

(b) The value of the activation energy $\Delta H_0 \sim 20$ kcals mole^{-1} precludes terminal desorption of CO_2 as the rate-determining step.

(c) The observed Tafel slopes for the pH range 0.3–12.5 and pressure range from 10^{-3} to 1 atm are b = 140–160 mV. At 80° C, the value of b = 2.3 × RT/αF for α = 0.5 is 140. Thus, it may be concluded that a charge transfer is a rate-determining step and the value of α is between 0.44–0.5.

(d) The observed Tafel slope is consistent only with the first charge transfer as r.d.s. or a later charge transfer from the species present at the electrode at full coverage as r.d.s. For the latter case however no pressure effect could be expected. Thus the value of b = 2.3 × 2RT/F together with the fact that $di/dp < 0$ (*Results, v*) fix the location of r.d.s. as the first charge transfer reaction.

(e) The negative pressure effect: $di/dp < 0$ shows that r.d.s. involves a substance which requires the surface *free* of ethylene (or any intermediate derived therefrom) to adsorb. Thus the likely rate-determining step is one of the two reactions.

$$H_2O \rightarrow OH + H^+ + e \qquad (5)$$

$$OH^- \rightarrow OH + e \qquad (6)$$

(f) The reaction sequence may then be represented by

$$C_2H_4 \rightleftharpoons C_2H_4 \text{ ads}$$

$$\text{r.d.s.} \begin{cases} H_2O \rightarrow OH_{ads} + H^+ + e, & \text{or} \\ OH^- \rightarrow OH_{ads} + e \end{cases}$$

$$C_2H_{4ads} + OH_{ads} \rightarrow C_2H_4OH (\text{or } C_2H_3\cdot + HOH)$$

$$C_2H_4OH + \ldots \rightarrow \ldots 2CO_2 + 11\,H^+ + 11e$$

The coverage of all intermediates will be negligible in comparison with the coverage of ethylenic radical, since they occur *after* the rate-determining step and are not in equilibrium because of the constant removal of the final product — CO_2. Thus it is justified to assume that $\theta_{Total} \sim \theta_{Ethylene}$.

(2) pH effect. As shown in Fig. 2 current-potential relation was investigated over a wide pH range (K_{water} at 80° = $10^{-12.5}$). The Tafel lines were of restricted extent in the middle range (curves 8–10) owing to the necessity of limiting the current to avoid pH changes in the diffuse layer. (The effect of those changes on Tafel slope is indicated by points corresponding to higher current densities of curves 6 and 7 in Fig. 2.) By extrapolating the Tafel lines so that the current values could be obtained at the same potential for all pH values, the plot of log *i versus* pH at constant potential (V = 100 mV) was obtained (Fig. 6).

In Table 1 the value of $(d \log i/d\,\text{pH})_V$ thus obtained is given, together with certain other relevant coefficients.

It may be seen that the present result is not consistent with the theoretical coefficients (derived on a simple model) for water or OH^- ions discharge as the rate-controlling step. This fact does not militate against the suggested mechanism but lends it support because similar anomalous pH effects have been observed by several authors (see Table 1) who were concerned with simple reactions in which the charge transfer from H_2O (or OH^-) is certainly the r.d.s.[19–22].

TABLE 1

EXPERIMENTAL AND THEORETICAL pH DEPENDENCE IN CERTAIN REACTIONS INVOLVING THE DISCHARGE OF H_2O OR OH^- IN PRESENCE OF EXCESS NEUTRAL SALT

Origin	$\left(\frac{d \log i}{d\,pH}\right)_V$	$\left(\frac{d\eta}{d\,pH}\right)_i$	$\left(\frac{d \log i_0}{dpH}\right)$
Theoretical consideration of the simple model — Discharge from water	0	RT/F	$-\alpha$
Theoretical consideration of the simple model — Discharge from OH^-	1	$-$ RT/F	α
BOCKRIS AND HUQ[19], O_2 evolution on Pt, (H_2SO_4)	0.25	α RT/F	
VETTER AND BERNDT[20], O_2 evolution on Pt wide pH range		0	
MACDONALD AND CONWAY[21], O_2 evolution on Pd and Au alloys (H_2SO_4, NaOH)		0	0
Present work	0.45	$\sim$ 0	$\sim$ 0

The value of $(d \log i/d\,\mathrm{pH})_V$ is constant over the entire investigated pH range, suggesting that the same mechanism applies in the cases of both acidic and alkaline solutions. Charge transfer from OH^- ions would cause, in acid solutions, a limiting current at very low current densities, several orders of magnitude lower than those observed in the Tafel region. It is thus concluded that the discharge occurs from water molecules over the whole pH range investigated.

A number of possibilities for the anomalous pH effect (at constant ionic strength) may be considered.

(a) Let it be supposed: (a) H_2O undergoes charge transfer only when oriented with the O atoms towards the electrode; (b) the potential of zero charge of Pt decreases with pH (see below). Then, the fraction of water molecules which could react increases with pH at constant potential, qualitatively in agreement with observation. However, such an effect would also occur during the potential interval corresponding to a Tafel line. Equations developed by BOCKRIS, DEVANATHAN AND MÜLLER show[23] that the change expected in water orientation over the relevant potential range is not consistent with the Tafel slope observed.

(b) Let it be supposed that the discharge of OH^- and H_2O both contribute to the current:

$$i = (k_5 a_{H_2O} + k_6 a_{OH^-}) e^{\alpha FV/RT}$$

$$\left(\frac{d \ln i}{d\,\mathrm{pH}}\right)_V = \frac{1}{\frac{k_5}{k_6}\frac{a_{H_2O}}{a_{OH^-}} + 1}$$

in disagreement with the observed coefficient $(d \ln i/d\,\mathrm{pH})_V = \text{const}$.

(c) Were reaction sequences of the type:

$$A \rightleftharpoons B + H^+ + e$$

$$B \rightleftharpoons 2C$$

$$C + D \rightarrow E \ldots,$$

both the observed Tafel slope and pH effect would be obtained. However, no reasonable model was found which would correspond to the above reaction sequence.

(d) Suppose that a pH effect on the potential of zero charge (V_{pzc}) exists. Then, for a given vaue of the measured Galvani potential difference across the interface, the Volta potential difference changes, *i.e.* a pH effect on the current densities at constant potential would be found. Evidence for such a change exists. Thus, KHEIFETZ AND KRASIKOV[24] found it for platinum but in systems in which Pt had been presaturated with hydrogen. BOCKRIS, SWINKELS AND GREEN[25] found that the potential of the maximum of the adsorption for naphthalene, $V_{max.\ napht.}$, on Pt depended on pH to the same degree as that observed by KHEIFETZ AND KRASIKOV. Assuming that $dV_{max.\ napht.}/dV_{pzc} = 1$, the empirical relation is:

$$V_{pzc} = V^{\circ}_{pzc} + \frac{RT}{F} \ln a_{H+}$$

Thus:

$$i = k_5 a_{H_2O} (1 - \theta)\, e^{[V - (V^{\circ}_{pzc} + \frac{RT}{F} \ln a_{H+})] \frac{\alpha F}{RT}}$$

or

$$\left(\frac{d \log i}{d\ pH}\right)_V = \alpha \simeq 0.5,$$

as observed.

Were OH^- ions to adsorb on the electrode surface according to a logarithmic isotherm, they would contribute to a change in potential across the interface equivalent in form to that here assumed.

(3) Pressure effect. The evidence that the inverse pressure effect (Figs. 3, 5, 5a) does not represent some artifacts, as for instance the effects of the presence of traces of some poisoning substance in ethylene gas, is as follows.

The pressure effects are reversible on repeated pressure changes without hysteresis. Similar effects have been observed on Pt with other hydrocarbons[4,26], but not during ethylene oxidation on other metals where positive pressure effects occur[17].

For a mechanism in which the rate-determining charge transfer occurs from water onto bare Pt sites:

$$i = k_5 a_{H_2O} (1 - \theta_E)\, e^{\alpha VF/RT} \qquad (7)$$

and at constant potential, the current decreases with pressure as the term $(1 - \theta_E)$ does.

From the theoretical plots of $(1 - \theta)$ *versus* pressure (eqn. 3a), for the limiting values of $K_p = 2.3$ and $K_p = 150$ (see *Discussion, i*), the values of $(1 - \theta)$ at $P_E = 1$, 0.1, 0.01 and 0.001 atm were found and introduced into equation (7). The term $k_5 a_{H_2O}\, e^{\alpha FV/RT}$ was calibrated from the experimental value of i at $P_E = 1$ atm and 520 mV and the theoretical i — log p relationship for seven potential values was plotted (Fig. 5, 5a, full lines $K_P = 150$, dotted lines $K_P = 2.3$). It may be seen that the general shape of the experimental i — log p curves fits much better the theoretical curve plotted for $K_P = 150$ than that for $K_P = 2.3$. Thus the experimental results are more consistent with a coverage close to 0.7 at $P_E = 1$ atm. The theoretical i — log p relation for $K_P = 150$ is in reasonable agreement with experimental data. The slope Q of the experimental i — log p curves varies with potential (Fig. 5 and 5a) $d \log Q/dV$ being

equal to $\sim 7\ V^{-1}$. From equation (7), the coefficent $d \log Q/dV$ should be equal to $\alpha F/2.3\ RT \simeq 7.2\ V^{-1}$ for $\alpha = 0.5$ and $t = 80°C$.

These are marked consistencies with the hypothetized mechanism.

(4) Control in the limiting current region. Figure 4 shows the existence of a limiting current, whose value depends on stirring and is roughly proportional to the partial pressure of ethylene (Fig. 3). Thus the control in this region is by diffusion of ethylene in solution. At sufficiently high pressures (*e.g.*, 1 atm) potential V = 0.9 V(R.H.E.) is reached earlier than the current corresponding to the diffusion control. At this potential, the current drops to negligible values for all pH and pressure values. This value of potential corresponds closely to the potential where surface oxide starts forming[18,20]. The "passivation" of the electrode with respect to ethylene oxidation may be understood of at $V \approx 0.9$ V (R.H.E.), the reaction between OH radicals, or OH and H_2O occurs fast enough for the accumulation of PtO, and water discharge onto the PtO covered surface drops to a negligible rate corresponding to the value

$$i = i_{0(O_2)}\, e^{-\alpha F\eta/RT} \simeq 10^{-10}\ A\ cm^{-2}$$

where $i_{0(O_2)}$ — exchange current for O_2 evolution reaction.

The dependence of the limit of the potential range of ethylene oxidation on oxide formation is to be noted.

(5) Rate constants of charge transfer from solution onto bare and O-covered platinum. The value of the exchange current of ethylene oxidation on smooth Pt $i_{0_E} = 10^{-10}$ A cm^{-2}, as compared with the exchange current of oxygen evolution occurring onto oxide covered surface $i_{0_{O_2}}$, is 10^{-10} to 10^{-8} (*cf.* ref. 27).

The ratio of rate constants for water discharge on bare and oxide covered surface is thus

$$\frac{k_E}{k_{O_2}} = \frac{i_{0_E}}{i_{0_{O_2}}}\, e^{\alpha F/RT(V_{rev_{O_2}} - V_{rev_E})} \approx 10^8$$

This large difference in the rate constants, and similar values of the activation energy of both reactions, is consistent with the model in which, in both cases, water discharges onto the bare surface, whose area in case of oxygen evolution is 10^8 times lower since the electrode is almost fully covered by PtO.

This assumption is supported by a consideration of the potential energy-distance profile diagrams which show that the bond energy of OH radicals with Pt–O would have been of the order of ~ 100 kcals to yield the observed activation energy of the oxygen evolution reaction. Such a high value of the Pt–O–OH bond energy is most unlikely. The assumption of H_2O discharging onto the bare surface sites only, is also supported by results of Bockris and Huq[19], who found that the overpotential of O_2 evolution increases with time, and attributed it to the filling up of the bare surface sites by an oxide.

ACKNOWLEDGEMENTS

Our thanks are due to the Pratt and Whitney Aircraft for financial support.

SUMMARY

The ethylene oxidation reaction on smooth and platinized platinum has been studied at 80°C in solutions of $H_2SO_4 + K_2SO_4$ and $NaOH + K_2SO_4$ of constant ionic strength = 1.5. Reaction rates were measured as a function of potential, pH and partial pressure of ethylene. Coulombic efficiency of the reaction was determined by measurements of CO_2 production in acidic solutions, and of C_2H_4 consumption in alkaline solutions. The following parameters have been found:

$$\left(\frac{dV}{d\log i}\right)_p = \frac{2.3 \cdot 2RT}{F}; \left(\frac{d\log i}{d\,pH}\right)_V \simeq 0.45; \left(\frac{d\eta}{d\,pH}\right)_i \simeq 0; \left(\frac{d\log i_0}{d\,pH}\right) \approx 0; \left(\frac{di}{dp}\right)_V < 0.$$

Coulombic efficiency is 100 ± 1% in acidic and 90 ± 5% in alkaline solutions. $i_0 = 10^{-8}$ A cm^{-2} on platinized and 10^{-10} A cm^{-2} on smooth Pt respectively. Activation energy A = 17 ± 2 kcals. At higher overpotentials diffusion limiting current was obtained. At V = 0.9 (R.H.E.), the current drops to negligible values due to the oxide formation. Coverage of the electrode with the ethylenic radical at 1 atm has been evaluated by two independent methods as $\theta_E = 0.55 \pm 0.2$.

The reaction mechanism in the Tafel potential range was interpreted in terms of water discharge as the rate-determining step over the complete pH range investigated. In the potential range higher than that of the Tafel region the rate control is shifted to mass transport of ethylene. At $P_E = 1$ atm, the Tafel potential range is limited by oxide formation before diffusion control sets in. A possible explanation of the anomalous pH effect in reactions concerning water discharge has been given.

REFERENCES

1 V. DRAZIC, M. GREEN AND J. WEBER, *J. Electrochem. Soc.*, in press.
2 J. WEBER AND M. GREEN, *J. Electrochem. Soc.*, in press.
3 J. O'M. BOCKRIS, I. A. AMMAR AND A. K. M. S. HUQ, *J. Phys. Chem.*, 61 (1957) 879
4 J. W. JOHNSON, H. WROBLOWA AND J. O'M. BOCKRIS, in process of publication.
5 G. H. TWIGG AND E. K. RIDEAL, *Trans. Faraday Soc.*, 36 (1940) 533.
6 G. K. T. CONN AND G. H. TWIGG, *Proc. Roy. Soc.*, A171 (1939) 70.
7 O. BEECK, A. E. SMITH AND A. WHEELER, *Proc. Roy. Soc.*, A177 (1940) 62.
8 O. BEECK, *Disc. Faraday Soc.*, 8 (1950) 118; *Rev. Mod. Phys.*, 17 (1945) 61.
9 B. M. W. TRAPNELL, *Trans. Faraday Soc.*, 48 (1952) 160.
10 C. A. COULSON, *Valence*, Oxford University Press, London, 1961.
11 B. E. CONWAY, *Proc. Roy. Soc.*, A247 (1958) 400.
12 B. M. W. TRAPNELL, *Chemisorption*, Academic Press Inc., New York, 1955.
13 H. DAHMS, M. GREEN AND J. WEBER, *Nature*, 196, No. 4861 (1962) 1310.
14 E. BLOMGREN, J. O'M. BOCKRIS AND C. JESCH, *J. Phys. Chem.*, 65 (1961) 2000.
15 "International Critical Tables," 5, McGraw-Hill, New York, 1929, p. 65.
16 B. RUBIN, private communication.
17 H. DAHMS AND J. O'M. BOCKRIS, in process of publication.
18 W. VISSCHER AND M. A. V. DEVANATHAN, in process of publication.
19 J. O'M. BOCKRIS AND A. K. M. S. HUQ, *Proc. Roy. Soc.*, 237 (1956) 277.
20 K. J. VETTER AND D. BERNDT, *Z. Elektrochem.*, 62 (1958) 378.
21 J. J. MACDONALD AND B. E. CONWAY, *Proc. Roy. Soc.*, A269 (1962) 419.
22 Y. YONEDA, *Bull. Chem. Soc., Japan*, 22 (1949) 266.
23 J. O'M BOCKRIS, M. A. V. DEVANATHAN AND K. MÜLLER, *Proc. Roy. Soc.*, in press.
24 V. L. KHEĬFETS AND B. S. KRASIKOV, *Zhur. Fiz. Khim.*, 31 (1957) 1992.
25 J. O'M. BOCKRIS, D. SWINKELS AND M. GREEN, *Rev. Sci. Instr.*, 33 (1962) 18.
26 H. WROBLOWA, B. J. PIERSMA AND J. O'M. BOCKRIS, in process of publication.
27 J. O'M. BOCKRIS, *Modern Aspects of Electrochemistry*, Vol. I, Butterworths Scientific Publications, London, 1954, p. 228.

Short Communication

Polarography of cyclic hydrazides

There have been, to our knowledge, two previous investigations on the polarographic reduction of cyclic hydrazides at a dropping mercury electrode in aqueous solutions. VOJIR[1] has reported the reduction of luminol (3-aminophthalhydrazide, I, R=NH_2) in 0.1 *F* sodium carbonate solution. MILLER[2,3] has described in detail the reduction of maleic hydrazide (II) at various pH's. MILLER[3] also demonstrated that the probable product from the reduction of maleic hydrazide, cyclic succinhydrazide (III), was not polarographically active.

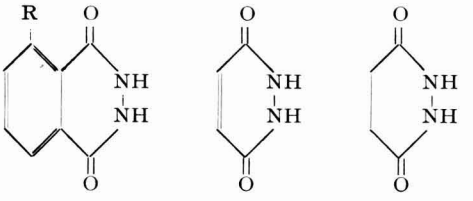

I II III

We attempted the polarographic reduction of luminol as part of an investigation which involved the anodic electro-generation of solution chemiluminescence[4]. We found that luminol was not reduced contrary to the work of VOJIR. Furthermore, the unsubstituted phthalhydrazide (I, R=H) was also inactive. 3-Nitrophthalhydrazide (I, R=NO_2), on the other hand, gave a wave ($E_{1/2}$ = −0.49 V *vs.* mercury pool) which appeared very similar to the one shown by VOJIR.

We believe that the wave, which VOJIR ascribed to luminol, was probably due to an impurity which may have been 3-nitrophthalhydrazide. Examination of the preparative methods for luminol shows that it can be made from (a) the action of hydrazine hydrate on 3-aminophthalimide[5] or (b) the reduction of 3-nitrophthalhydrazide with stannous chloride[5] or sodium hydrosulfite[6]. The first method can yield a side product of 3-N-diaminophthalimide, but this compound is insoluble in dilute carbonate solutions. In the second procedure, a likely contaminant can be the starting material itself. A sample of luminol prepared according to FIESER[6], indeed gave a wave corresponding to the starting nitro-compound. Commercial samples without further purification, however, failed to produce any reduction waves.

The results obtained above were also duplicated on a carbon-paste electrode. It was also interesting to note that oxidation of the nitro-compound (I, R=NO_2) produced an anodic current-voltage curve with $E_{p/2}$ of +0.36 V *vs.* saturated calomel reference electrode and a photo-polarogram similar to luminol[4] in a solution of carbonate containing oxygen.

MILLER attributed the cathodic activity of maleic hydrazide to the reduction of the carbon-carbon double bond which led to the postulated product, cyclic succinhydrazide. We performed a macro-scale electrolysis of maleic hydrazide at a mercury cathode in aqueous ethanol solution containing lithium chloride and produced a product identified as cyclic succinhydrazide by infrared spectrophotometric comparison with

an authentic sample. (Solvent composition was similar to the one used in the preparation of cyclic succinhydrazide from maleic hydrazide by aluminum amalgam reduction[7].) Our voltammetric and product analysis data, therefore, support the results and conclusions of MILLER.

EXPERIMENTAL

The dropping mercury electrode polarograms were obtained with a Sargent Model XV Polarograph using a Sargent-Heyrovsky cell with a mercury pool as the reference anode. This reference electrode was chosen to permit comparison with VOJIR's data. The cell was thermostatted at 25 $\pm$ 0.05°C. The carbon-paste electrode has been described by ADAMS[8]. Current-voltage curves using this electrode were obtained with a triangular-voltage apparatus[9].

The phthalhydrazides were prepared by reacting the appropriate phthalimides with excess hydrazine hydrate[5,10]. The commercial samples of luminol were obtained from the Eastman Kodak Company and the Aldrich Chemical Company.

The most reliable and satisfactory samples of luminol were obtained by reacting a highly purified sample of 3-aminophthalimide with hydrazine. However, whether the luminol was synthesized as above or obtained commercially, a modified purification procedure of Drew and Pearman gave the most consistent spectral and electrochemical results. As suggested by Drew and Pearman, a concentrated solution of luminol in 5% sodium hydroxide was cooled to 0°C in an icebath. The resulting crystals were dissolved in water and reprecipitated by the addition of 10% acetic acid. We have found, that, at this stage of the procedure, a product which was more easily isolated and dried was obtained as follows: luminol was redissolved in an excess of 10% aqueous ammonia, decolorized with charcoal (if necessary), diluted with an equal volume of 95% ethanol and then warmed to 50–60°C. The slow addition of 10% acetic acid (until it was in slight excess) brought about the gradual formation of needle-like crystals. The product should not be heated during drying and should be stored under dry nitrogen, protected from light.

ACKNOWLEDGEMENT

Partial financial support for this work provided by the University of California, (Riverside) under Intramural Grant No. 4003 is gratefully acknowledged.

Department of Chemistry,
University of California,
Riverside, California (U.S.A.)

EDDIE T. SEO
THEODORE KUWANA

1 V. VOJIR, *Chem. Listy*, 48 (1954) 520; *Coll. Czech. Commun.*, 19 (1954) 868.
2 D. M. MILLER, *Can. J. Chem.*, 33 (1955) 1806.
3 D. M. MILLER, *Can. J. Chem.*, 34 (1956) 1760.
4 T. KUWANA, *J. Electroanal. Chem.*, 6 (1963) 164.
5 H. D. K. DREW AND F. H. PEARMAN, *J. Chem. Soc.*, (1937) 26.
6 L. F. FIESER, *Experiments in Organic Chemistry*, 3rd Edition, D. C. Heath and Co., Boston, 1955, pp. 199–201.
7 H. FEUER, G. V. BACHMAN AND E. H. WHITE, *J. Am. Chem. Soc.*, 73 (1951) 4716.
8 R. N. ADAMS, *Progress in Polarography*, 2 (1962) 503.
9 J. R. ALDEN, J. Q. CHAMBERS AND R. N. ADAMS, *J. Electroanal. Chem.*, 5 (1963) 152.
10 H. D. K. DREW AND H. H. HATT, *J. Chem. Soc.*, (1937) 16.

Received August 9, 1963

CONTENTS

ELSEVIER PUBLISHING COMPANY, AMSTERDAM

Printed in The Netherlands by

NEDERLANDSE BOEKDRUK INRICHTING N.V., 'S-HERTOGENBOSCH

Elsevier
and the Nobel Foundation

jointly announce the publication of the

NOBEL PRIZE LECTURES

CHEMISTRY · PHYSICS · PHYSIOLOGY OR MEDICINE

Each category to be contained in three volumes:
1901-1921/1922-1941/1942-1962

In the world of science, the history of research and progress in the last sixty years is largely a history of the accomplishments of the Nobel Prize winners. Annually these achievements are placed in perspective at the Nobel Prize ceremonies held each December in Stockholm.

Published for the Nobel Foundation, the collected Nobel Lectures will be issued, for the first time in English, by Elsevier. The lectures will be arranged in chronological order according to subject, beginning in 1901 and continuing through 1962. Each Lecture will be preceded by the presentation address to the prizewinner and followed by his or her biography. Initially, the Nobel Prize Lectures in Chemistry, in Physics, and in Physiology or Medicine will be issued, each in three volumes, to be completed in about two years.

- **The first volumes are scheduled to appear in December 1963**
- **Special subscription terms**
- **A large descriptive brochure available upon request**

ELSEVIER PUBLISHING COMPANY

AMSTERDAM LONDON NEW YORK

272 E